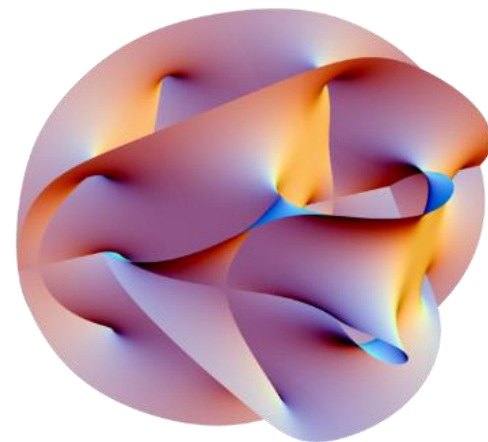
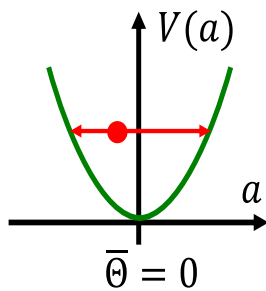
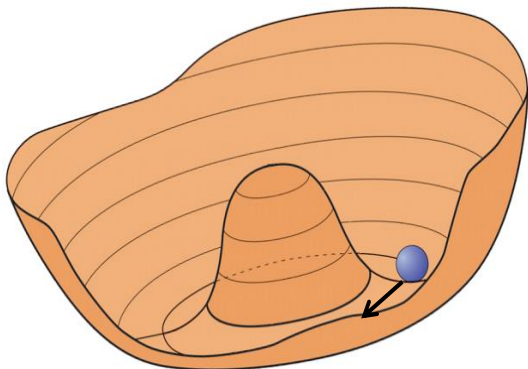


Dark Matter Axion and ALPs

Where do they come from?

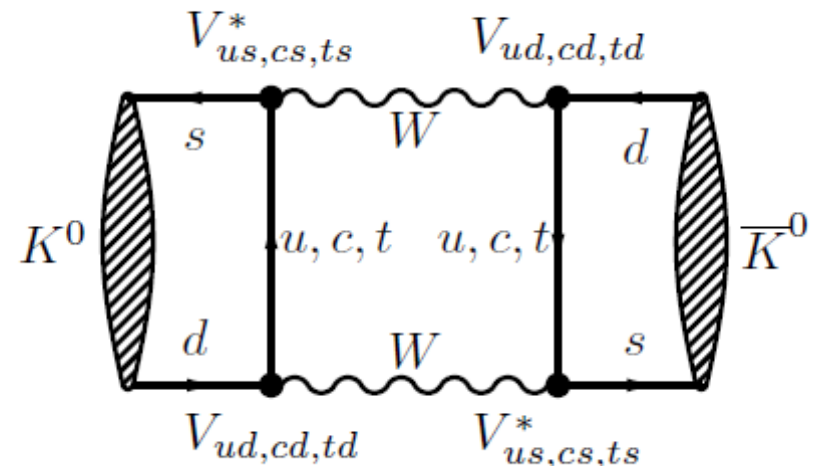
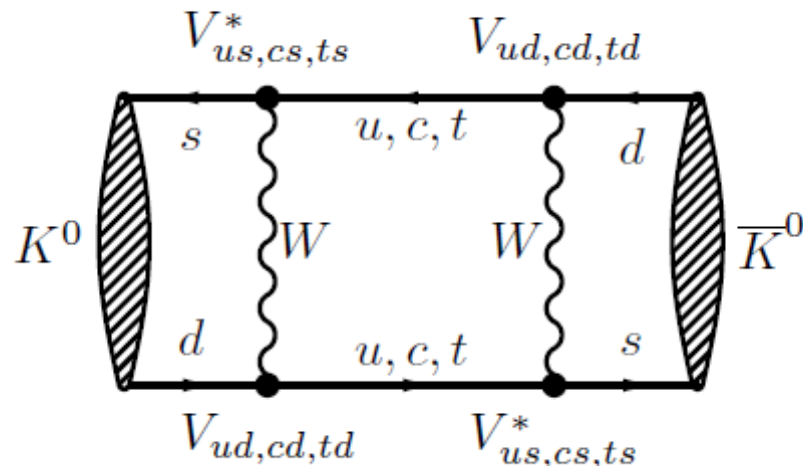


- CP violation in QCD
- The strong CP problem
- Peccei Quinn symmetry breaking & the axion
- Axion production in the early universe

CP violation in the quark sector

$K^0 - \bar{K}^0$ Oscillation via quark mixing

$$\begin{bmatrix} |V_{ud}| & |V_{us}| & |V_{ub}| \\ |V_{cd}| & |V_{cs}| & |V_{cb}| \\ |V_{td}| & |V_{ts}| & |V_{tb}| \end{bmatrix} = \begin{bmatrix} 0.97427 \pm 0.00015 & 0.22534 \pm 0.00065 & 0.00351^{+0.00015}_{-0.00014} \\ 0.22520 \pm 0.00065 & 0.97344 \pm 0.00016 & 0.0412^{+0.0011}_{-0.0005} \\ 0.00867^{+0.00029}_{-0.00031} & 0.0404^{+0.0011}_{-0.0005} & 0.999146^{+0.000021}_{-0.000046} \end{bmatrix}.$$



CP violation in the quark sector

For Kaons (negative parity):

$$C|K^0, \mathbf{p} > = -|\overline{K^0}, \mathbf{p} >$$

$$P|K^0, \mathbf{p} = \mathbf{0} > = -|K^0, \mathbf{p} = \mathbf{0} > \text{ and } P|\overline{K^0}, \mathbf{p} = \mathbf{0} > = -|\overline{K^0}, \mathbf{p} = \mathbf{0} >$$

Thus:

$$CP|K^0, \mathbf{p} = \mathbf{0} > = |\overline{K^0}, \mathbf{p} = \mathbf{0} > \text{ and } CP|\overline{K^0}, \mathbf{p} = \mathbf{0} > = |K^0, \mathbf{p} = \mathbf{0} >$$

Thus there are two CP Eigenstates:

$$|K_{1/2}^0, \mathbf{p} = \mathbf{0} > = \frac{1}{\sqrt{2}}\{|K^0, \mathbf{p} = \mathbf{0} > \pm |\overline{K^0}, \mathbf{p} = \mathbf{0} >\}$$

With

$$CP|K_{1/2}^0, \mathbf{p} = \mathbf{0} > = \pm|K_{1/2}^0, \mathbf{p} = \mathbf{0} >$$

K_1^0 ALWAYS has to decay into states with $CP=1$

K_2^0 ALWAYS has to decay into states with $CP=-1$

CP violation in the quark sector

Experimentally two states observed:

$$K_S^0 \rightarrow \pi\pi \quad \text{and} \quad K_L^0 \rightarrow \pi\pi\pi$$

$$\tau_S = 0.9 \cdot 10^{-10} s, \quad \tau_L = 0.5 \cdot 10^{-7} s$$

corresponding to (CP states)

$$K_L^0 = K_2^0 \text{ and } K_S^0 = K_1^0$$

1964: Christenson, Cronin, Fitch and Turlay at Brookhaven national Lab also **observed**:

$$\rightarrow K_L^0 \rightarrow \pi\pi$$

This is a CP violating decay!
 (similar CP violating decays appear in b-mesons: BELLE/Babar)

→ Nobel Prize 1980

The Nobel Prize in Physics 1980



Photo from the Nobel Foundation archive.

James Watson
Cronin

Prize share: 1/2

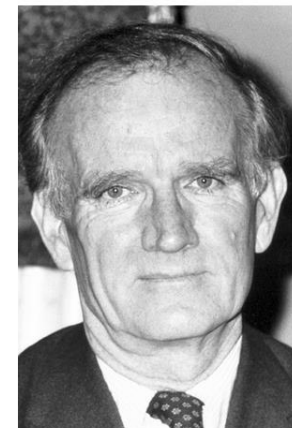


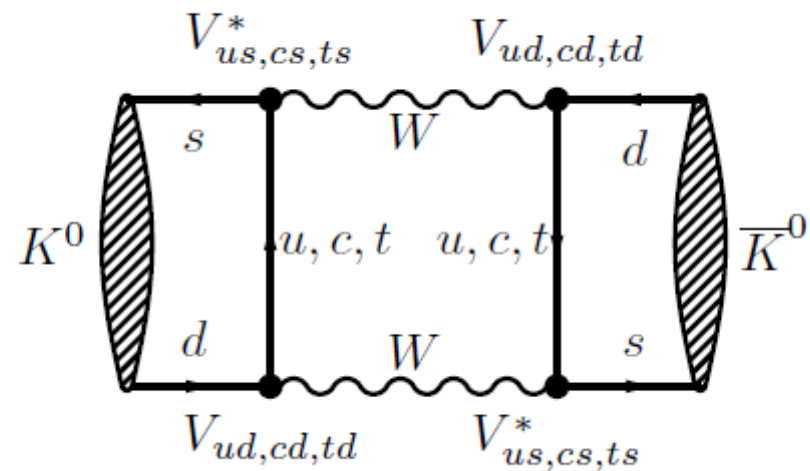
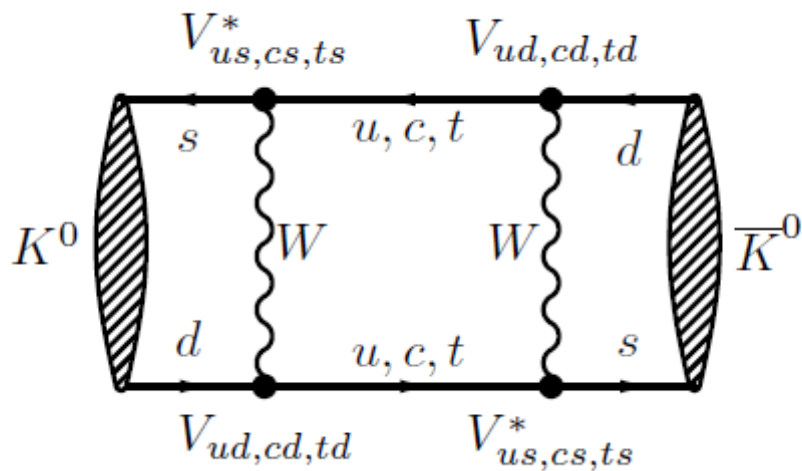
Photo from the Nobel Foundation archive.

Val Logsdon Fitch
Prize share: 1/2

CP violation in the quark sector

$K^0 - \bar{K}^0$ Oscillation

$$\begin{bmatrix} |V_{ud}| & |V_{us}| & |V_{ub}| \\ |V_{cd}| & |V_{cs}| & |V_{cb}| \\ |V_{td}| & |V_{ts}| & |V_{tb}| \end{bmatrix} = \begin{bmatrix} 0.97427 \pm 0.00015 & 0.22534 \pm 0.00065 & 0.00351^{+0.00015}_{-0.00014} \\ 0.22520 \pm 0.00065 & 0.97344 \pm 0.00016 & 0.0412^{+0.0011}_{-0.0005} \\ 0.00867^{+0.00029}_{-0.00031} & 0.0404^{+0.0011}_{-0.0005} & 0.999146^{+0.000021}_{-0.000046} \end{bmatrix}.$$



$$\begin{bmatrix} 1 & 0 & 0 \\ 0 & c_{23} & s_{23} \\ 0 & -s_{23} & c_{23} \end{bmatrix} \begin{bmatrix} c_{13} & 0 & s_{13} e^{-i\delta_{13}} \\ 0 & 1 & 0 \\ -s_{13} e^{i\delta_{13}} & 0 & c_{13} \end{bmatrix} \begin{bmatrix} c_{12} & s_{12} & 0 \\ -s_{12} & c_{12} & 0 \\ 0 & 0 & 1 \end{bmatrix}$$

$$\theta_{12} = 13.04 \pm 0.05^\circ, \theta_{13} = 0.201 \pm 0.011^\circ, \theta_{23} = 2.38 \pm 0.06^\circ, \text{ and } \delta_{13} = 1.20 \pm 0.08 \text{ radians}$$

Axions and ALPs: where do they come from, how to detect them?

CP violation in the QCD vacuum

QCD gauge group $SU(3)_c$ is a **non-Abelian**:
gauge transformations of the Lie group are **not commutative!**

Consequence: QCD has “large gauge transformations”, which come with
gauge in-equivalent **ZERO energy states** $|n\rangle$, separated by potential barrier.

→ No single $|n\rangle$ (including $|0\rangle$) can be a stable vacuum state due to quantum tunelling

Physical ground state of QCD vacuum is defined by
gauge invariant superposition of vacuum states:

$$|\theta\rangle = \sum_n e^{in\theta} |n\rangle$$

For couplings this means: Need to evaluate “possible amplitudes”

→ **NEED** to add a general CP violating term to the QCD Lagrangian:

$$\Theta \frac{\alpha_s}{8\pi} G_{\mu\nu a} \tilde{G}_a^{\mu\nu}$$

CP violation in QCD

→ There are **two INDEPENDENT sources for CP violation** in QCD.

Physically only one CP violating phase will appear:

$$\theta_{eff} = \bar{\theta} = \theta - (\text{phase of CKM matrix})$$

leading to additional CP violating term in the QCD Lagrangian:

$$\overline{\Theta} \frac{\alpha_s}{8\pi} G_{\mu\nu a} \tilde{G}_a^{\mu\nu}$$

With α_s the strong coupling constant and $G_{\mu\nu a}$ and $\tilde{G}_a^{\mu\nu}$ the gluon field and its dual.

Electric Dipole Moment (EDM)

Nonzero EDMs imply P and T (and CP) violation if the system has a non-degenerate ground state. This can be seen as follows:

$$\vec{d} = \left| \vec{d} \right| \frac{\vec{\sigma}}{|\sigma|} \rightarrow \Delta E = \left| \vec{d} \right| \frac{\vec{\sigma}}{|\sigma|} \cdot \vec{E}$$

$$P(\vec{\sigma} \cdot \vec{E}) = -(\vec{\sigma} \cdot \vec{E})$$

$$T(\vec{\sigma} \cdot \vec{E}) = -(\vec{\sigma} \cdot \vec{E})$$

EDM energy Eigenstates are neither P nor T conserving

→ Together with CPT theorem:

Non vanishing dipole moment is CP violating!

→ Consequence of non-vanishing cp violating $\bar{\theta}$:

Finite electric dipole moment (EDM) of elementary particles

The strong CP problem:

CP violation in QCD should induce EDM in neutron

$$d_n = \bar{\theta} \cdot 10^{-16} e \text{ cm}$$

Experimental limit: $d_n < 3 \cdot 10^{-26} e \text{ cm}$

$$\rightarrow \bar{\Theta} = \Theta - \arg \det M_q < 10^{-10}$$

Why do two INDEPENDENT sources for CP violation
eliminate each other to 1 in 10^{10} ?

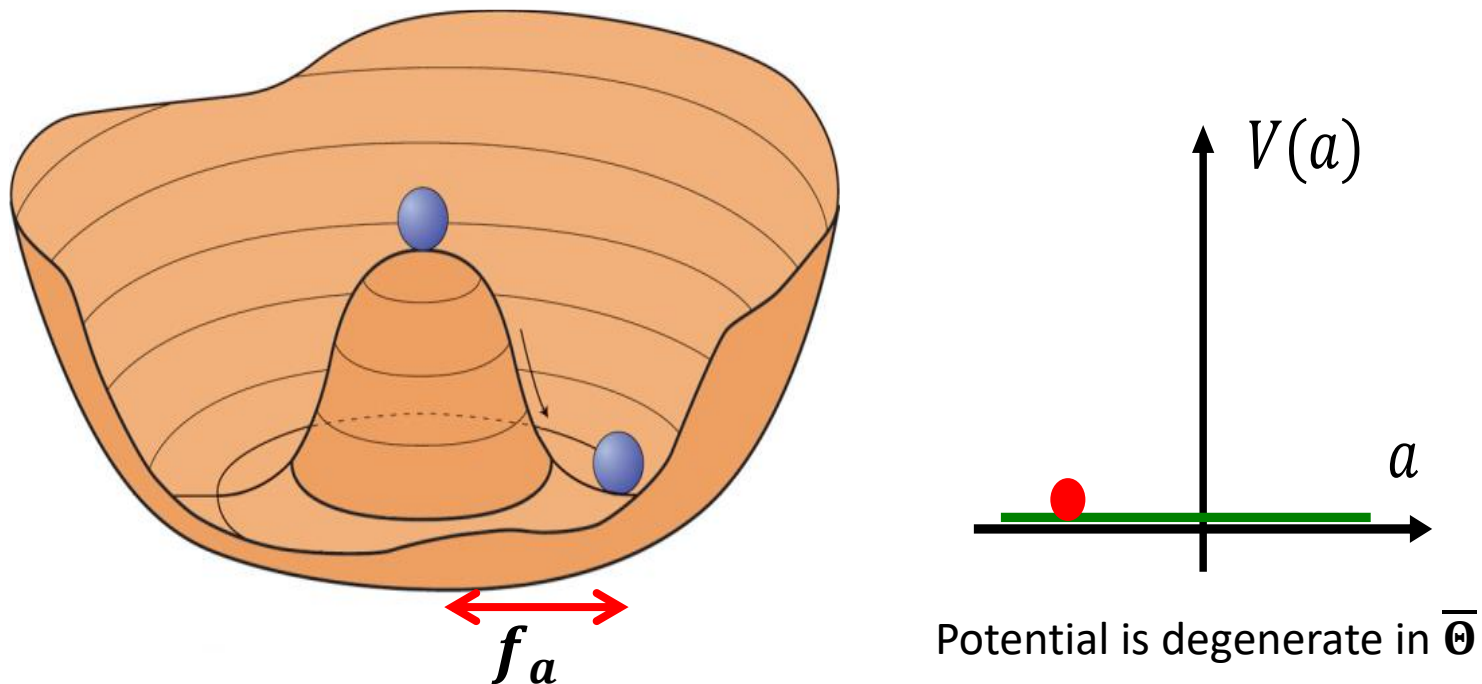
Anthropic principle does not help!

Universe would look the same with $\bar{\Theta} \sim 0.001$

The Peccei Quinn mechanism

“Make $\bar{\Theta}$ a field that is dynamically driven to 0”

Introduce U(1) symmetry with $\bar{\Theta}$ the complex phase



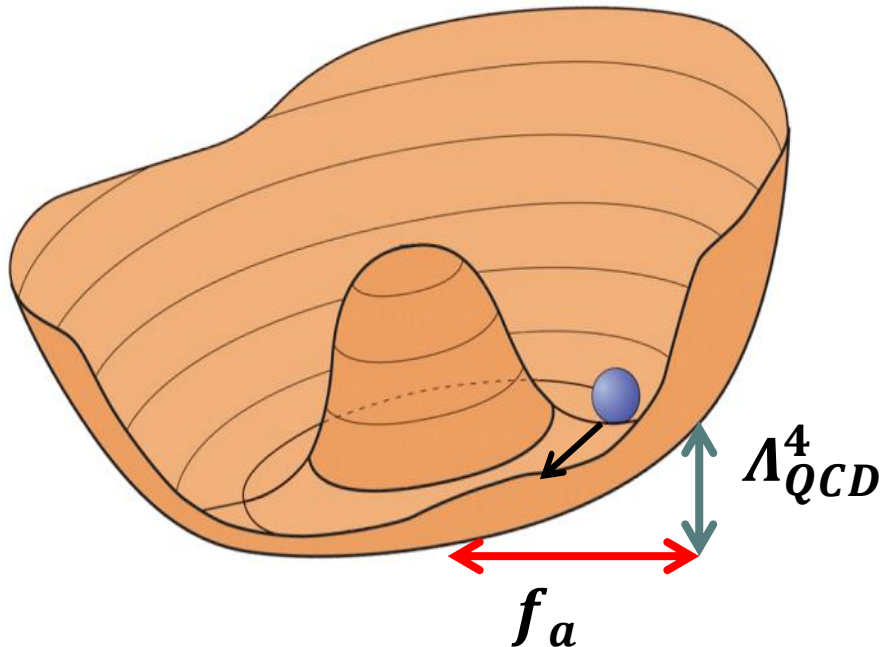
U(1) symmetry is spontaneously broken at Peccei Quinn scale f_a
 $(f_a$ also sometimes called axion decay constant)

→ Massless Nambu-Goldstone-Boson $a(x) = \bar{\Theta}(x) \cdot f_a$

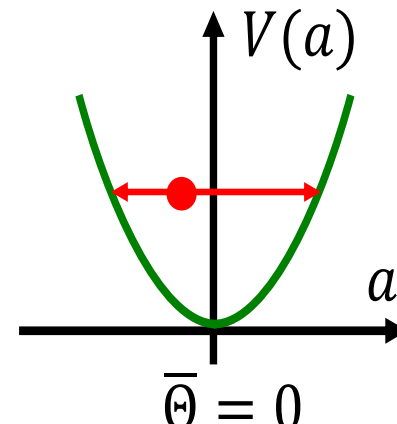
Axions and ALPs: where do they come from, how to detect them?

The Peccei Quinn mechanism

→ Explicit symmetry breaking during QCD phase transition



Potential develops minimum:



„Topological susceptibility“ of QCD vacuum :

dependence of term $G_{\mu\nu a} \tilde{G}_a^{\mu\nu}$ on $\bar{\Theta}$

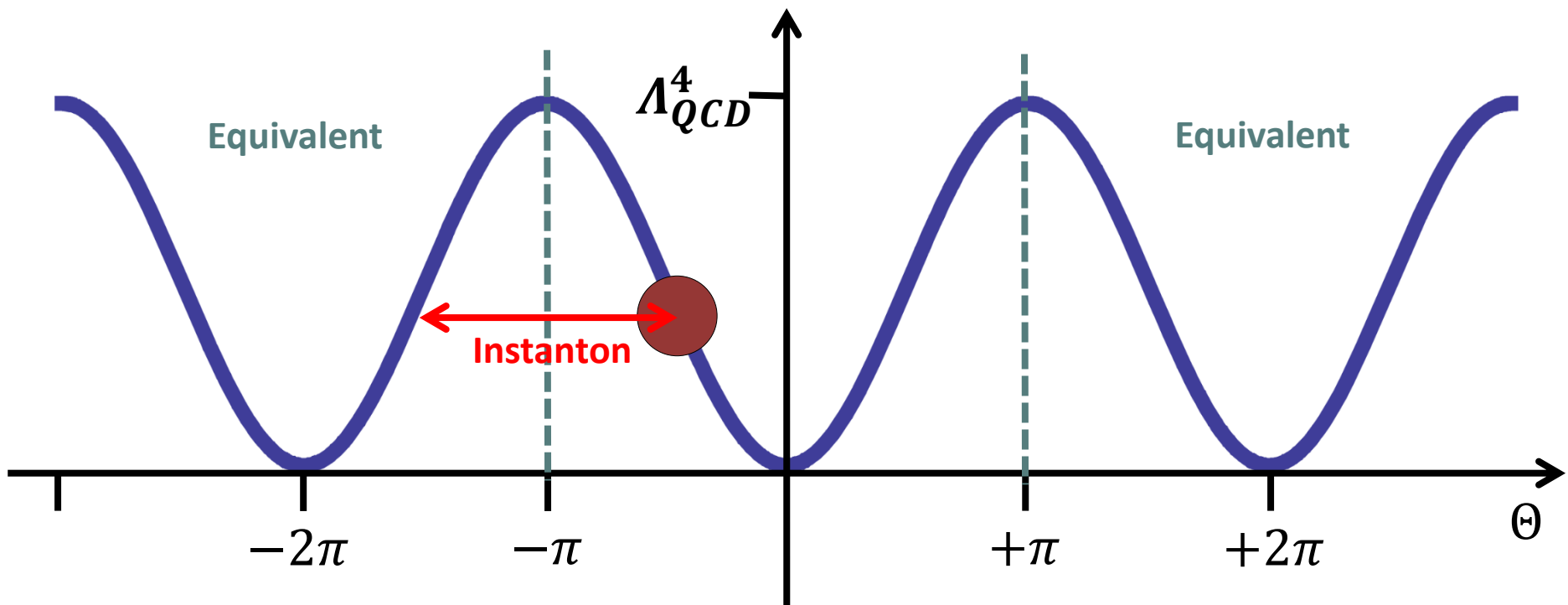
→ Dependence of field potential on $\bar{\Theta}$:

→ Potential minimum at $V(\bar{\Theta} = 0)$ due to “Instanton dynamics”

→ Massive pseudo Nambu-Goldstone-Boson

The Peccei Quinn mechanism

“Make $\overline{\Theta}$ a field that is dynamically driven to 0”



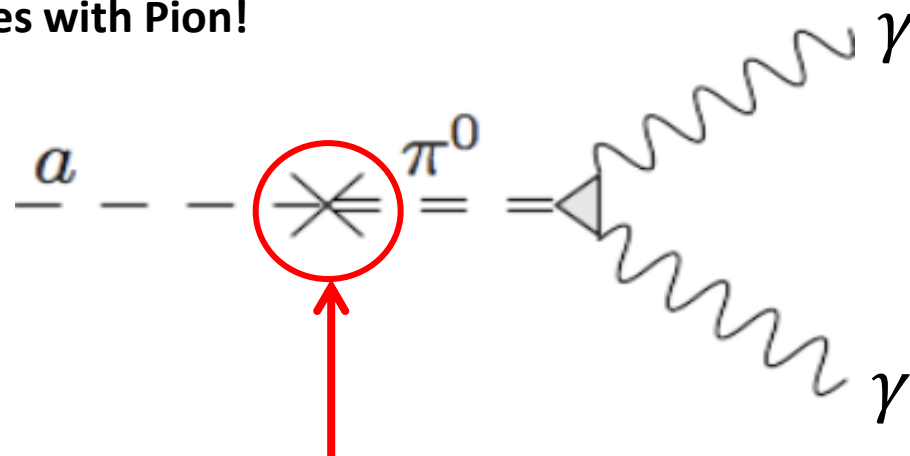
Axion as massive pseudo Nambu-Goldstone-Boson

→ generation of mass by chiral symmetry breaking
 (mass: second derivative of potential at minimum)

$$m_a = 5.7 \mu eV \left(\frac{10^{12}}{f_a} \right) \quad \text{Correlated to } f_a \text{ by QCD}$$

Chiral symmetry breaking is process giving π^0 its mass!!
 → Mass generation by “mixing with mesons!”

→ Axion mixes with Pion!

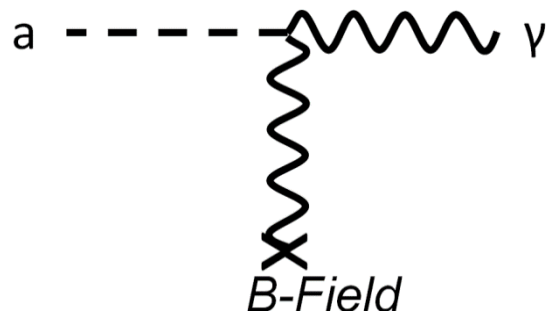


Coupling to Photons: $g_{a\gamma\gamma} \propto 1/f_a$

Axion Photon mixing

→ Axion photon conversion in external B-field

**Inverse Primakoff
effect**



Coupling to Photons: $g_{a\gamma\gamma} \propto 1/f_a$

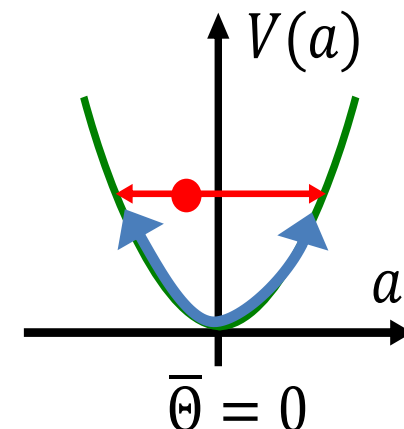
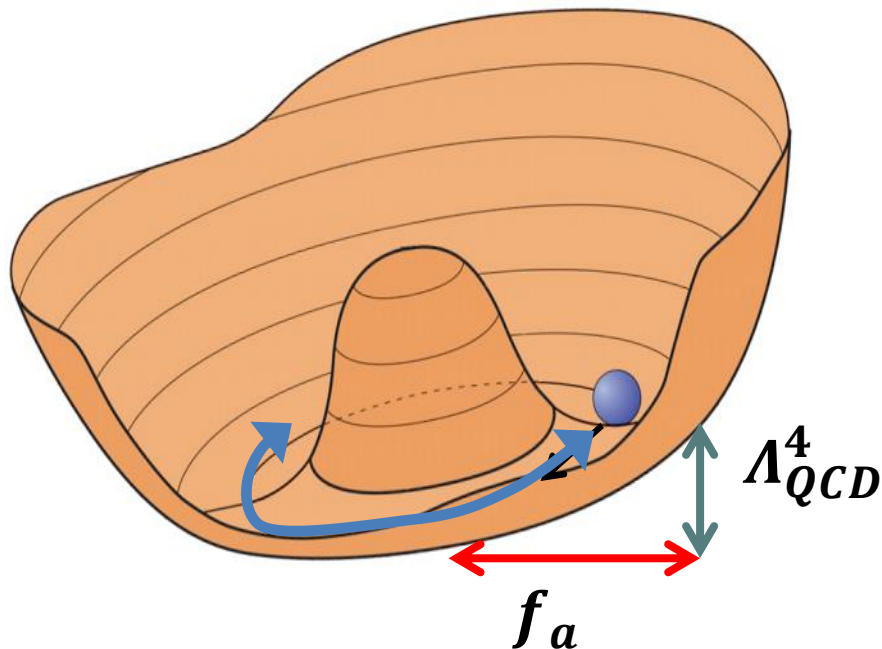
In general: Presence of axion field modifies Maxwell's equations:

$$\begin{aligned}\nabla \cdot \mathbf{E} &= \rho - g_{a\gamma} \mathbf{B} \cdot \nabla a, \\ \nabla \times \mathbf{B} - \dot{\mathbf{E}} &= \mathbf{J} + g_{a\gamma} (\mathbf{B} \dot{a} - \mathbf{E} \times \nabla a), \\ \nabla \cdot \mathbf{B} &= 0, \\ \nabla \times \mathbf{E} + \dot{\mathbf{B}} &= 0, \\ \ddot{a} - \nabla^2 a + m_a^2 a &= g_{a\gamma} \mathbf{E} \cdot \mathbf{B}.\end{aligned}$$

Axions in the early universe

Axions are produced as **NON-THERMAL** local field oscillations,

→ particle population without initial momentum → **NON RELATIVISTIC!**



After phase transition: axion field oscillations:

frequency proportional to axion mass

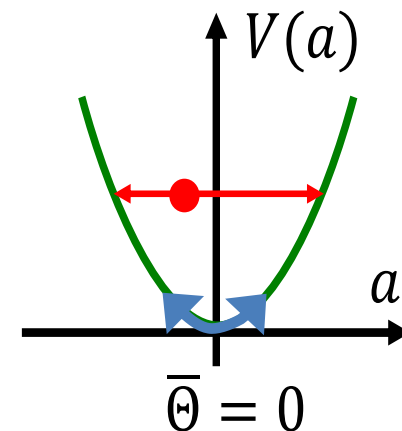
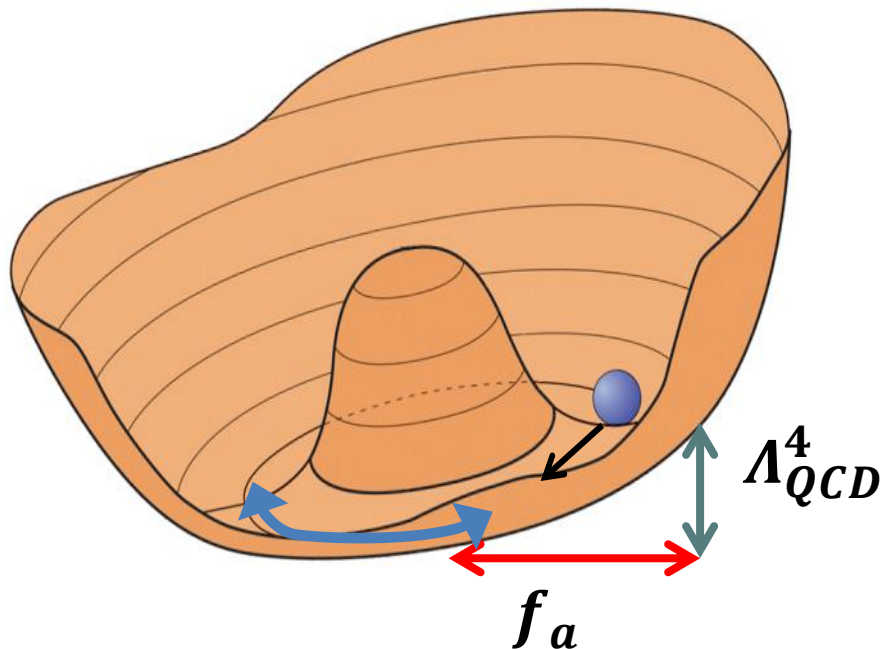
Quantization of oscillations → huge particle density

→ Ideal cold Dark Matter candidate

Axions in the early universe

Axions are produced as **NON-THERMAL** local field oscillations,

→ particle population without initial momentum → **NON RELATIVISTIC!**



Energy stored, i.e. particle number density:

depends on initial alignment of $\bar{\Theta}_i$ after symmetry breaking.

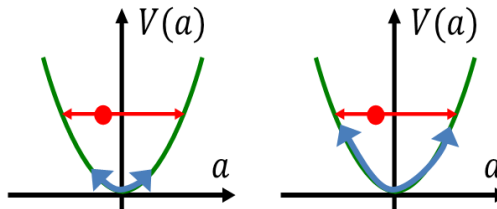
Assume: Axions make up all dark matter:

If we can calculate axion relic density → prediction for their mass!

Axions in the early universe

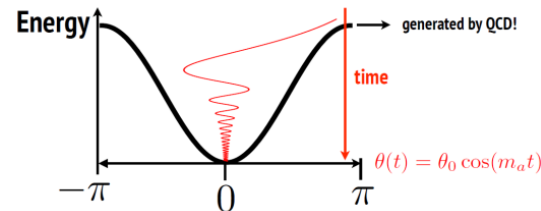
Axion relic density depends on:

- Initial misalignment $\overline{\Theta}_i$



- Damping of oscillation** amplitude due to **Hubble expansion** of universe during QCD phase transition:
Damping: proportional to ratio between Hubble expansion rate and axion field oscillation frequency (mass)

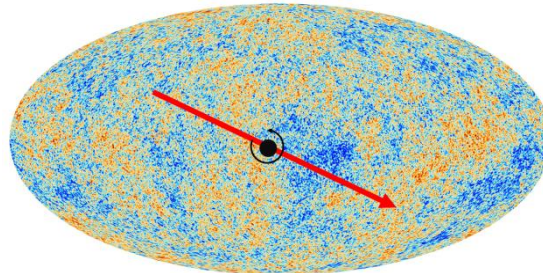
$$\ddot{\theta} + 3H\dot{\theta} + m_a^2(T) \sin \theta = 0$$



- Energy scale of f_a : Peccei-Quinn symmetry breaking before or after inflation?

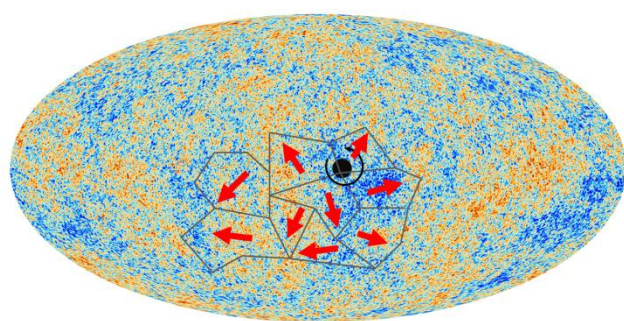
Axions in the early universe

Pre-inflationary scenario: Peccei Quinn symmetry breaking occurred before inflation: $\overline{\Theta}_i$ the same everywhere in the observable universe $\rightarrow 0 < |\overline{\Theta}_i| < \pi$

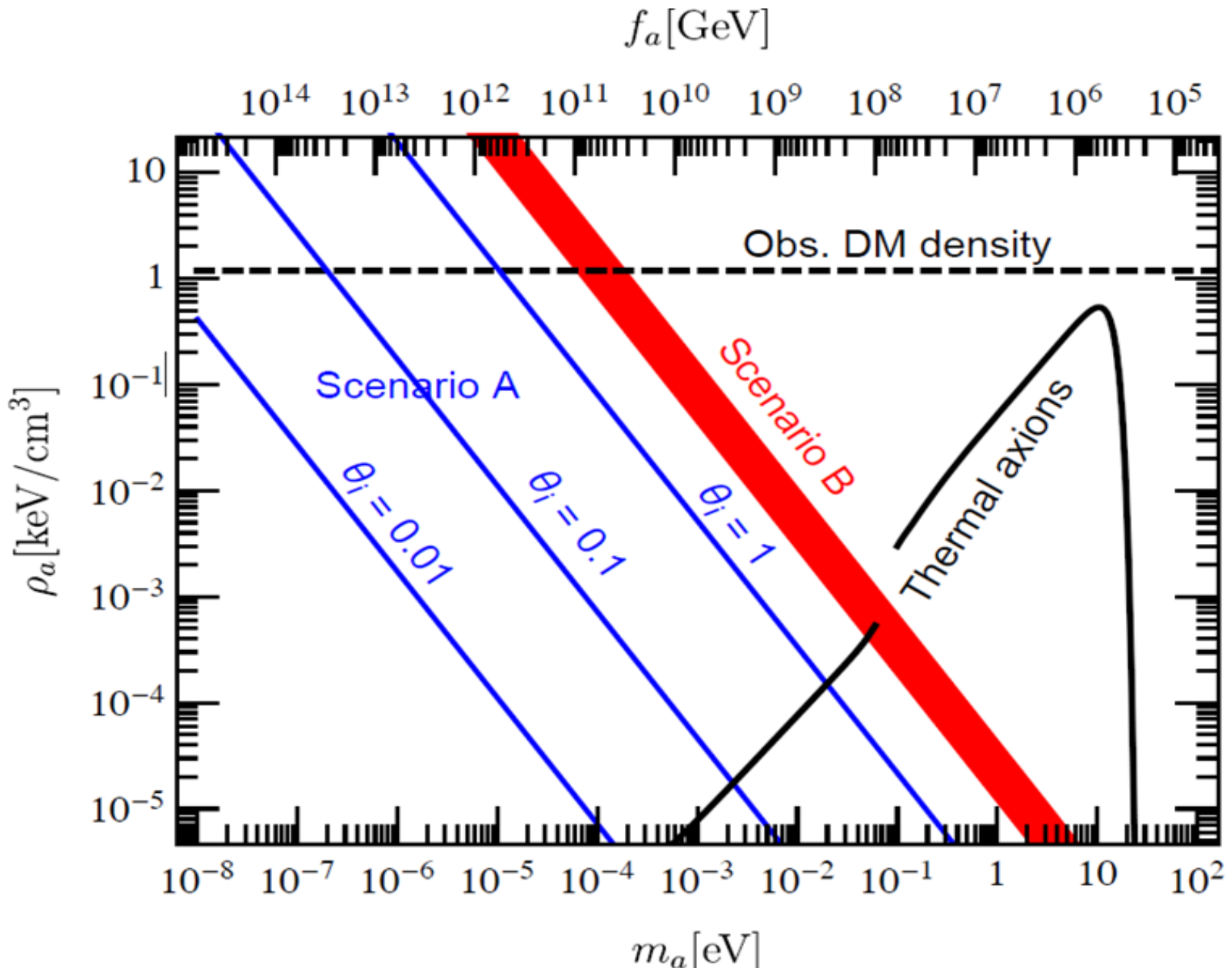


Post-inflationary scenario: Observable universe consists of many patches not in causal contact during Peccei Quinn symmetry breaking

- Today we see average of all $\overline{\Theta}_i$ from many patches now in causal contact
- $|\widehat{\overline{\Theta}}_i| \sim \pi/2!$



Problem: Topological defects lead to additional axion population \rightarrow large uncertainties

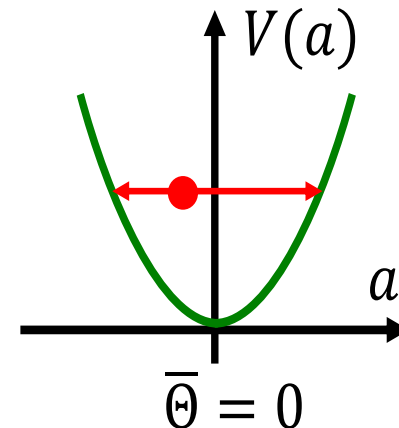
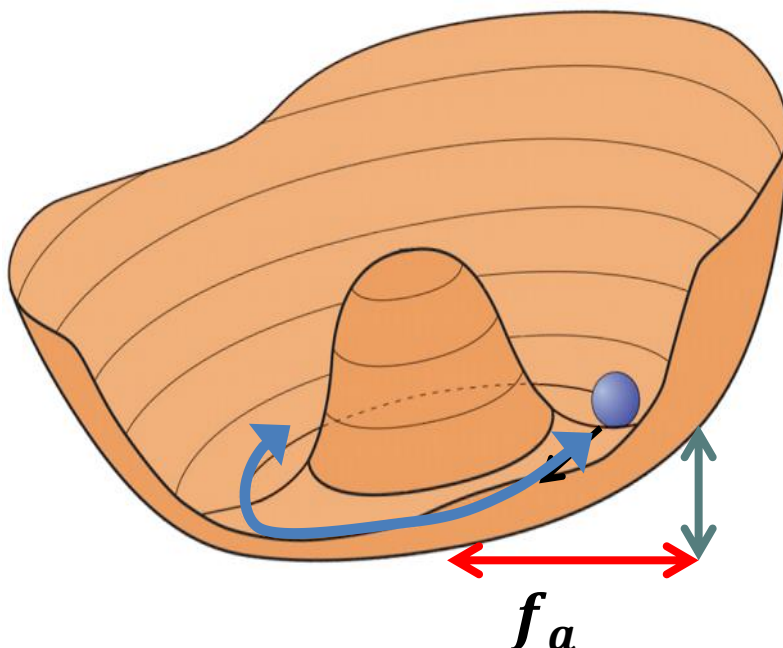


Axion Like Particles (ALPs)

Any spontaneously broken U1 symmetry with explicit symmetry breaking:
Pseudo Nambu Goldstone Boson
→ Axion like particle

For axion:

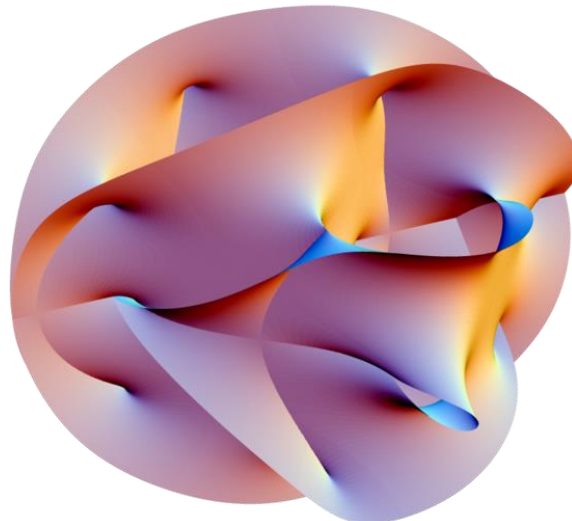
mass correlated by QCD to spontaneous symmetry breaking energy scale f_a



Axion Like Particles (ALPs)

Many other pNGBs:

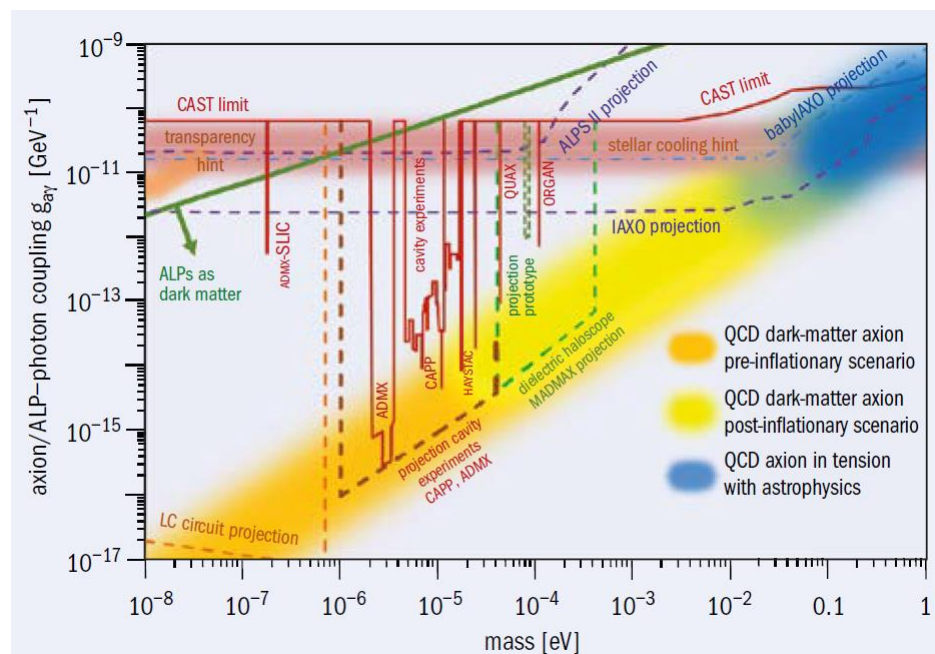
- The **Axiverse** from string theory arising from compactification of dimensions (Calabi-Yau manifold of extra dimensions)!
- No correlation between energy scale of spontaneous symmetry breaking and mass, but coupling to photon suppressed by energy scale of spontaneous symmetry breaking
- Same mechanism of ALP photon mixing and Primakoff effect!
- Axion searches also good for ALP searches

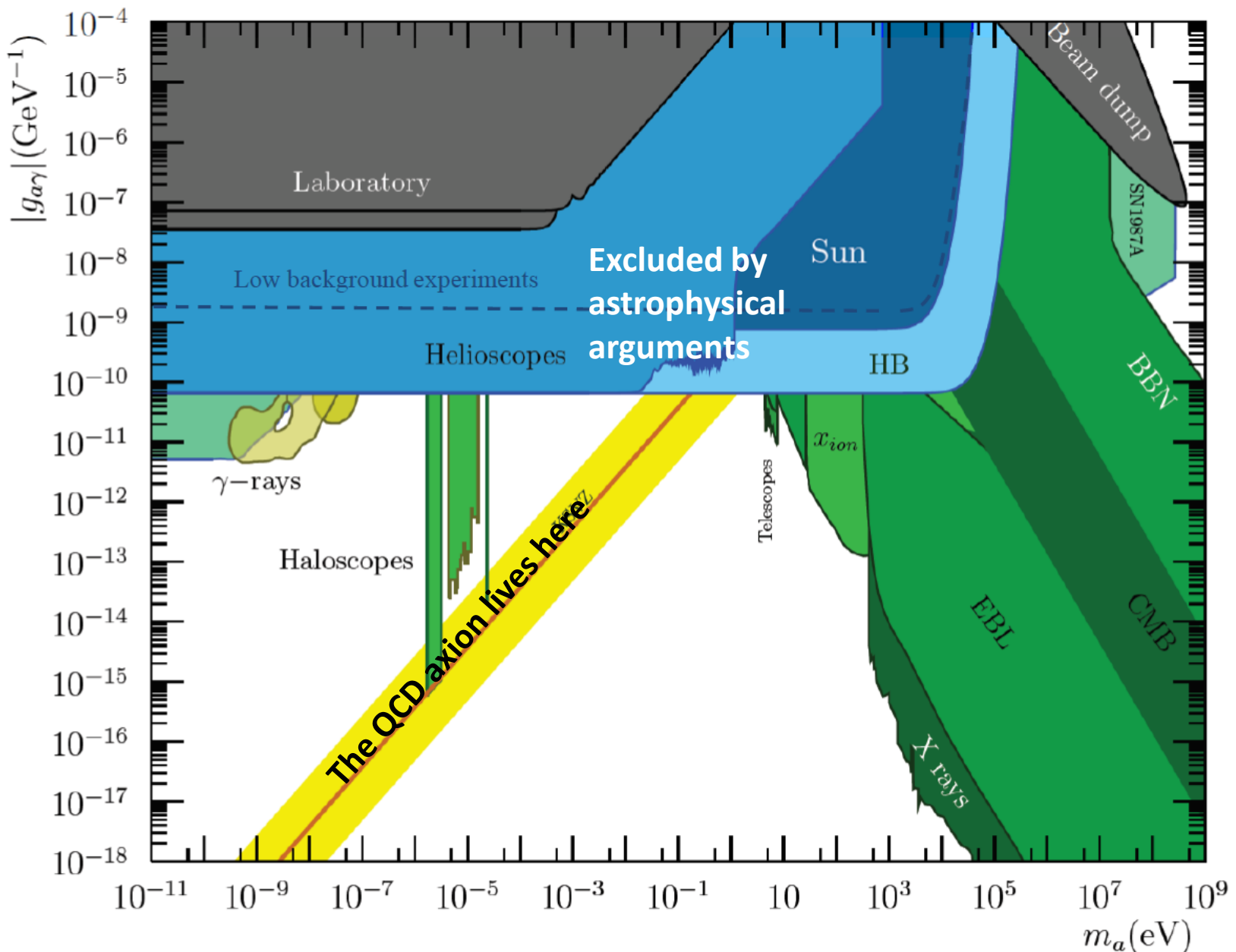


Dark Matter Axion and ALPs

How to detect them?

- Axion couplings and sources
- Cavity experiments
- Dielectric haloscopes
- LC circuits
- NMR experiments
- Solar axion search
- Light shining through the wall
- Some astrophysical constraint



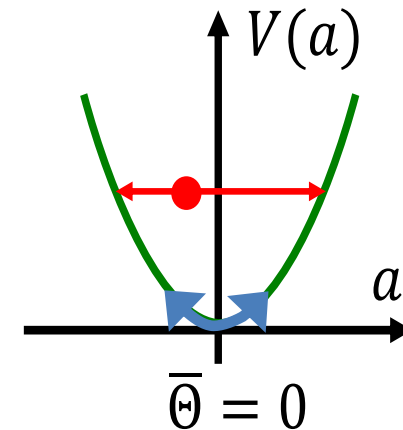
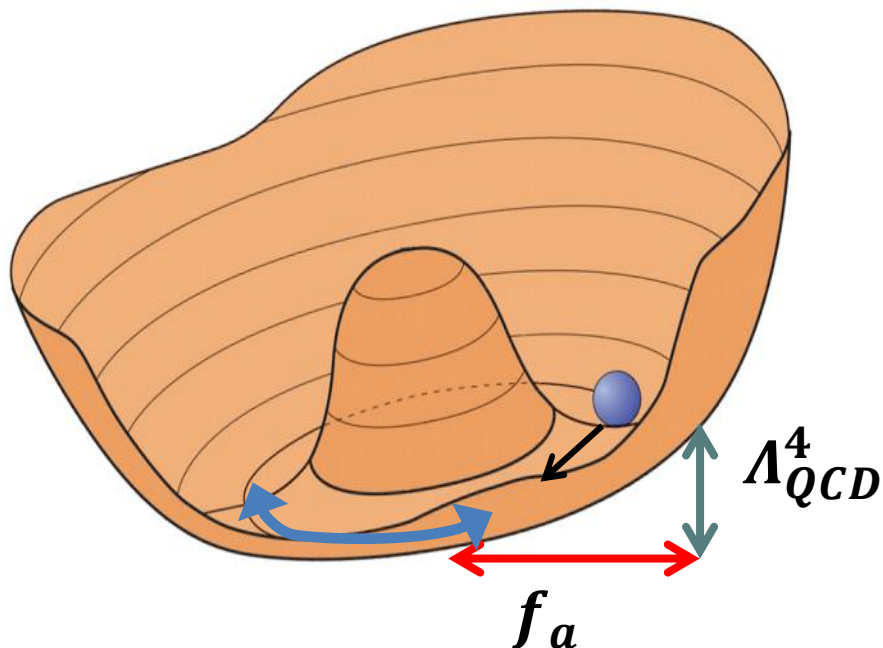


Axion production in the early universe

Axions are produced as **NON-THERMAL** local field oscillations,

→ particle population without initial momentum → **NON RELATIVISTIC!**
 → Production by misalignment as relic-oscillation of $\bar{\Theta}_i$

$$\langle v_{DM} \rangle = 10^{-3}c$$



Axion as massive pseudo Nambu-Goldstone-Boson

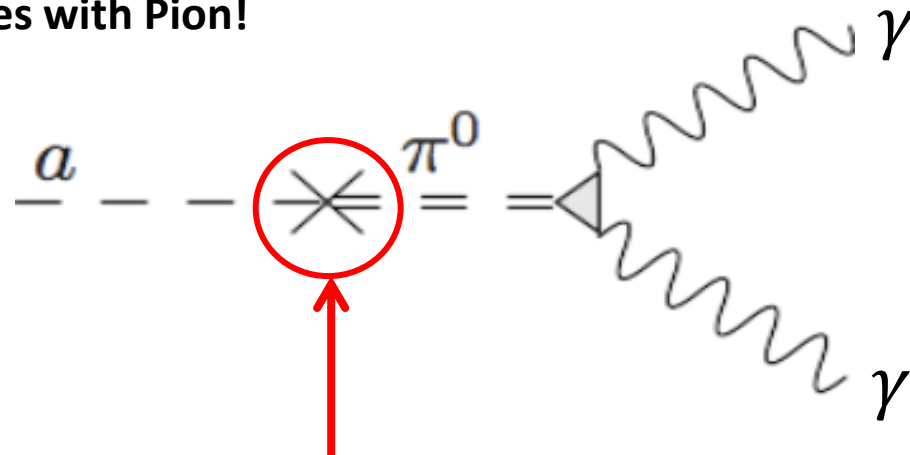
→ generation of mass by chiral symmetry breaking
 (mass: second derivative of potential at minimum)

$$m_a = 5.7 \mu eV \left(\frac{10^{12}}{f_a} \right) \quad \text{Correlated to } f_a \text{ by QCD}$$

Chiral symmetry breaking is process giving π^0 its mass!

→ Mass generation by “mixing with mesons!”

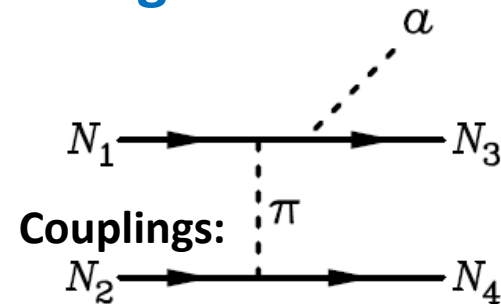
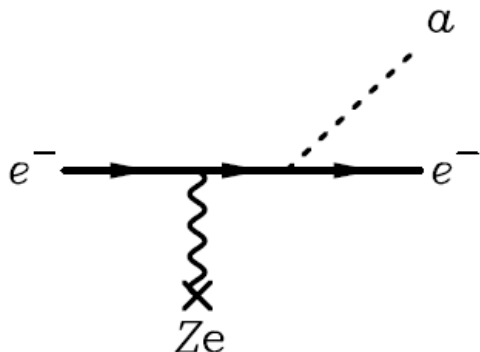
→ Axion mixes with Pion!



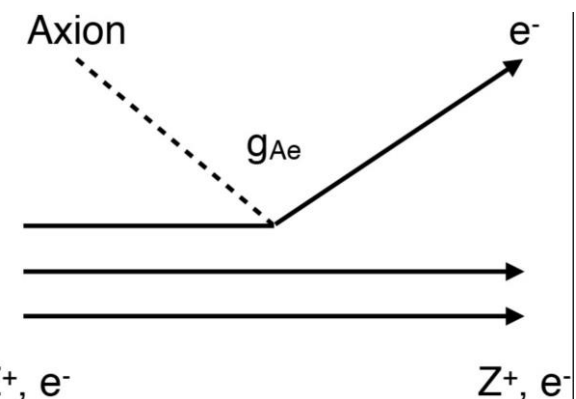
Coupling to Photons: $g_{a\gamma\gamma} \propto 1/f_a$

Other axion couplings $\propto 1/f_a$:

Axion Bremsstrahlung



Axioelectrif effect



Oscillating EDM

$$d_n = \bar{\theta} \cdot 10^{-16} e \text{ cm}$$

$\rightarrow \frac{\partial \bar{\theta}}{\partial t}$ leads to \dot{d}_n

\rightarrow Spin coupling $\propto \sigma \cdot E$

Axion Photon mixing

In general: Presence of axion field modifies Maxwell’s equations:

$$\nabla \cdot \mathbf{E} = \rho - g_{a\gamma} \mathbf{B} \cdot \nabla a ,$$

$$\nabla \times \mathbf{B} - \dot{\mathbf{E}} = \mathbf{J} + g_{a\gamma} (\mathbf{B} \dot{a} - \mathbf{E} \times \nabla a) ,$$

$$\nabla \cdot \mathbf{B} = 0 ,$$

$$\nabla \times \mathbf{E} + \dot{\mathbf{B}} = 0 ,$$

$$\ddot{a} - \nabla^2 a + m_a^2 a = g_{a\gamma} \mathbf{E} \cdot \mathbf{B} .$$

\dot{a} : Oscillation of axion field

∇a : Gradient in axion field

→ \dot{a} : **Sources E – field oscillation!**

Primakoff Effect:



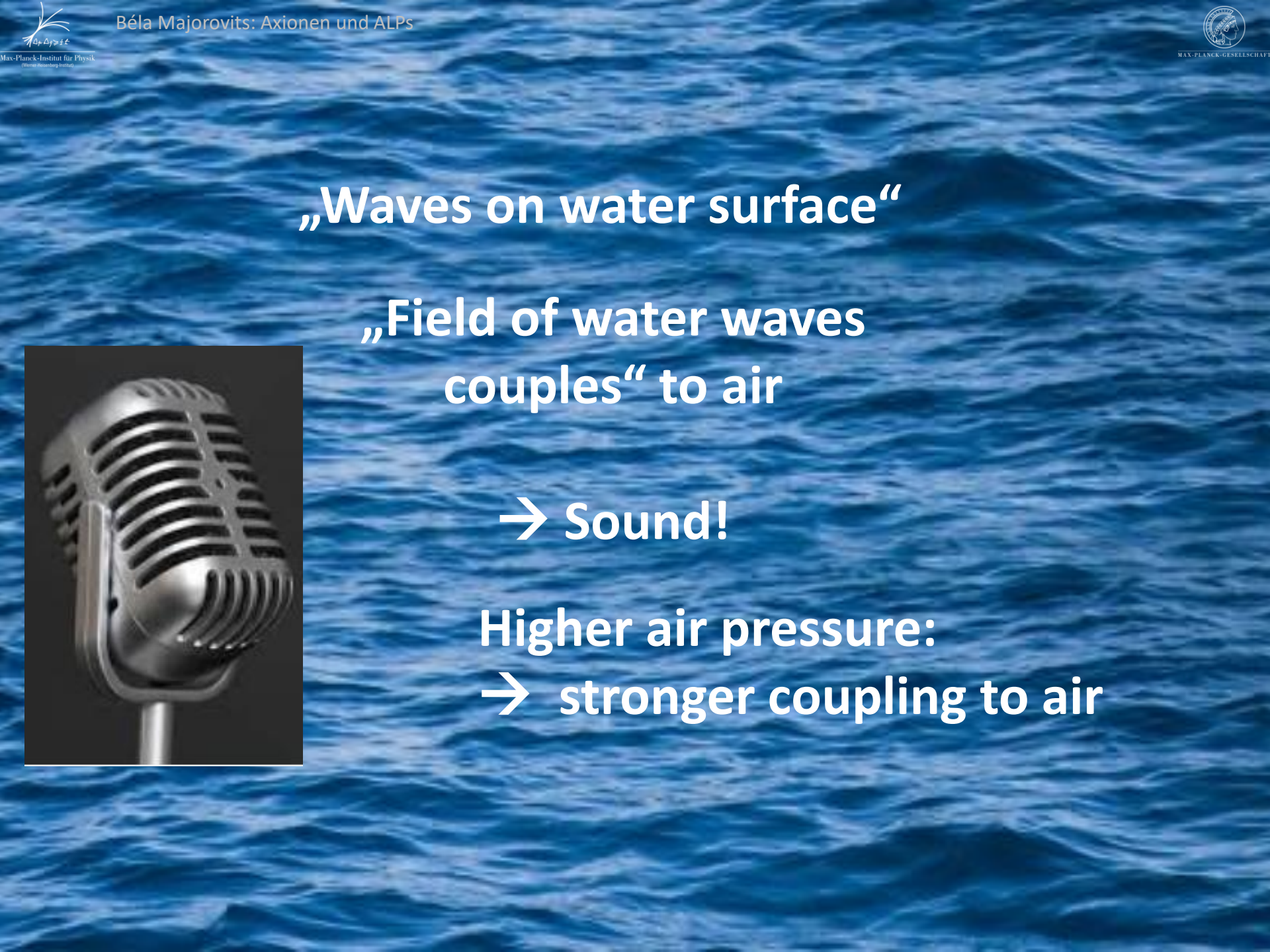
Real photon

$$E = mc^2 = h\nu$$

$$C_{a\gamma} \propto g_{a\gamma} \cdot f_a$$

B-Field

$$\mathcal{L}_{a\gamma} = \frac{\alpha}{2\pi} C_{a\gamma} \frac{a(t)}{f_a} E \cdot B$$



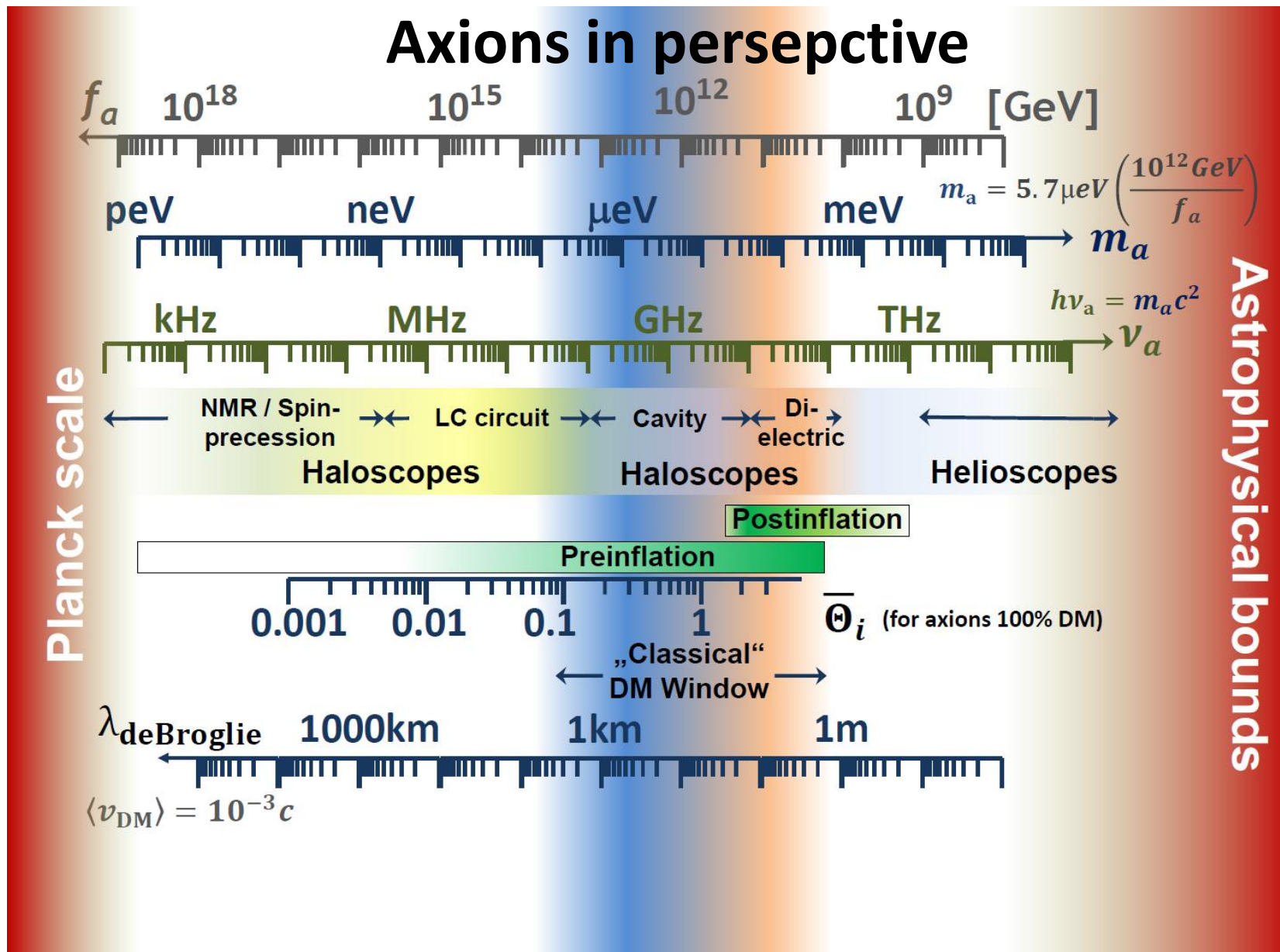
„Waves on water surface“

„Field of water waves
couples“ to air



→ Sound!

Higher air pressure:
→ stronger coupling to air



Axion and ALPs experiments: categorization in source of axions

DM axions: Haloscopes

Detect axions from galactic DM Halo

Model dependence:

- Assume axions make up DM (100%)
- Halo density distribution
- Velocity distribution

Solar axions: Helioscopes

Production of axions/ALPs in the sun:

Inverse Primakoff effect → thermal distribution depends on solar modeling

Production in lab: Laboratory experiments

Use photon sources (lasers) to measure effects

Axion "size":

Local DM velocity distribution

$$\langle v_{DM} \rangle = 10^{-3}c$$

De Broglie wavelength:

$$\lambda_{deBroglie} = \frac{h}{p}$$

$$\begin{aligned}\lambda_{deBroglie} &= \frac{h}{p} \sim \frac{h}{m_a \langle v_{DM} \rangle} \sim \frac{h}{\frac{h v_a}{c^2} 10^{-3} c} \\ &= 10^3 \frac{c}{v_a} = \frac{3 \cdot 10^{11} m/s}{v_a} = \\ &300 m \cdot \left(\frac{1 \text{ GHz}}{v_a} \right) \sim 75 m \cdot \left(\frac{\mu eV/c^2}{m_a} \right)\end{aligned}$$

→ Experiment fits into particle!

Axion-experiment "coherence time":

Local DM velocity distribution

$$\langle v_{DM} \rangle = 10^{-3}c$$

axion mass vs. frequency

$$m_a = \frac{h\nu_a}{c^2}$$

Interaction time of axions for experiment determined by $\lambda_{deBroglie}$:

$$dt \sim \frac{\lambda_{deBroglie}}{\langle v_{DM} \rangle} \sim \frac{300 \text{ m}}{10^{-3}c} \cdot \left(\frac{1 \text{ GHz}}{\nu_a} \right) = 10^{-3} \text{ s} \cdot \left(\frac{1 \text{ GHz}}{\nu_a} \right)$$

→ Number of oscillation phases during propagation through experiment:

$$dt \cdot \nu_a \sim 10^6$$

→ Many oscillations periods during transition

Axion local DM number density:

Local DM density

$$\rho_{DM} \sim 0.3 \frac{GeV/c^2}{cm^3}$$

$$\begin{aligned} N_a &= \frac{\rho_a}{m_a} = 0.3 \frac{(GeV/c^2)/m_a}{cm^3} \\ &= 0.3 \frac{(GeV/c^2)/(\mu eV/c^2)}{cm^3} \left(\frac{1\mu eV/c^2}{m_a} \right) \\ &= \frac{3 \cdot 10^{14}}{cm^3} \left(\frac{\mu eV/c^2}{m_a} \right) \\ &= 3 \cdot 10^{14} \left(\frac{\mu eV/c^2}{m_a} \right) \frac{4 \cdot 10^{12}}{\lambda_{deBroglie}^3} \left(\frac{\mu eV/c^2}{m_a} \right)^3 \sim \frac{10^{27}}{\lambda_{deBroglie}^3} \left(\frac{\mu eV/c^2}{m_a} \right)^4 \end{aligned}$$

De Broglie wavelength:

$$\lambda_{deBroglie} \sim 7500 \text{ cm} \cdot \left(\frac{\mu eV/c^2}{m_a} \right)$$

$$\lambda_{deBroglie}^3 \sim 4 \cdot 10^{12} \text{ cm}^3 \cdot \left(\frac{\mu eV/c^2}{m_a} \right)^3$$

$$1 \text{ cm}^3 \sim 2.5 \cdot 10^{-13} \lambda_{deBroglie}^3 \cdot \left(\frac{m_a}{\mu eV/c^2} \right)^3$$

→ Highly degenerate Bose-Einstein condensate!

Axion-Photon Coupling: Oscillations of E-Field!



→ Use of
resonance effects!

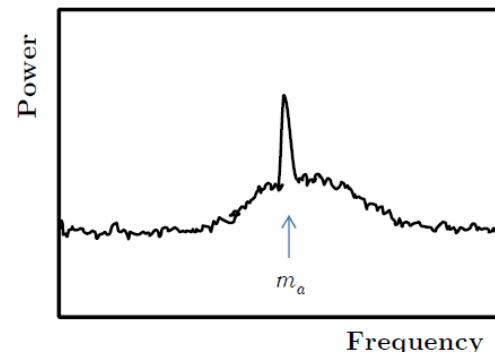
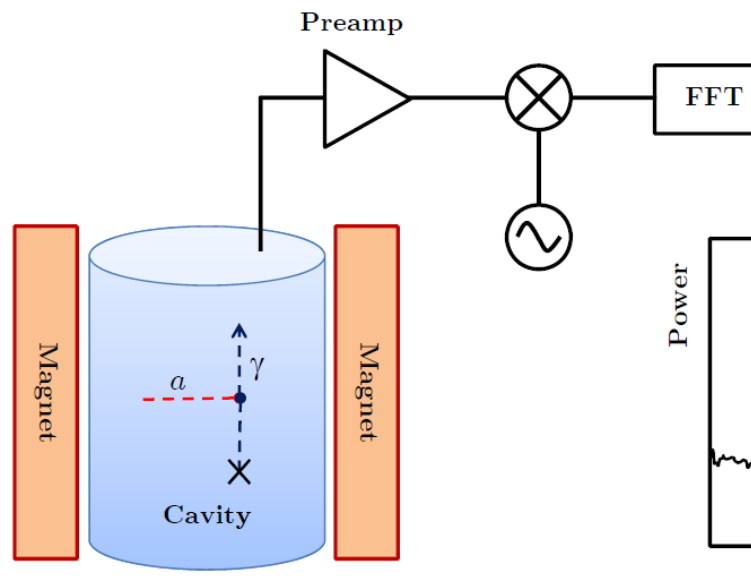
Cavity HALOSCOPES

High Q-factor cavities in strong B-field:

- Coherent E-field oscillation
- If at resonant frequency: cavity is “pumped”
- Power can be detected

$$Q = \frac{\text{Energy in cavity}}{\text{Energy dissipated in walls}}$$

$$Q_L = \frac{\text{center frequency}}{\text{frequency bandwidth}}$$



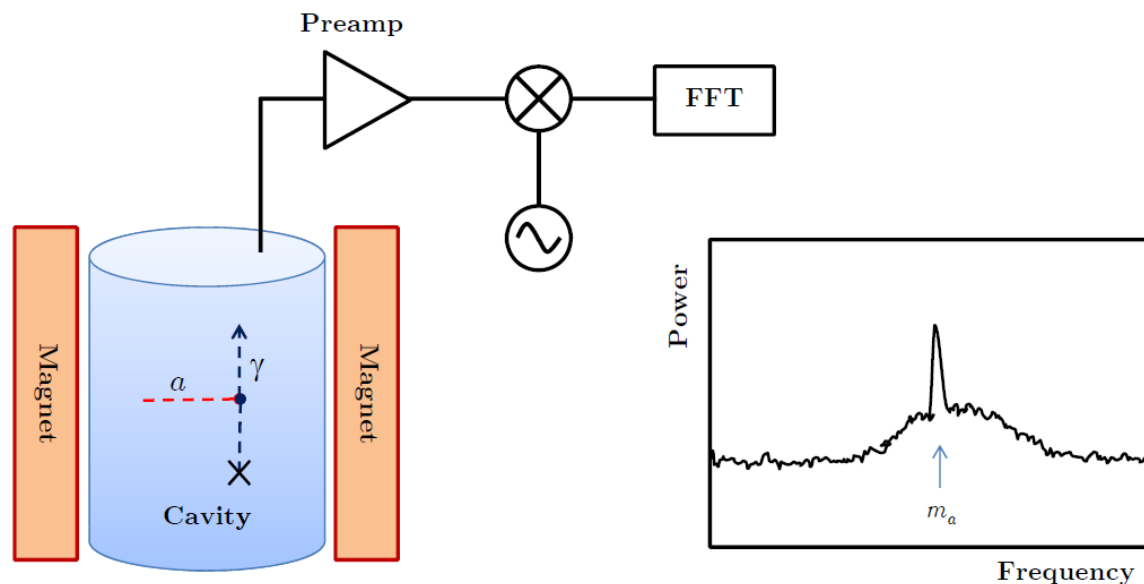
Cavity HALOSCOPES

Total power expected from resonant DM axion to photon conversion:

$$P_{sig} = g_{a\gamma}^2 \left(\frac{\rho_a}{m_a} \right) B^2 V Q_L C$$

$$C = \frac{\left| \int_V d^3x \overrightarrow{E(\nu)} \cdot \vec{B} \right|^2}{\int_V d^3x \epsilon |E(\nu)|^2}$$

V : Volume of cavity, Q_L : Loaded Quality factor of cavity (if axion signal width narrower), C : Overlap integral of B-field with axion induced E-field of mode

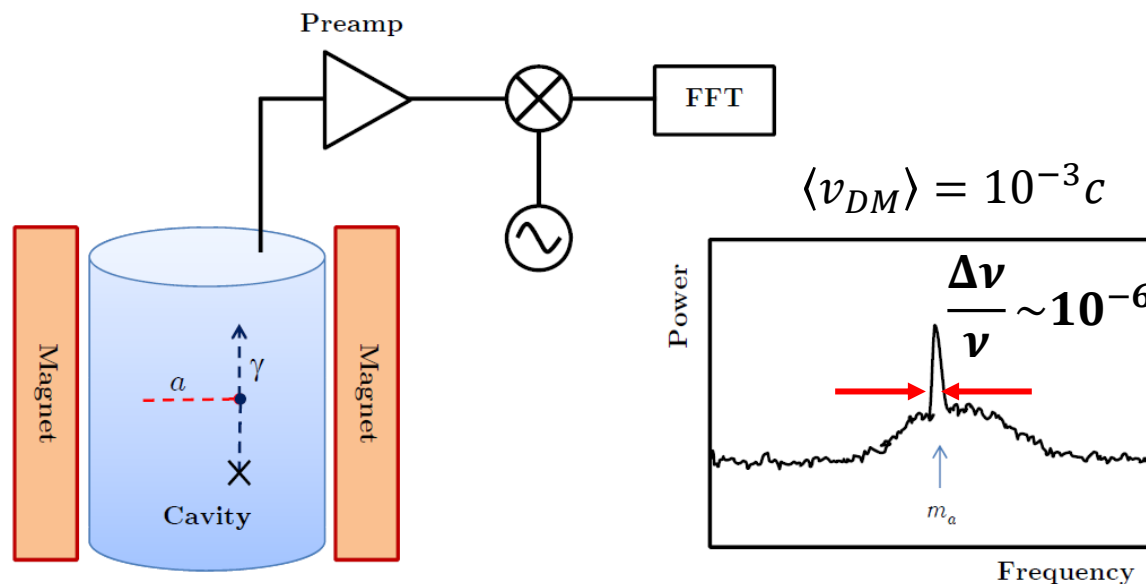


Cavity HALOSCOPES

Total power expected from resonant DM axion to photon conversion:

$$P_{sig} = 7 \cdot 10^{-23} W \left(\frac{\mu eV/c^2}{m_a} \right) \left(\frac{B}{8T} \right)^2 \left(\frac{V}{200l} \right) \left(\frac{Q_L}{10^5} \right) \left(\frac{C}{0.35} \right)$$

V : Volume of cavity, Q_L : Loaded Quality factor of cavity (if axion signal width narrower), C : Overlap integral of B-field with axion induced E-field of mode



Cavity HALOSCOPES

Sensitivity of experiment: Use "Dicke's radiometer equation":

$$\frac{S}{N} = \frac{P_{sig}}{k_b T_{sys}} \sqrt{\frac{t_{scan}}{\Delta\nu}}$$

$P_{sens} \sim 10^{23} W$

roughly 5σ

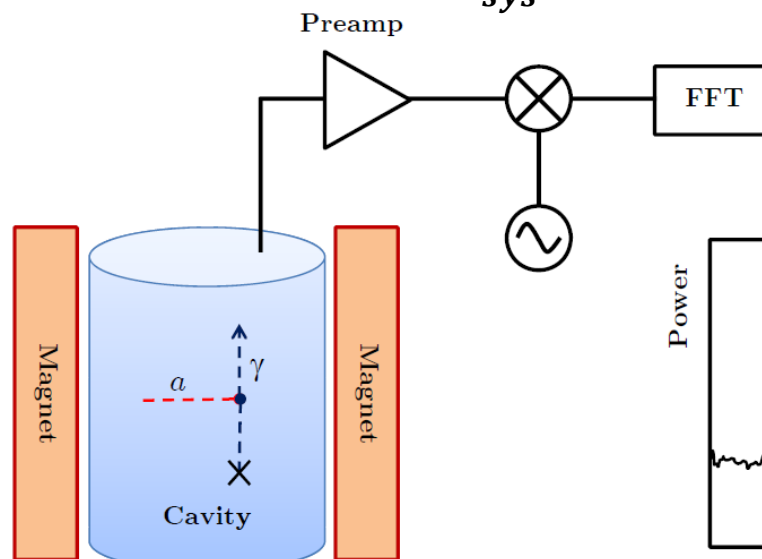
$$\frac{S}{N} \sim 5$$

Dilution fridge +
noise temp receiver

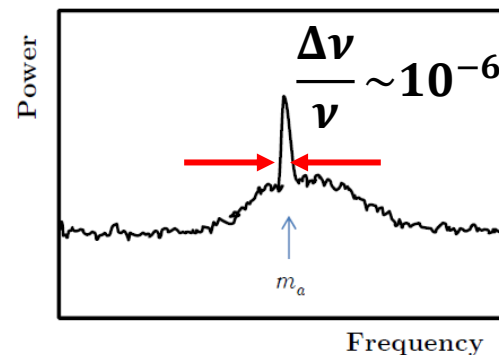
$$T_{sys} \sim 0.2 K$$

Many individual
measurements!

$$t_{scan} \sim 100 \text{ sec}$$



$$\langle v_{DM} \rangle = 10^{-3} c$$



Cavity HALOSCOPES

Sensitivity of experiment: Use "Dicke's radiometer equation":

Scan rate:

$$\frac{dm_a}{dt} \sim 0.4 \text{ } \mu\text{eV/yr} \left(\frac{B}{8T} \right)^4 \left(\frac{V}{136l} \right)^2 \left(\frac{Q_L}{3 \cdot 10^4} \right)^2 \left(\frac{0.2 \text{ K}}{T_{sys}} \right)^2 \left(\frac{m_a}{3 \mu\text{eV}} \right)^2$$

roughly 5σ

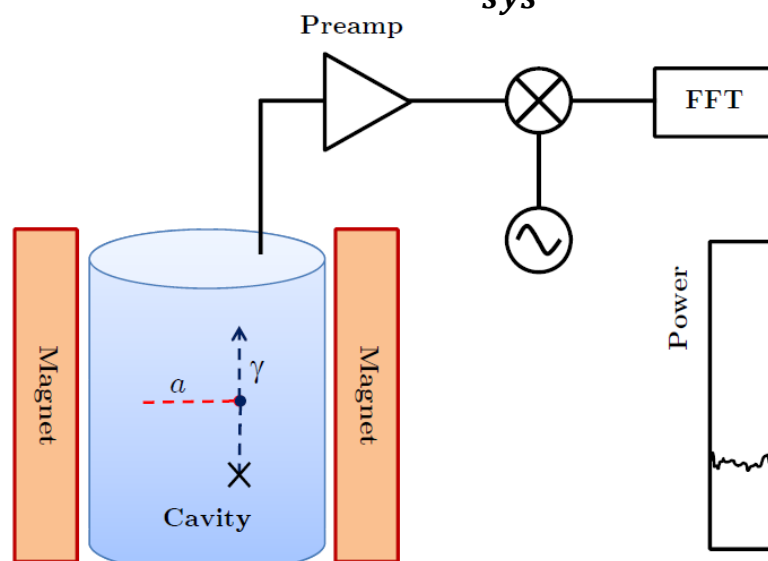
$$\frac{S}{N} \sim 5$$

Dilution fridge +
noise temp receiver

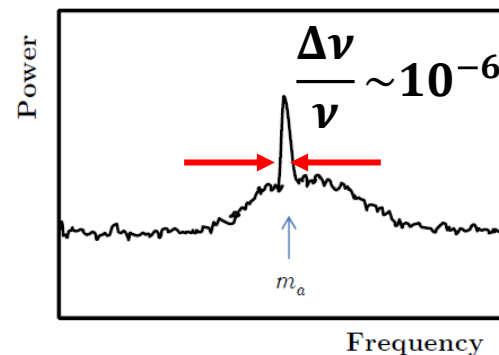
$$T_{sys} \sim 0.2 \text{ K}$$

Many individual
measurements!

$$t_{scan} \sim 100 \text{ sec}$$



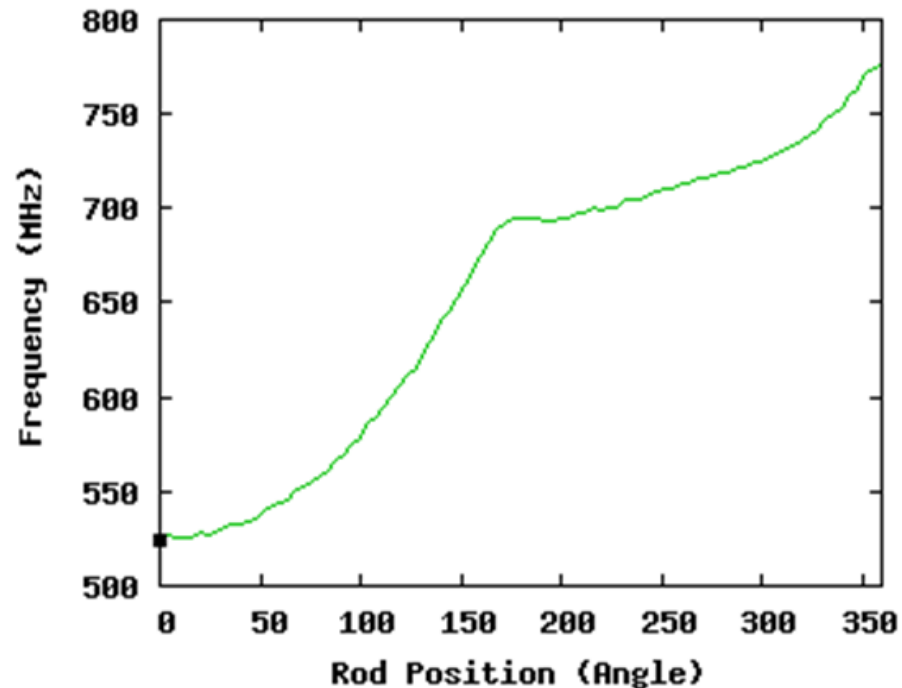
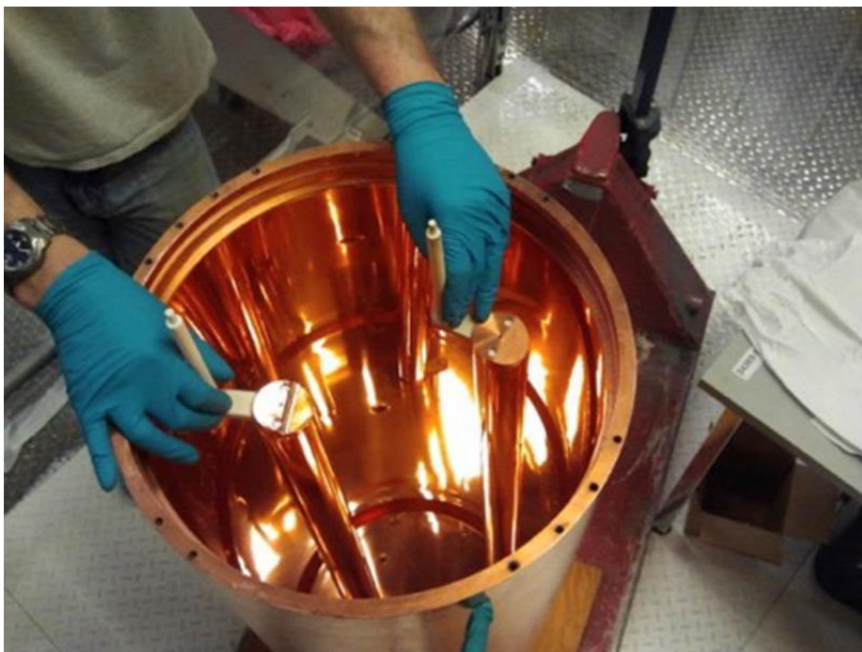
$$\langle v_{DM} \rangle = 10^{-3} c$$



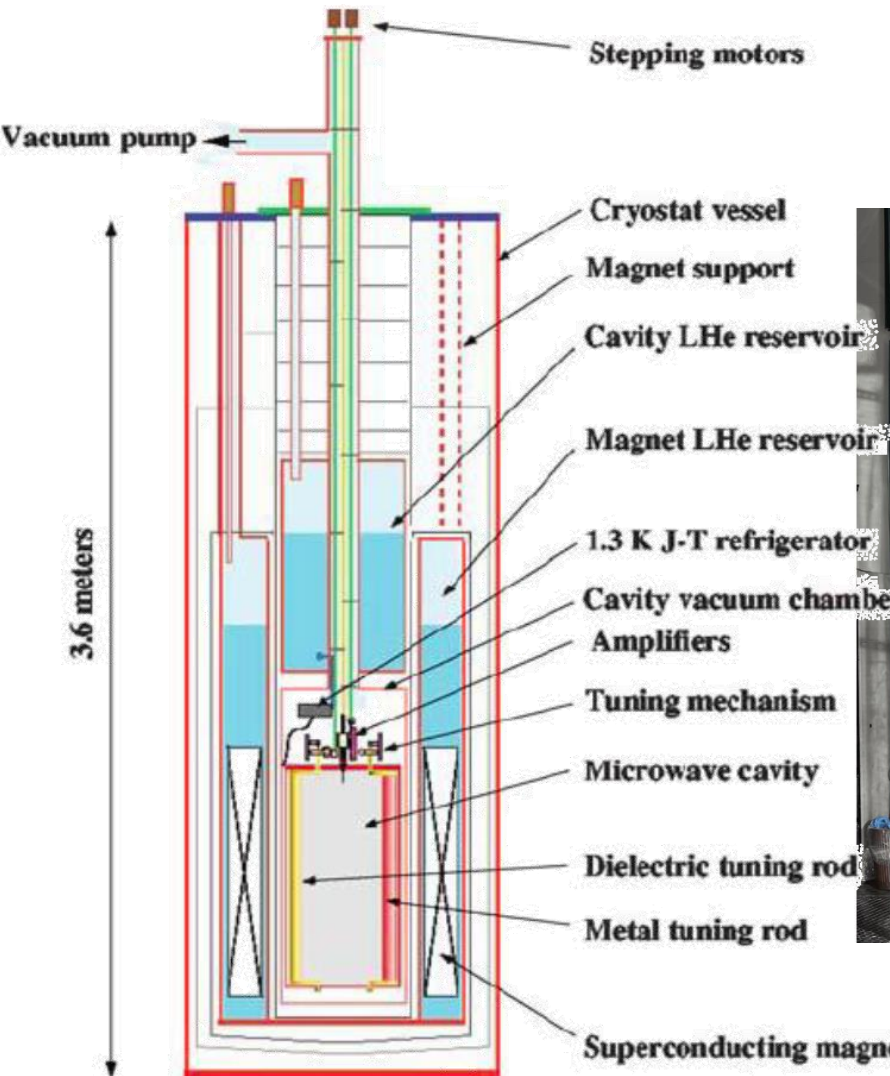
Cavity HALOSCOPE: ADMX

Scan mass range: need to tune

- Use dielectric low loss tuning rod
- Change resonance frequency of cavity



Cavity HALOSCOPE: ADMX

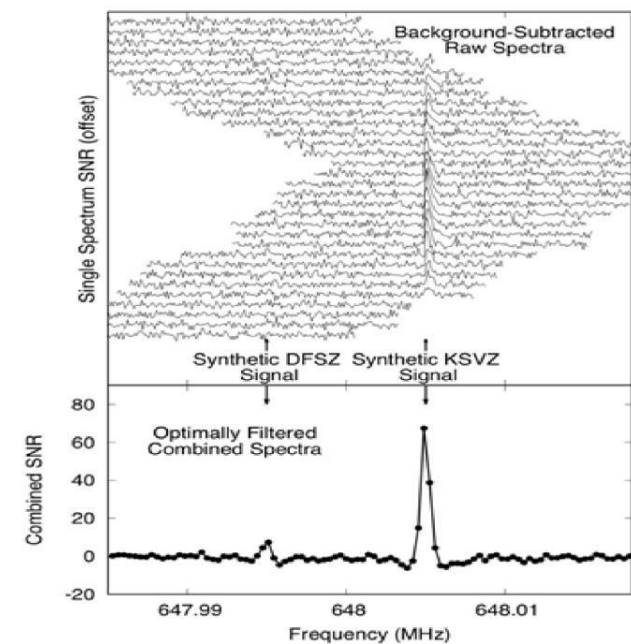


Sensitivity range: 0.5 – 2.5 GHz → ~2 – 10 μeV

Axions and ALPs: where do they come from, how to detect them?

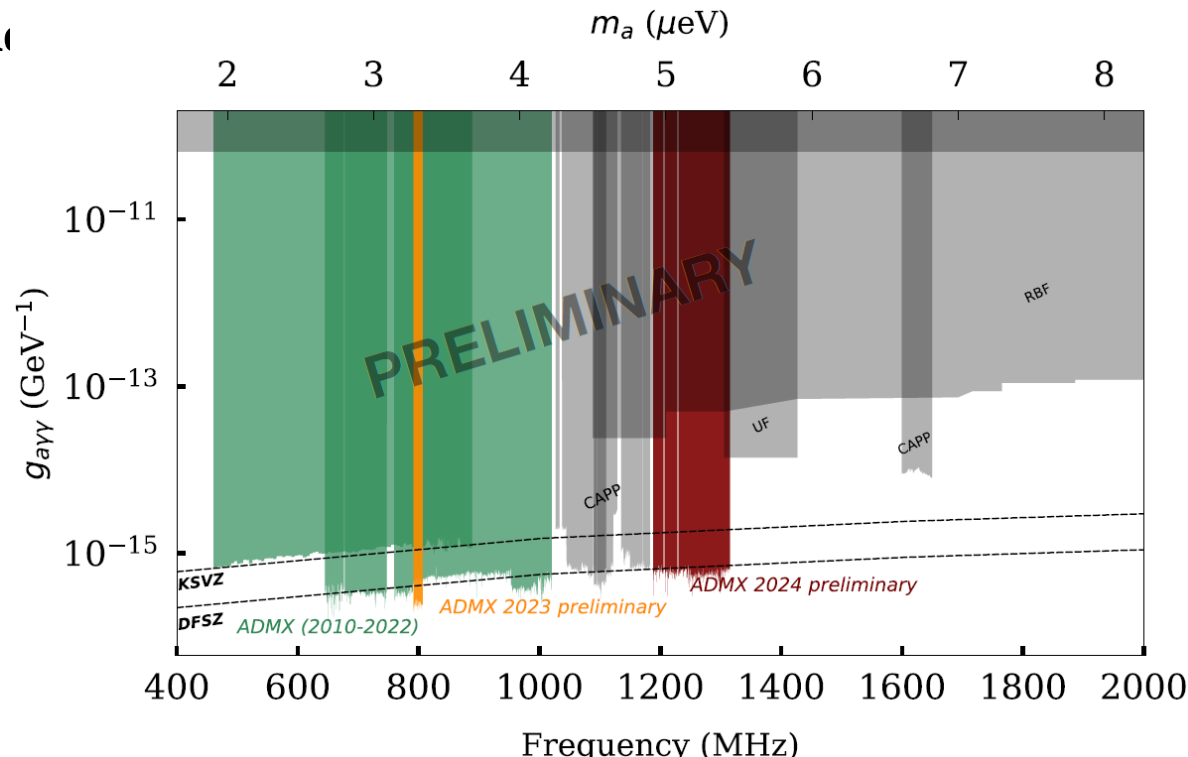
Cavity HALOSCOPE: ADMX

individual ~ 100s measurements
With different tuning rod positions



individual measurements
With different tuning rod positions

No excess signal found

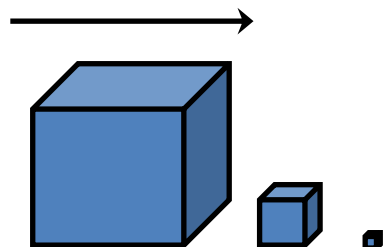


arXiv:2408.15227

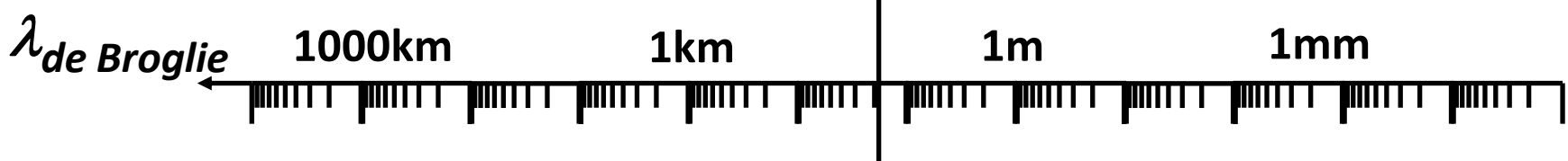
Scan rate:

$$\frac{dm_a}{dt} \sim 0.4 \text{ } \mu\text{eV/yr} \left(\frac{B}{8T} \right)^4 \left(\frac{V}{136l} \right)^2 \left(\frac{Q_L}{3 \cdot 10^4} \right)^2 \left(\frac{0.2 K}{T_{sys}} \right)^2 \left(\frac{m_a}{3 \mu\text{eV}} \right)^2$$

Volume of cavities & Q_L decrease with wavelength



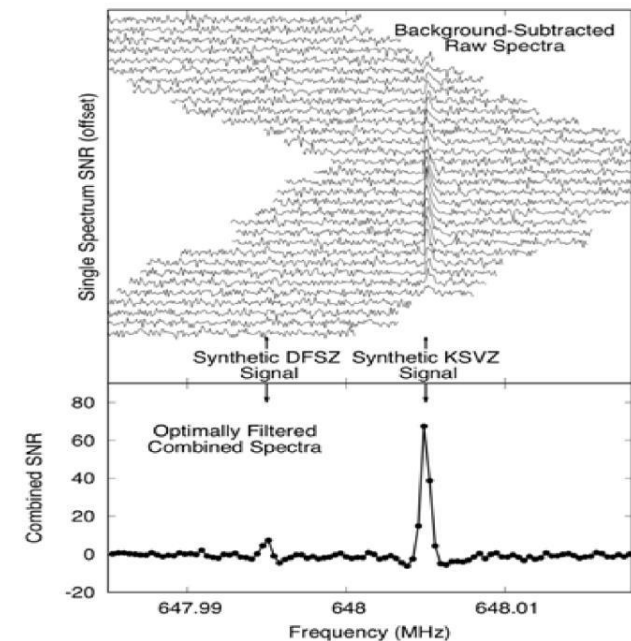
Alternative Approaches:
Couples cavities
Dish Antenna
Dielectric Haloscope



$$P_{sig} \propto B^2 V Q_{cav}$$

Cavity HALOSCOPE: ADMX

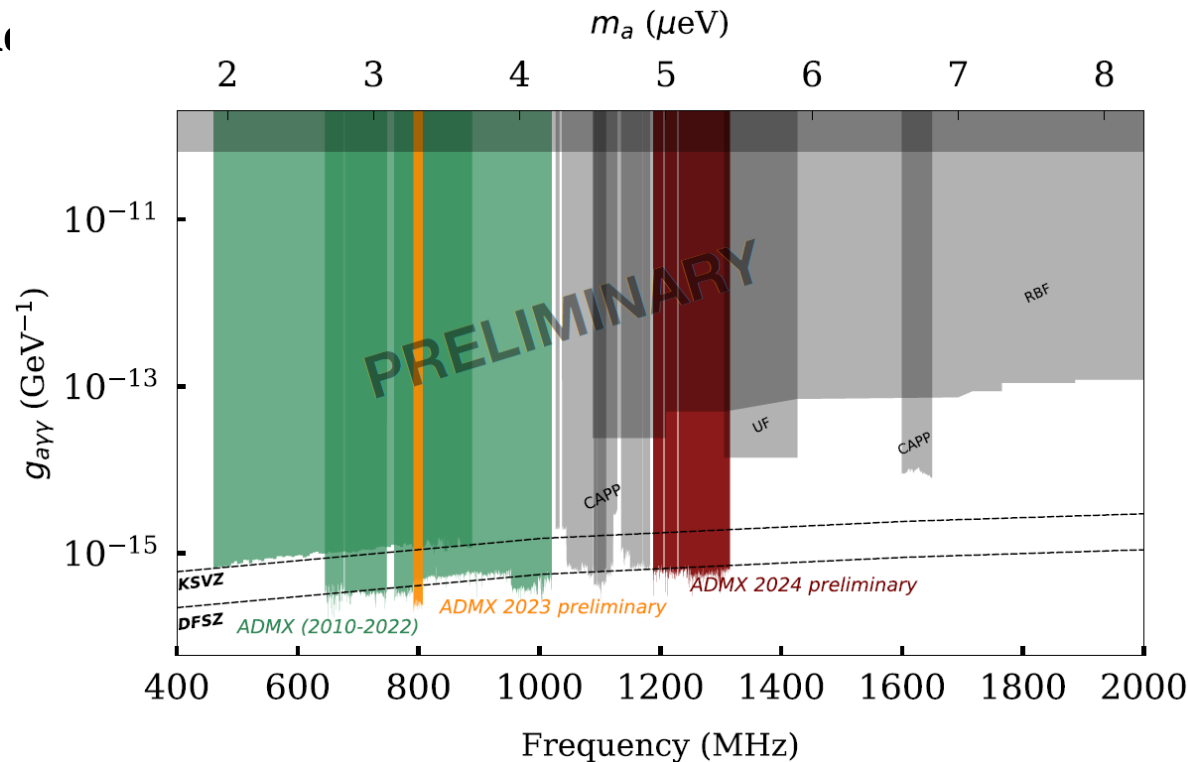
individual ~ 100s measurements
With different tuning rod positions



individual measurements
With different tuning rod positions

$$\frac{dm_a}{dt} \sim 0.4 \mu eV/yr \left(\frac{B}{8T} \right)^4 \left(\frac{V}{136l} \right)^2 \left(\frac{Q_L}{3 \cdot 10^4} \right)^2 \left(\frac{0.2 K}{T_{sys}} \right)^2 \left(\frac{m_a}{3 \mu eV} \right)^2$$

No excess signal found



arXiv:2408.15227

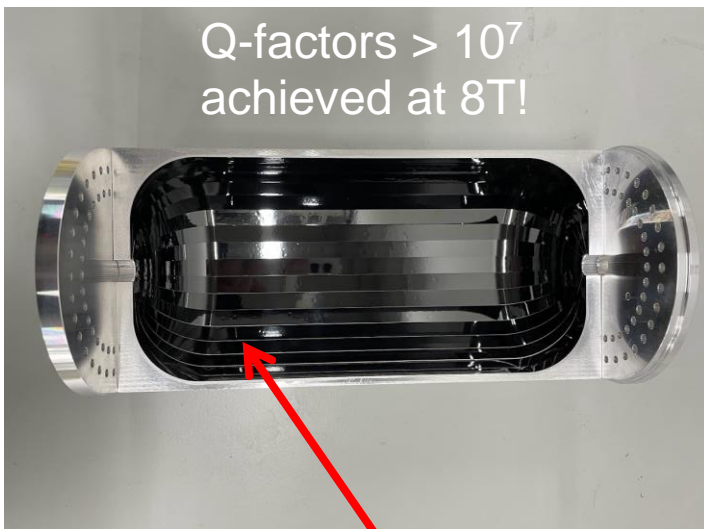
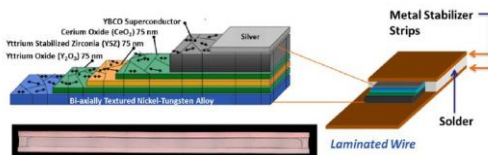
Scan rate:

Axions and ALPs: where do they come from, how to detect them?

Superconducting and dielectric cavities:

Increase of cavity Q-value:

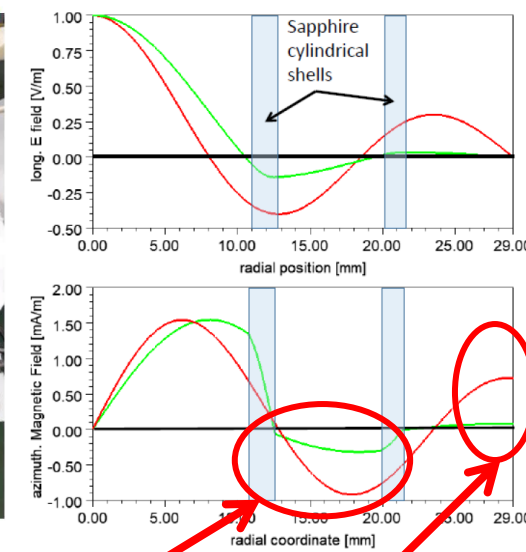
- Avoid high frequency losses:
use superconducting wall lining Problem: Superconductor $Tc(B)$
→ limits B –field → use HTS!
- Minimize field at cavity walls: Use (low-loss) dielectric cylinders



Coating with high T_c superconductor

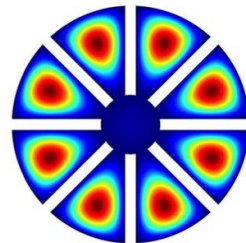
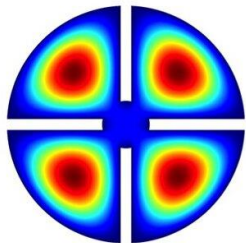
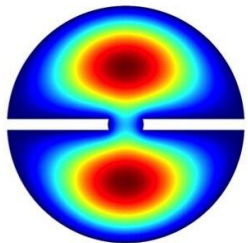


Negative field values
→ cancellation of coupling



High field values at walls → losses

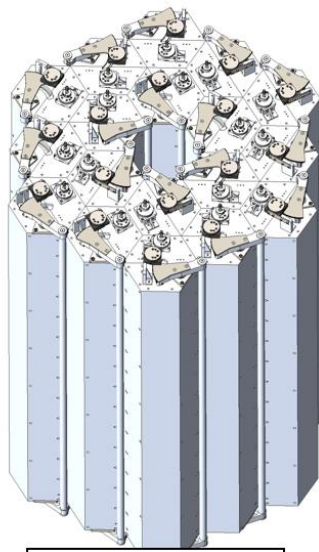
Superconducting and multiple cavities:



**Many small cavities
Mode matched**

PRL 125, 221302 (2020)

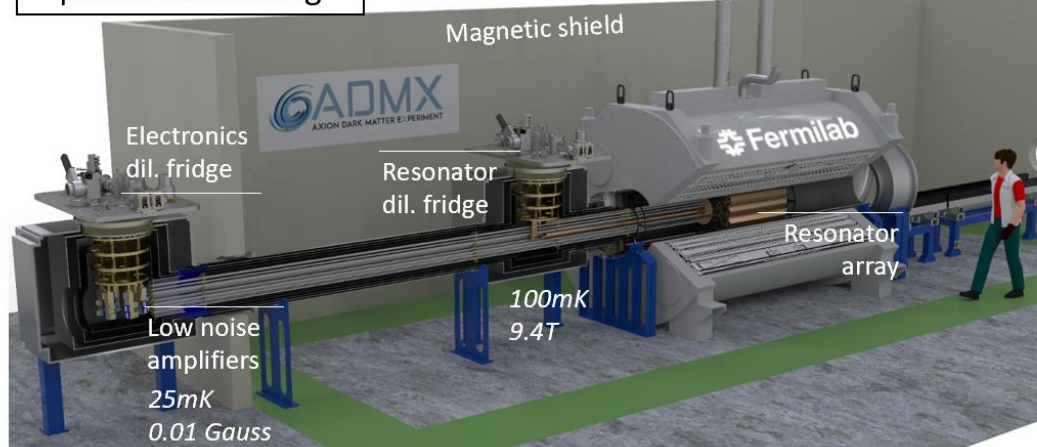
ADMX-EFR (Extended Frequency Range): 2 – 4 GHz (9 – 16 μ eV)



18 cavity array

digital power combining

horizontal magnet:
9.4 T, 258 L

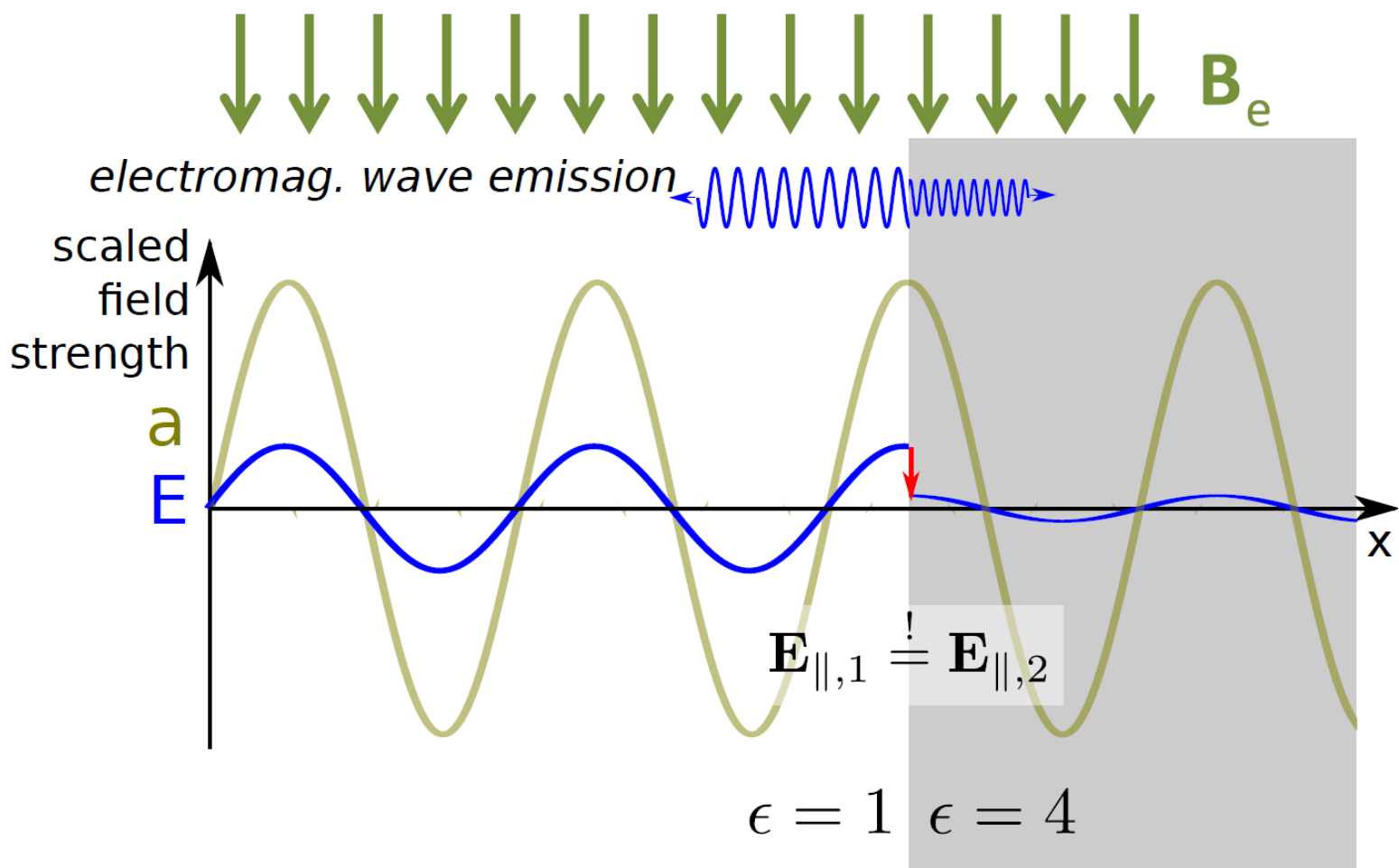


Goal: Search 2-4GHz @ DFSZ sensitivity in 3 years scan time

S. Knirck at Patras 2024 workshop

Axions and ALPs: where do they come from, how to detect them?

Effect of Dielectric discontinuity

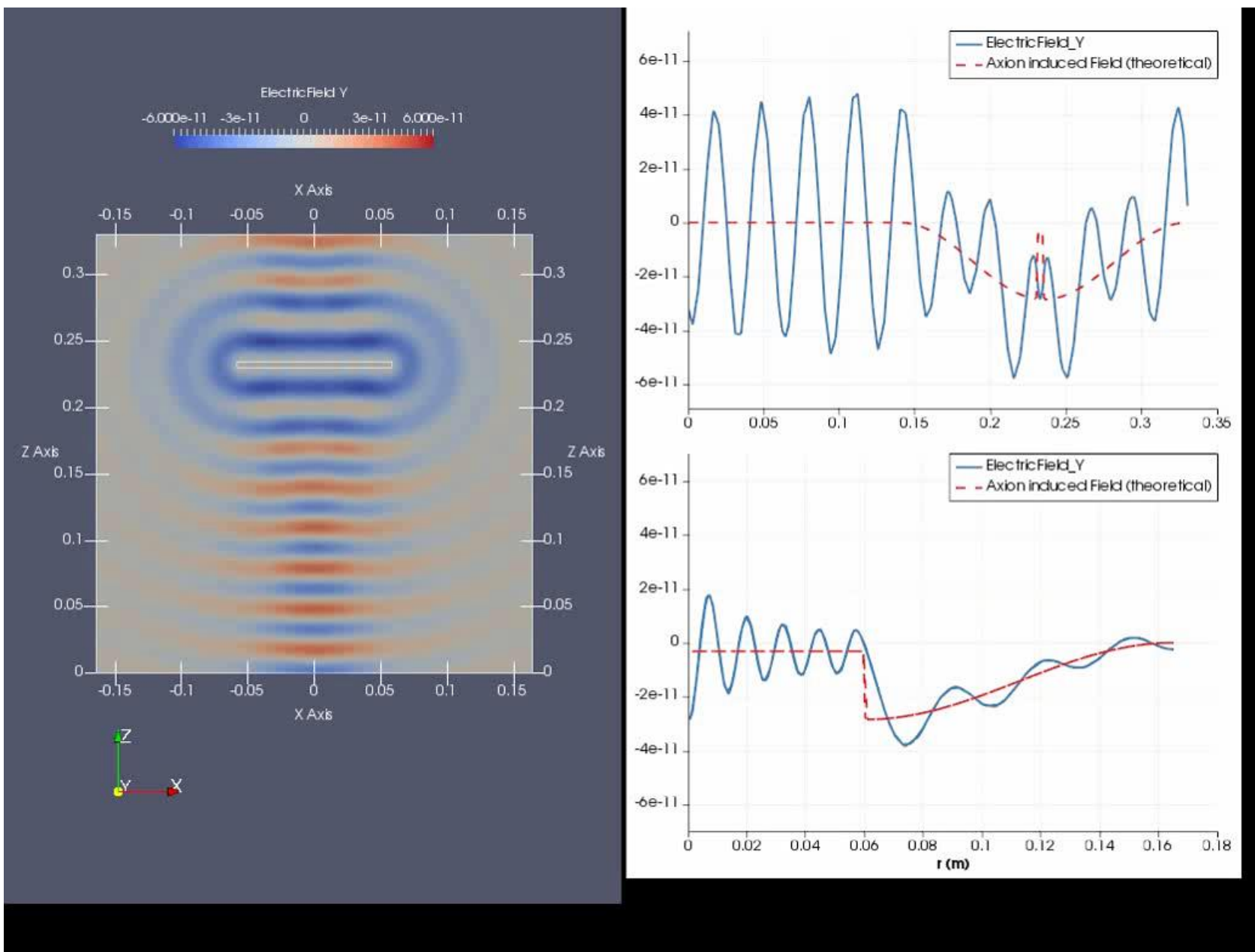


Discontinuity in ϵ

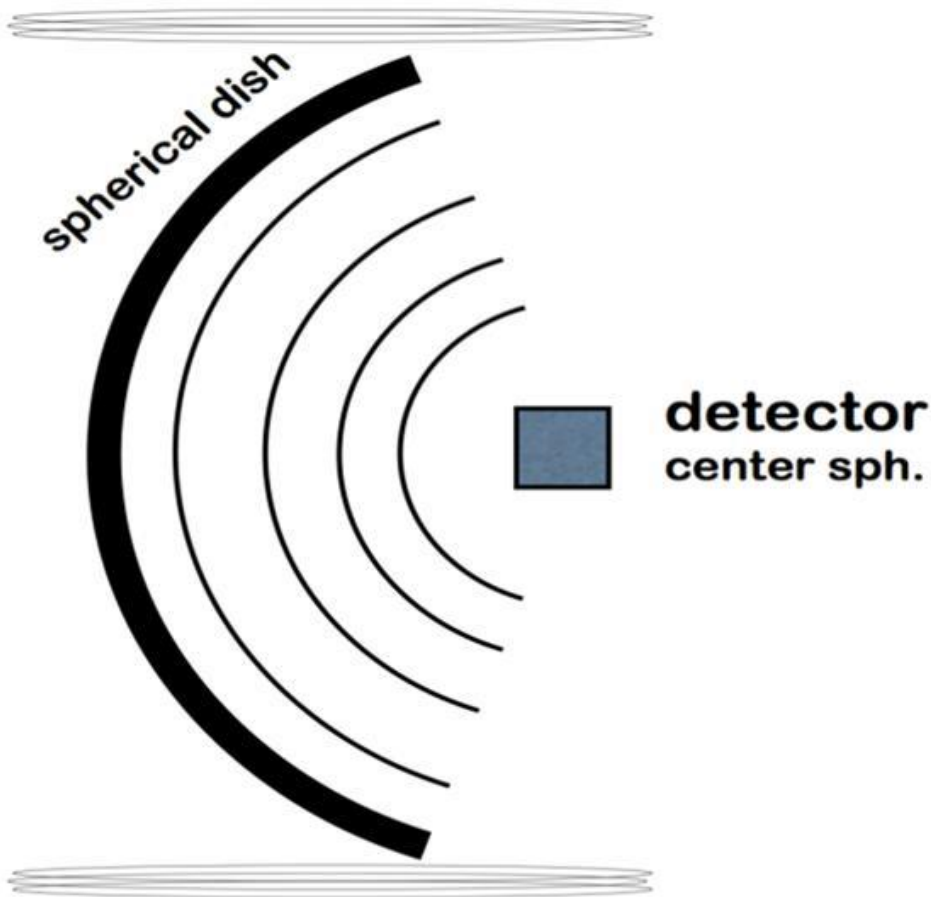
→ Emission of power Perpendicular to surface

$$\left(\frac{P}{A}\right)_{\text{mirror}} \sim 2 \cdot 10^{-27} \frac{W}{m^2} \left(\frac{B_{||}}{10 T}\right)^2 (g_{a\gamma\gamma} m_a)^2$$

Axions and ALPs: where do they come from, how to detect them?



Dish antenna



Broadband approach

Works independent of frequency (axion mass)!

$$P_{\text{sig}} \sim B^2 A$$

For axion search:

**Need large area and
Extremely sensitive detector
BRASS @ Uni Hamburg/DESY
BREAD @ Fermilab**

$$B=10 \text{ T}$$

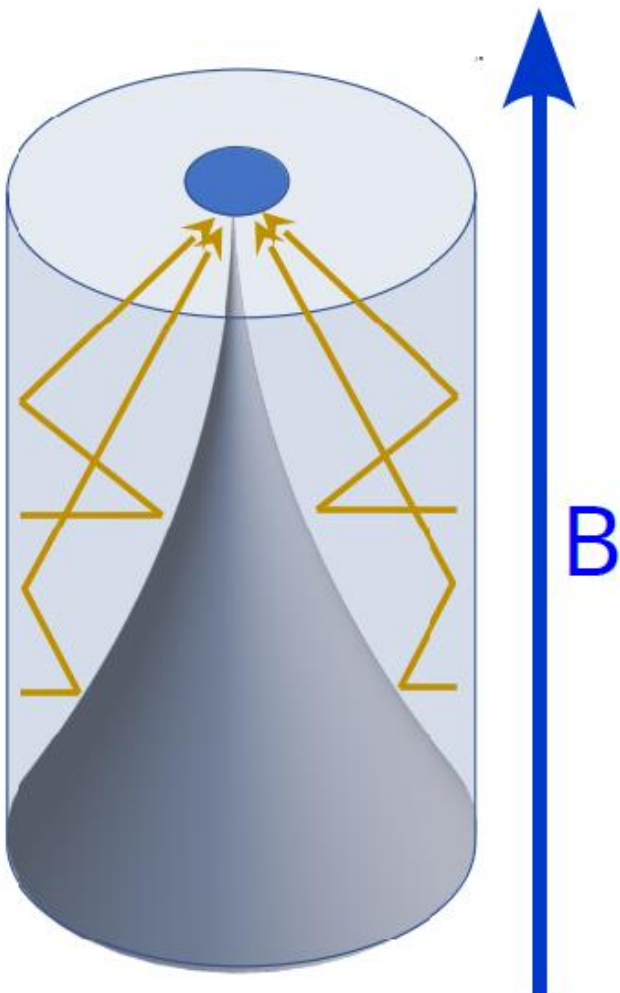
$$T_{\text{sys}} = 8 \text{ K}$$

$$P_{\text{sens}} = 10^{-23} \text{ W}$$

$$\rightarrow A = 1.000 \text{ m}^2$$

Dish antenna BREAD experiment

Broadband Reflector Experiment for Axion Detection



Use “lighthouse” geometry

Photon emission from cylinder walls
→ Fits into solenoid magnet

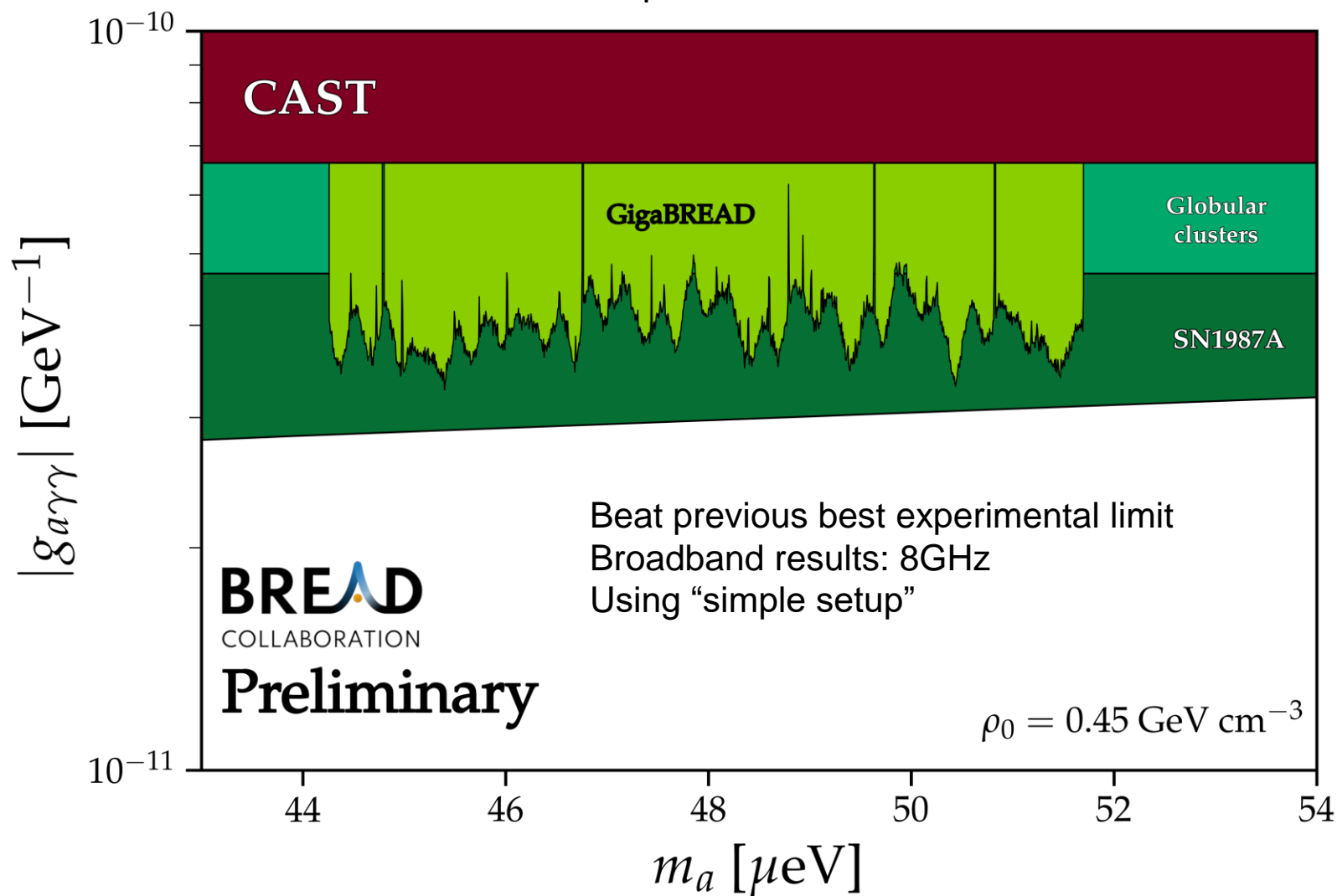


$$A=0.5 \text{ m}^2, B=3.9 \text{ T}, T_{\text{sys}}=400 \text{ to } 600 \text{ K}, t \sim 30 \text{ days}$$

Axions and ALPs: where do they come from, how to detect them?

Dish antenna BREAD experiment

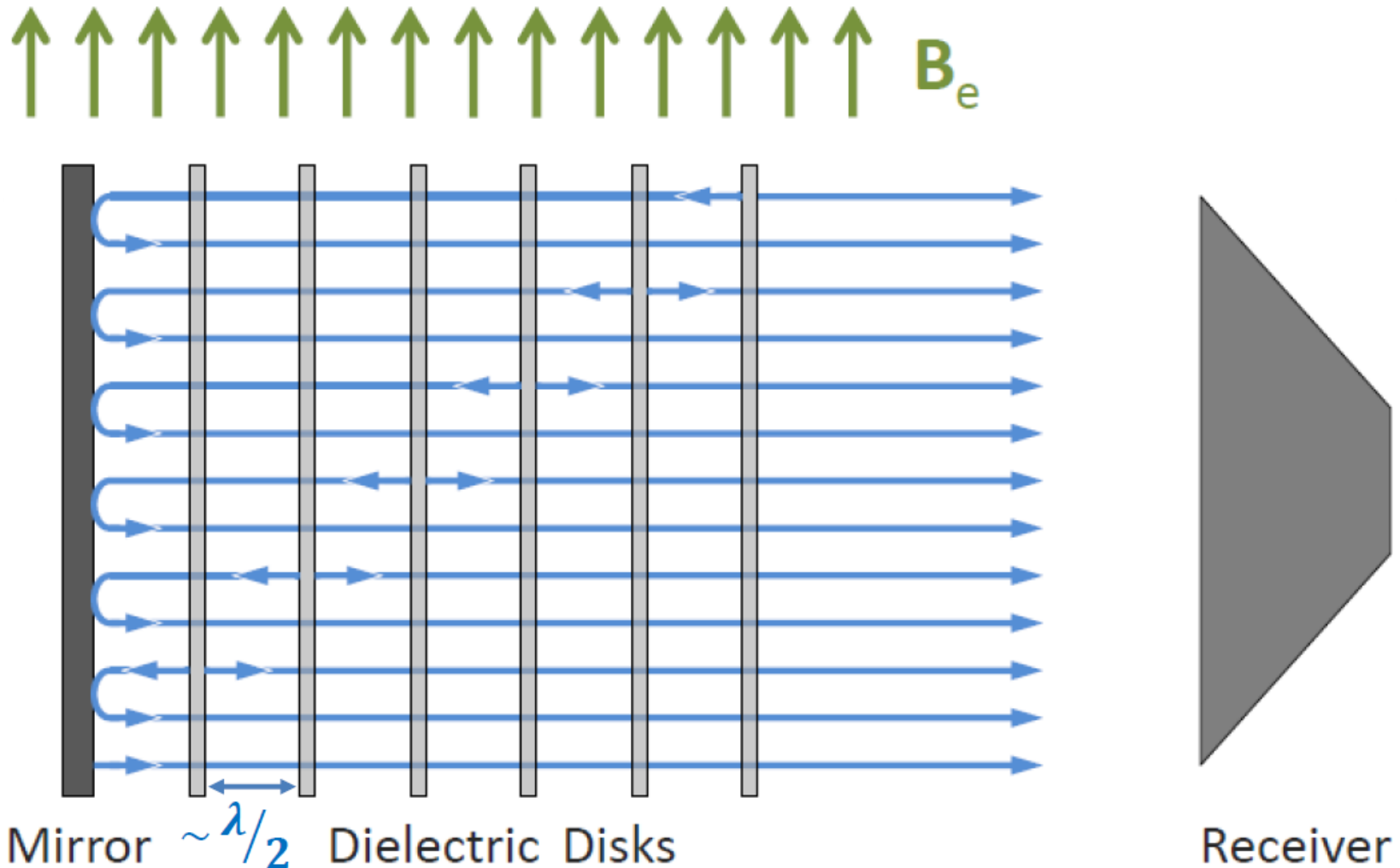
Broadband Reflector Experiment for Axion Detection



Taken from G. Hohshino at PATRAS 2024

Dielectric haloscopes:

“Quasi broadband” approach



Dielectric haloscopes:

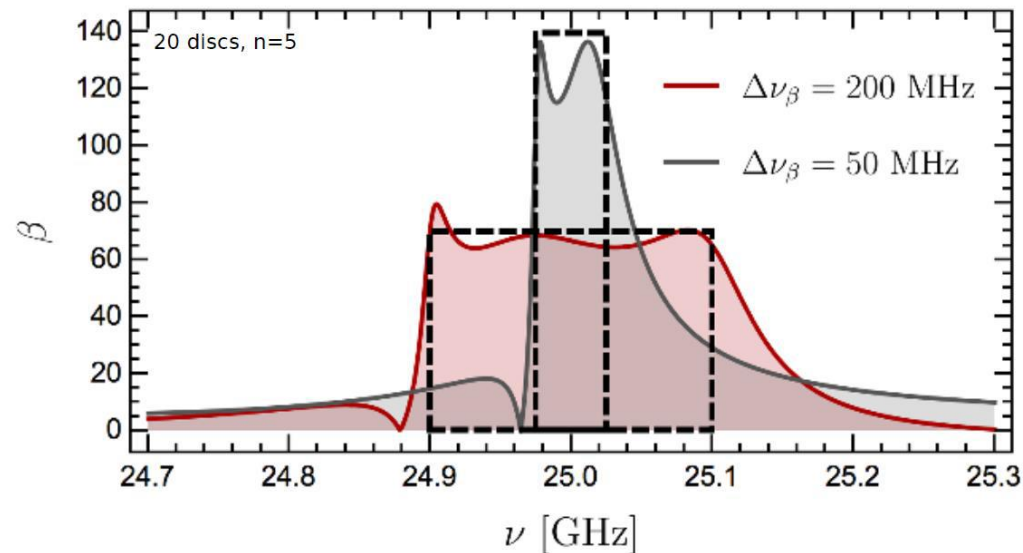
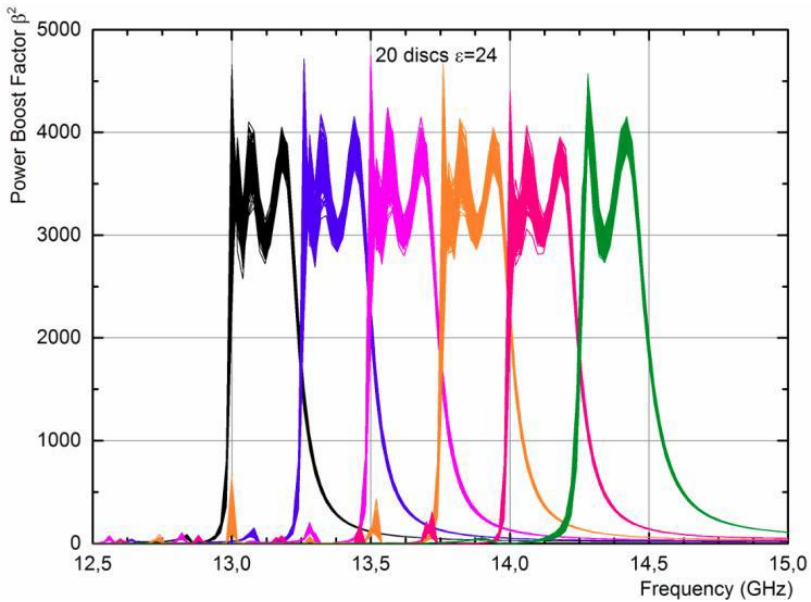
“Quasi broadband” approach

Two effects:

1. **Coherent emission** from all surfaces
2. **Resonant enhancement** of emission at surfaces

- Set disk distances to tune resonant effects
- Changing distances changes sensitive frequency range

mean distance $\sim \lambda/2 \rightarrow$ frequency distance variation \rightarrow width „boost factor“



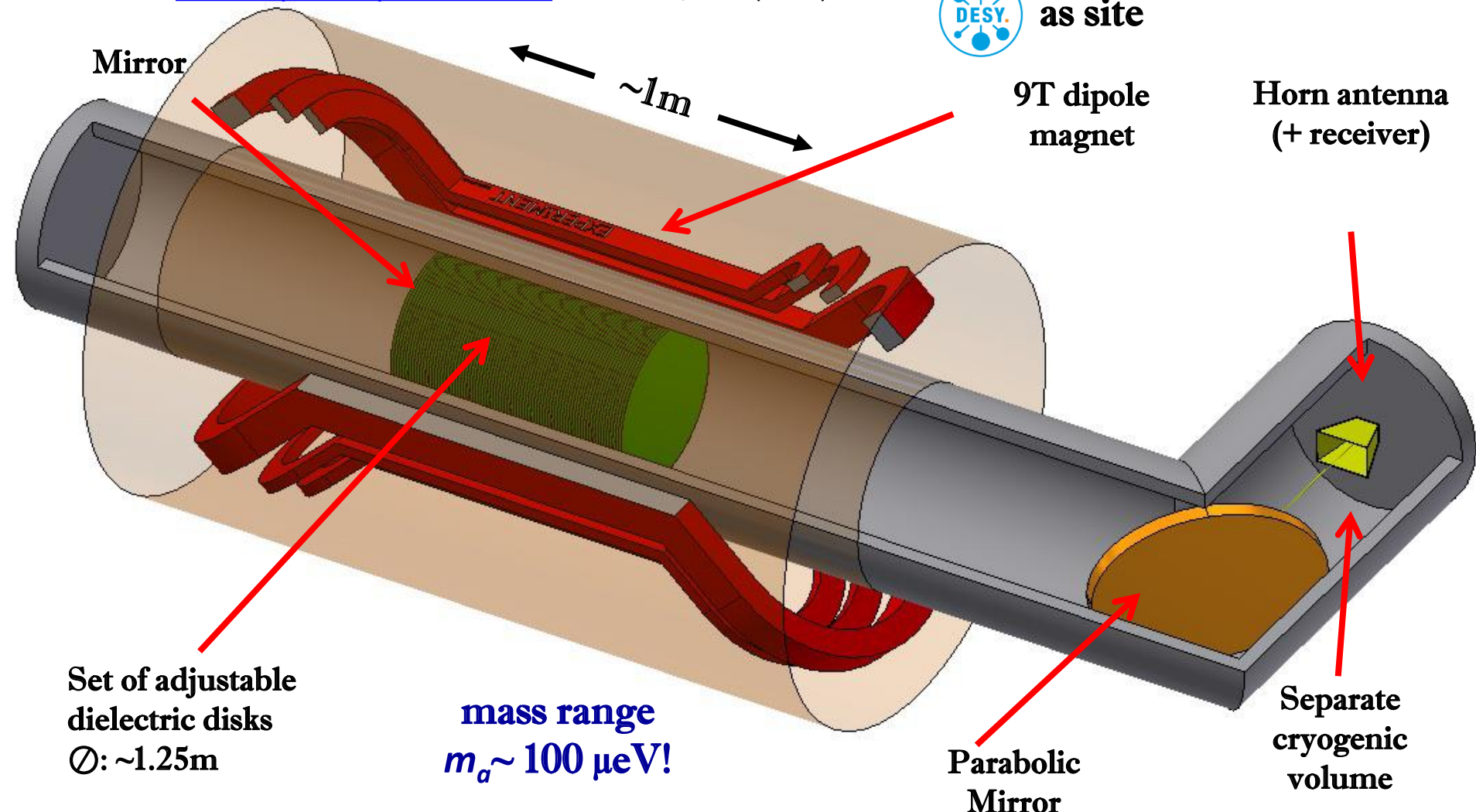


MAgnitized disk and Mirror Axion eXperiment

[The European Physical Journal C](#) volume 79, 186 (2019)



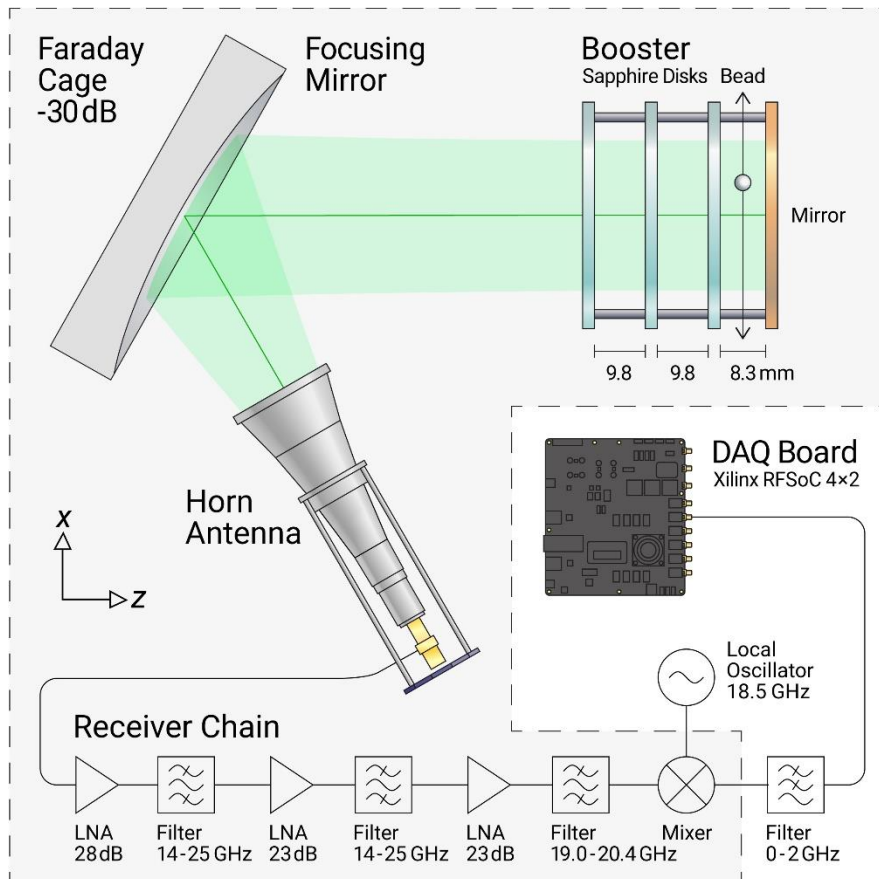
as site





MAgnetized disk and Mirror Axion eXperiment

Prototype booster → Obtain boost factor from E-field measurements

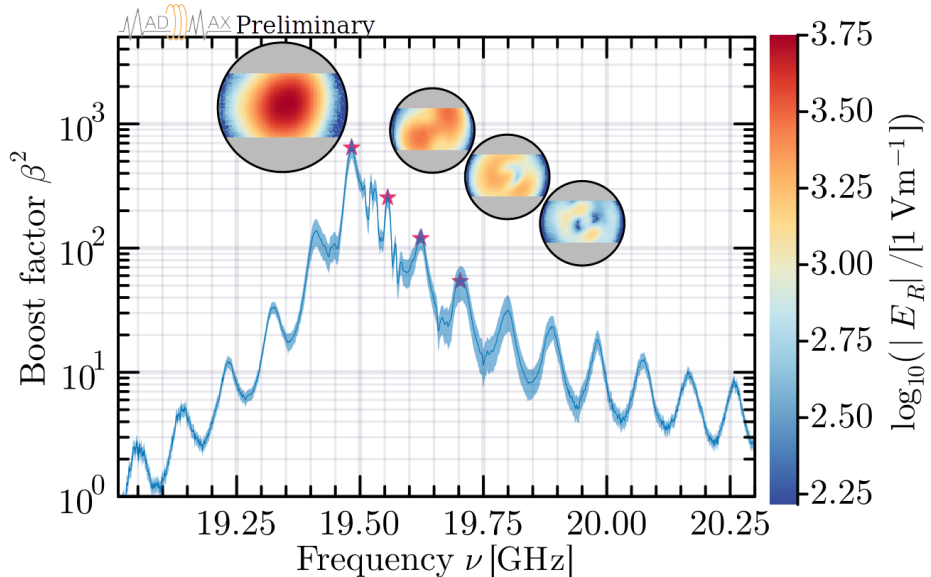


- Set up a simple three disk open booster
- Fixed distances
- Study electromagnetics with „bead-pull“ method

$$\beta^2 \propto \left| \int_{V_a} dV E \right|^2$$

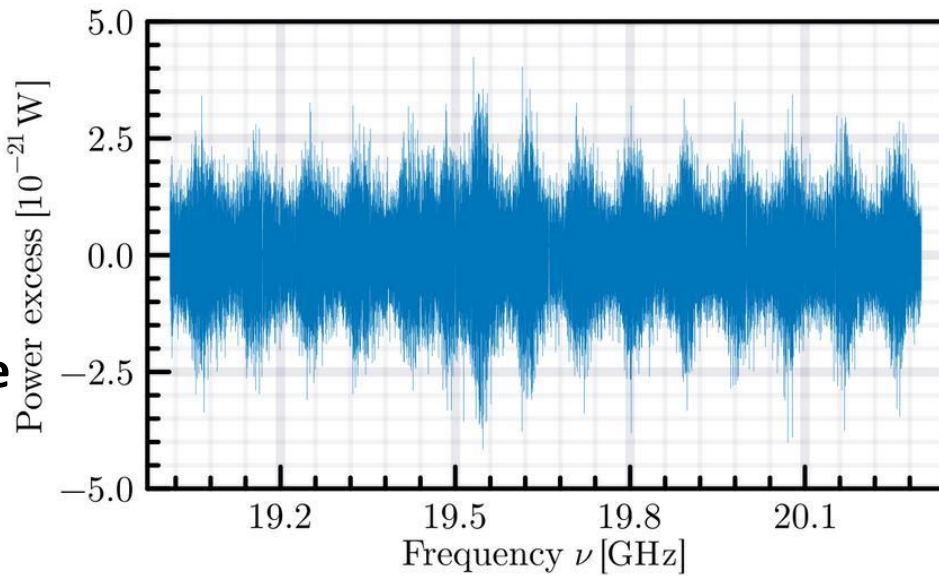


MAgnitized disk and Mirror Axion eXperiment



**Measure electric field
Calculate boost factor from
measurement**

$$\beta^2 \propto \left| \int_{V_a} dV E \right|^2$$

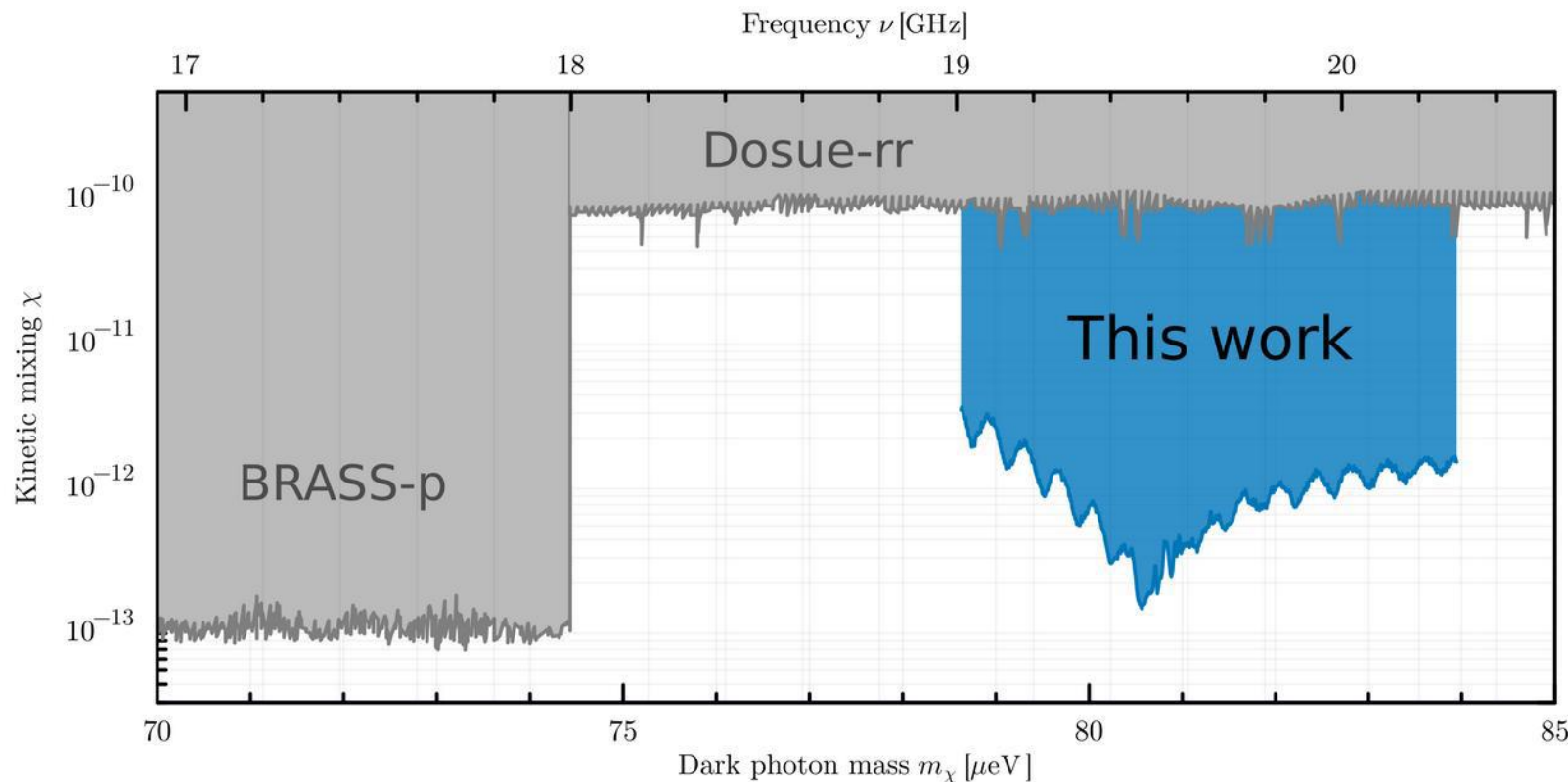


- No signals of unknown origin
- Sensitive to dark photon signals $\sim 10^{-21} \text{ W}$
- Compute 95%-CI upper limit
- Convert to limit on kinematic mixing angle



MAgnetized disk and Mirror Axion eXperiment

“Simple” 3-disk 300mm prototype booster at room temperature:

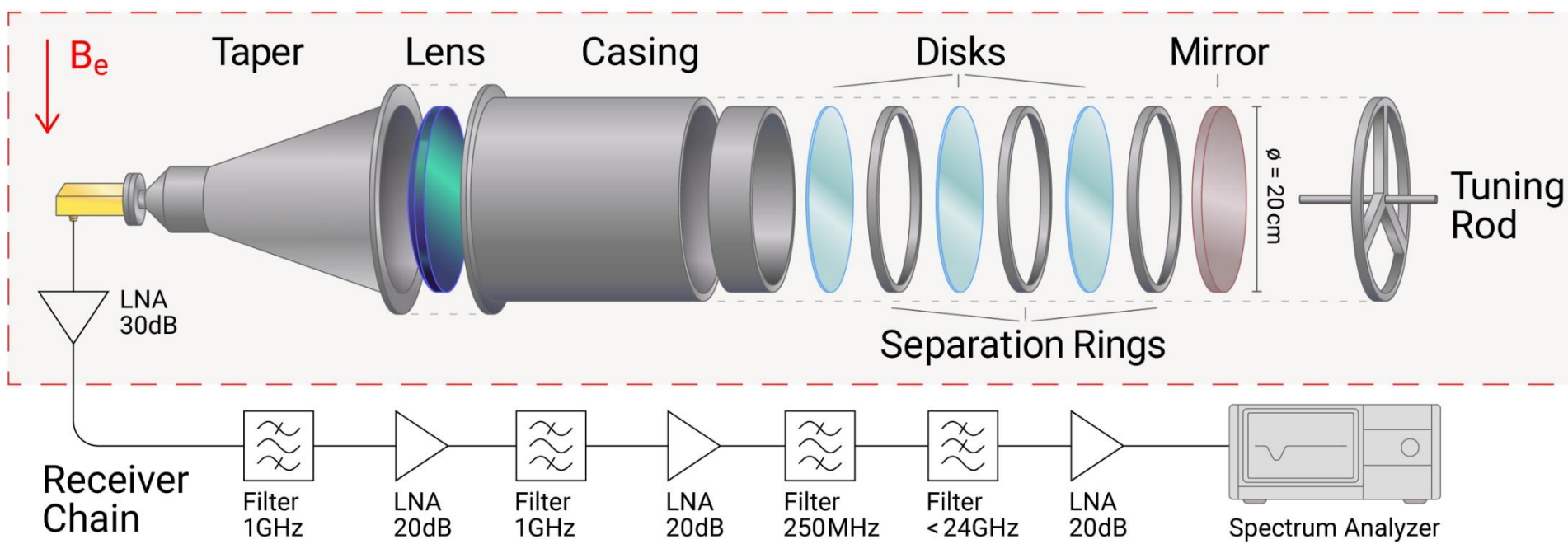


**Improve existing limits by ~3 orders of magnitude
Resonant and broadband at the same time**



MAgnetized disk and Mirror Axion eXperiment

"Simple" 3-disk 200mm "closed" booster at room temperature:

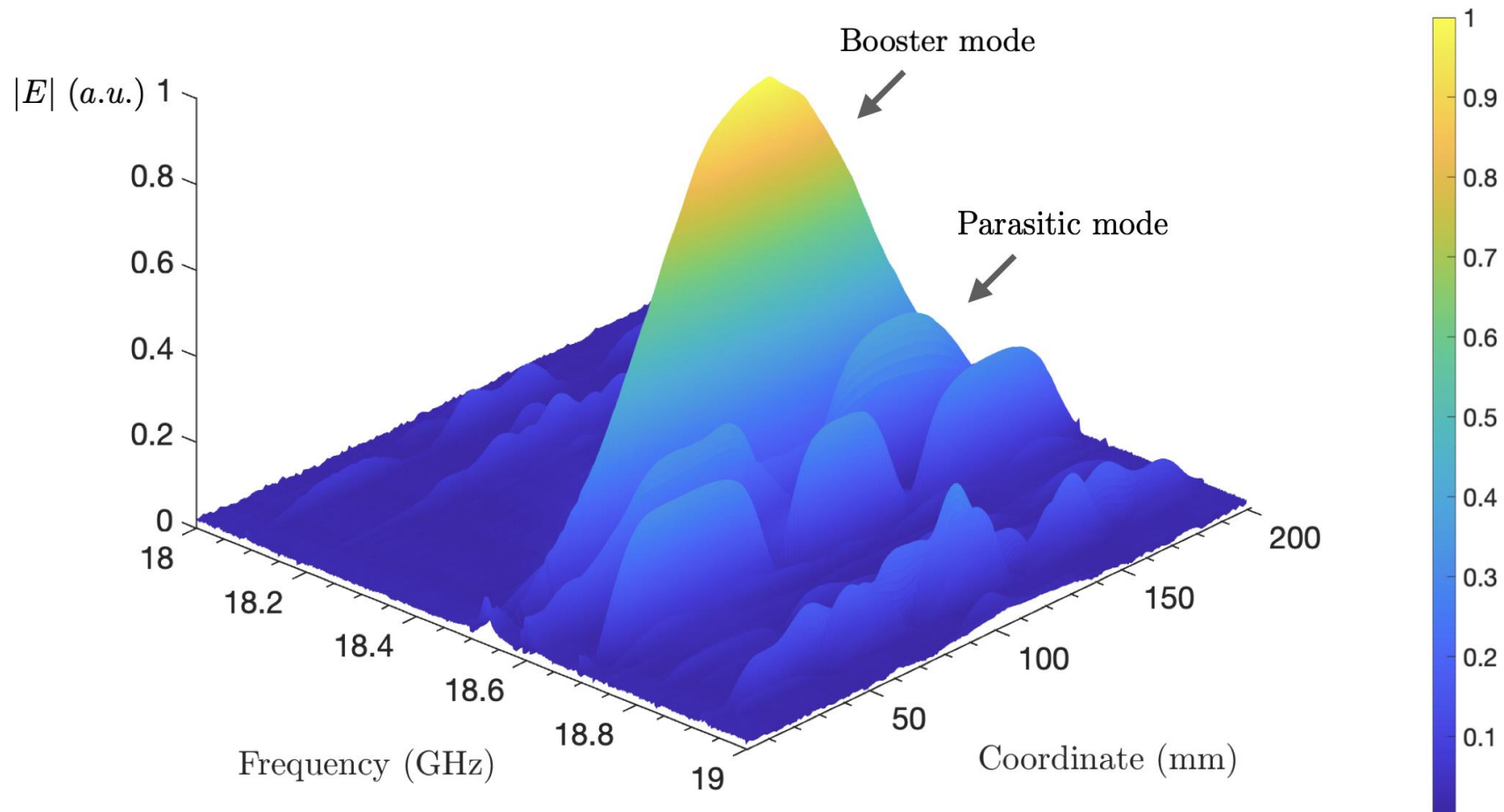


Closed boundary conditions: finite number of modes

- Easier to model
- Boost factor can be determined from 1D model
- Separation rings can be exchanged → Tune frequency
- Use 1.6 T dipole magnet at CERN



MAgnetized disk and Mirror Axion eXperiment



Identification of correct mode via “bead pull measurements”



MAgnitized disk and Mirror Axion eXperiment

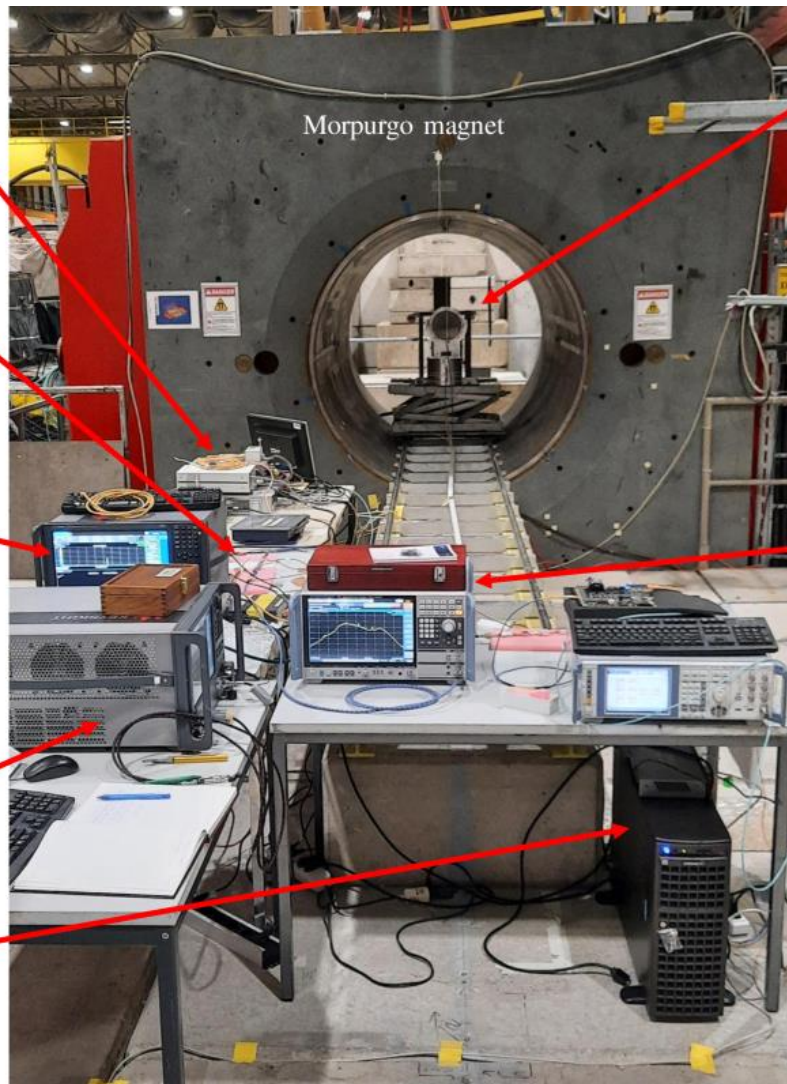
B-field &
T - monitors

Receiver
chain
outside the
B-field

Spectrum
analyzer for
RFI
measurement

VNA for S11
calibration
measurements

Computer
with GPU

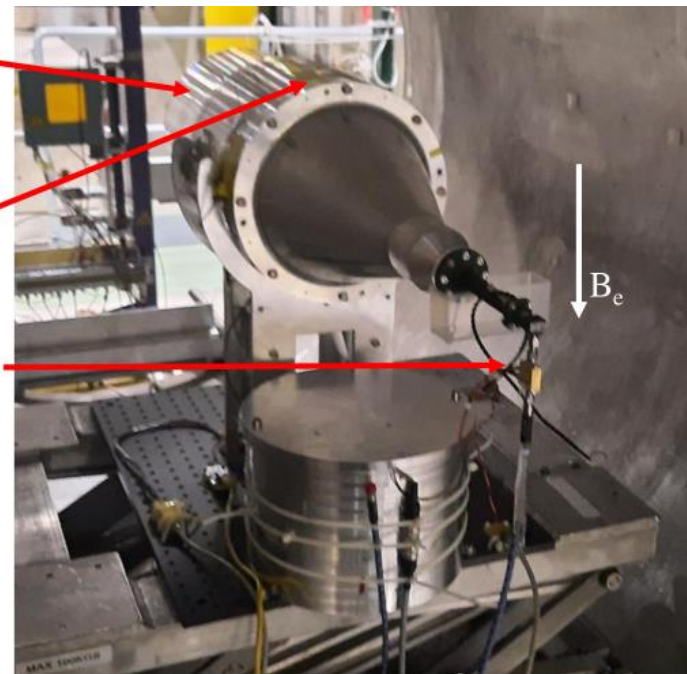


CB200

B-field
probe

First LNA
with T-
sensor
attached

R&S
spectrum
analyzer
FSW43



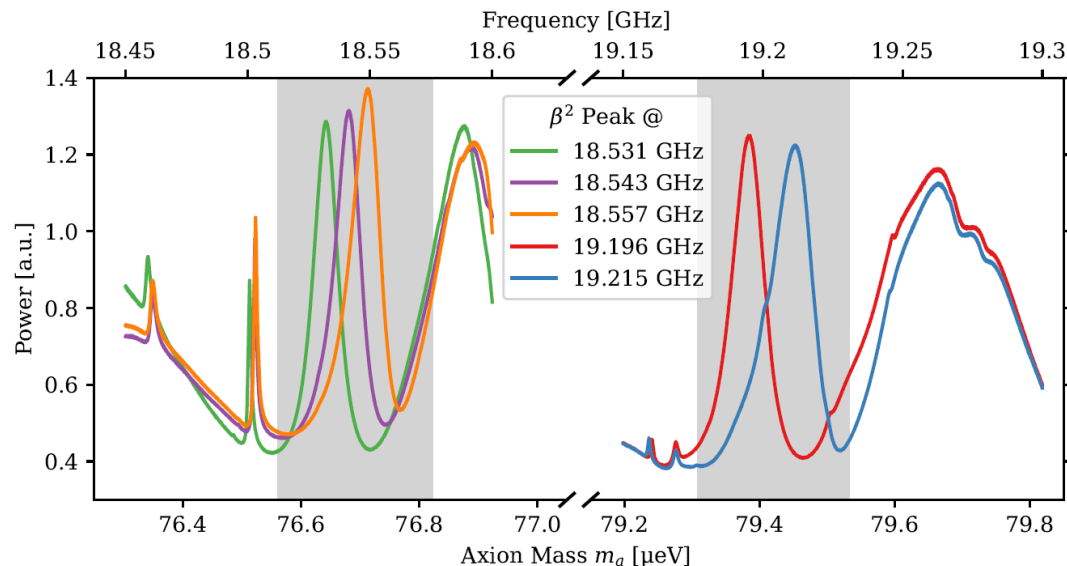
Receiver chain outside the B-field

arXiv: 2409.11777

Axions and ALPs: where do they come from, how to detect them?

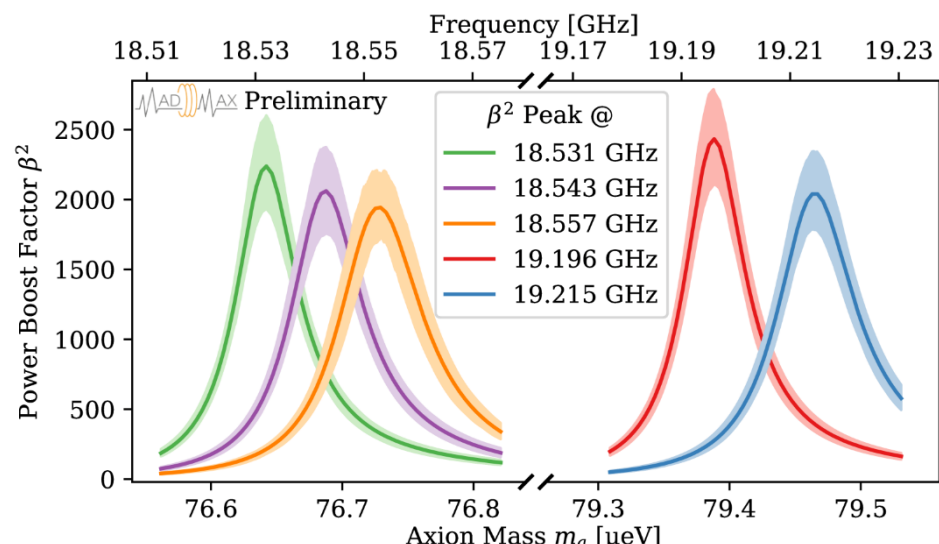


MAgnitized disk and Mirror Axion eXperiment



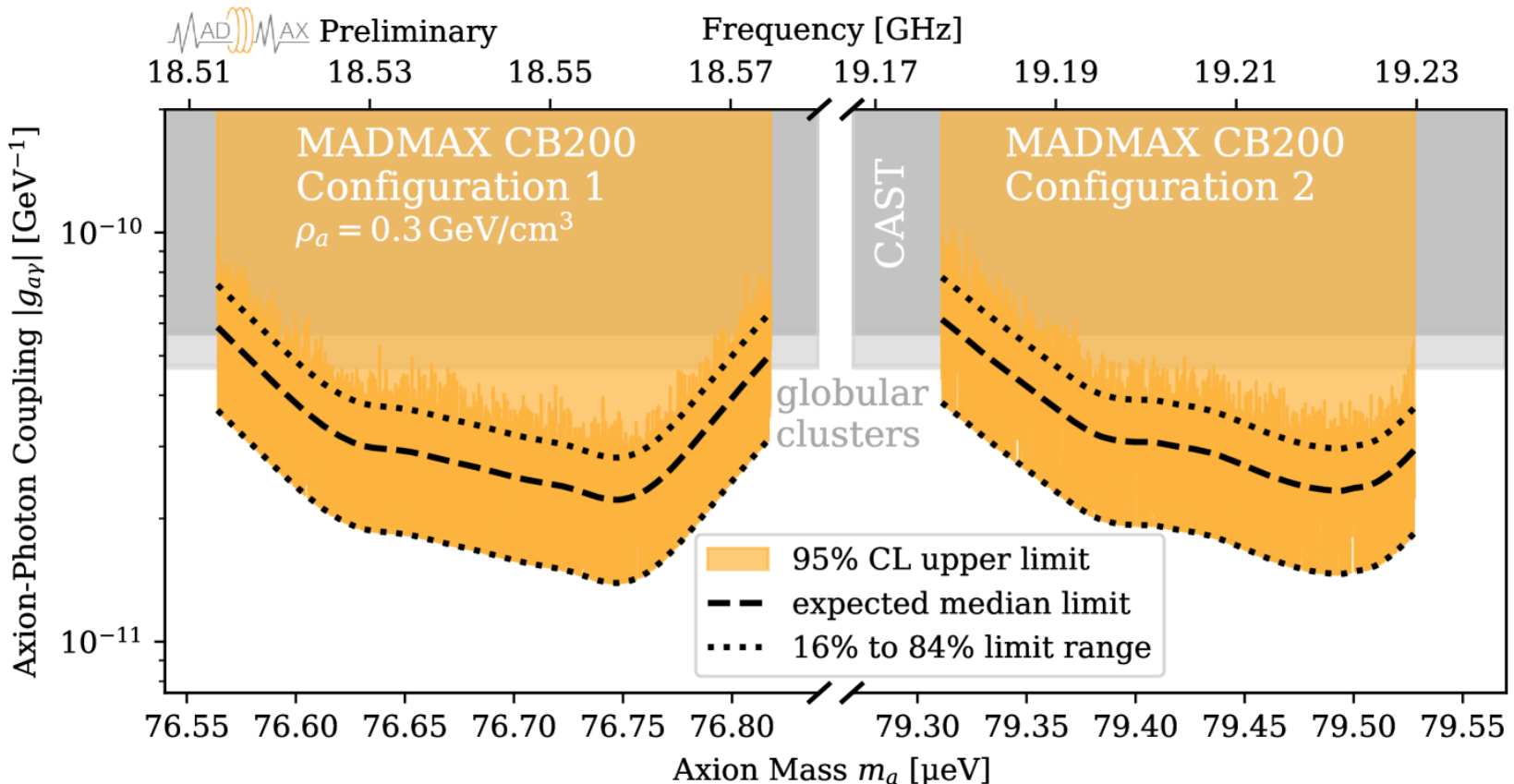
Tuned booster to 5 different frequency bands
 RF behavior via reflectivity
 Data taking: Measure power spectrum inside magnet

1D modelling of booster RF behavior
 → Calculate boost factors





MAgnitized disk and Mirror Axion eXperiment



Improve existing limits by factor ~ 2

Good understanding of boost factor determination:

Measuremet + Modelling

→ Proof of concept!



MAgnitized disk and Mirror Axion eXperiment

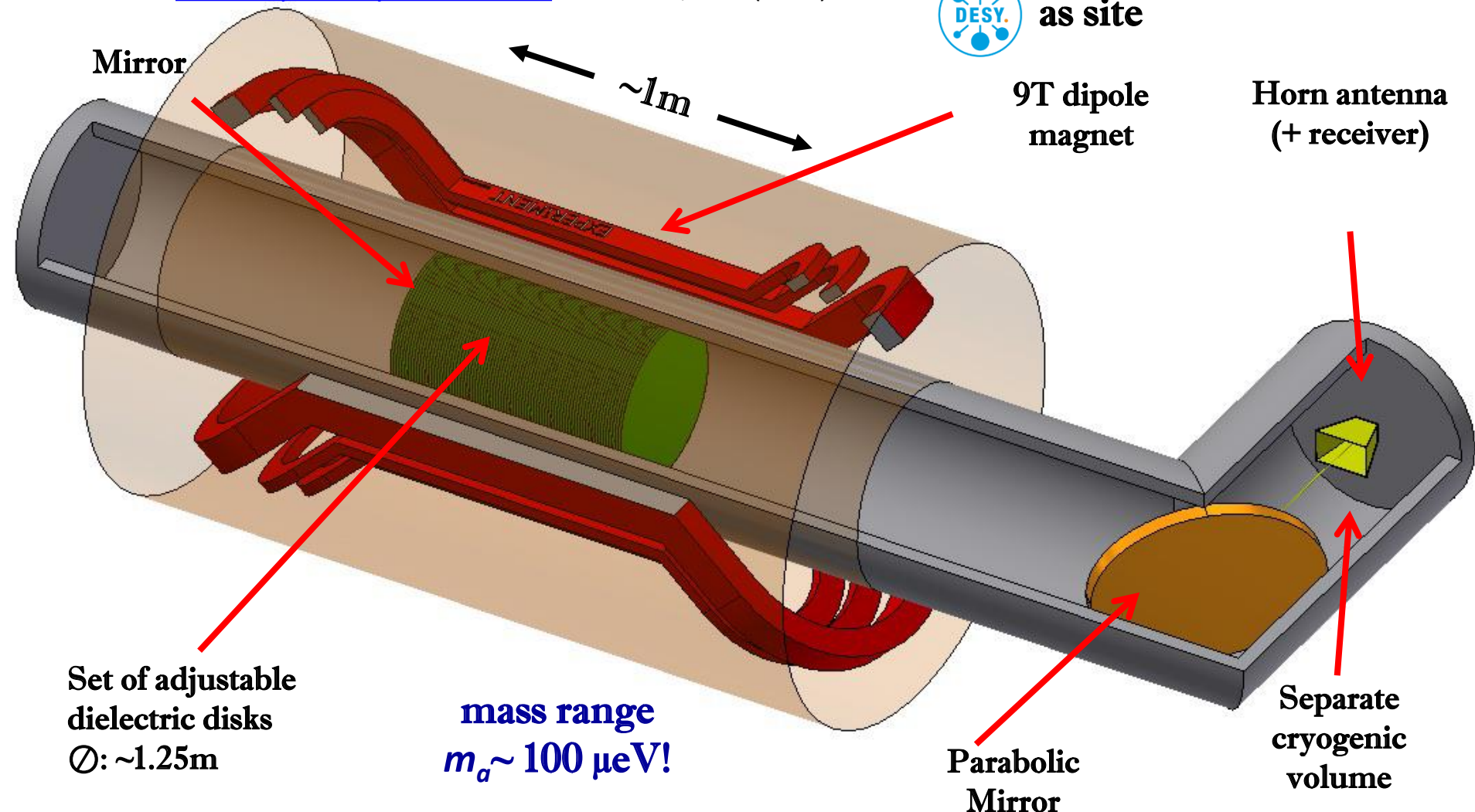
[The European Physical Journal C](#) volume 79, 186 (2019)



as site

9T dipole
magnet

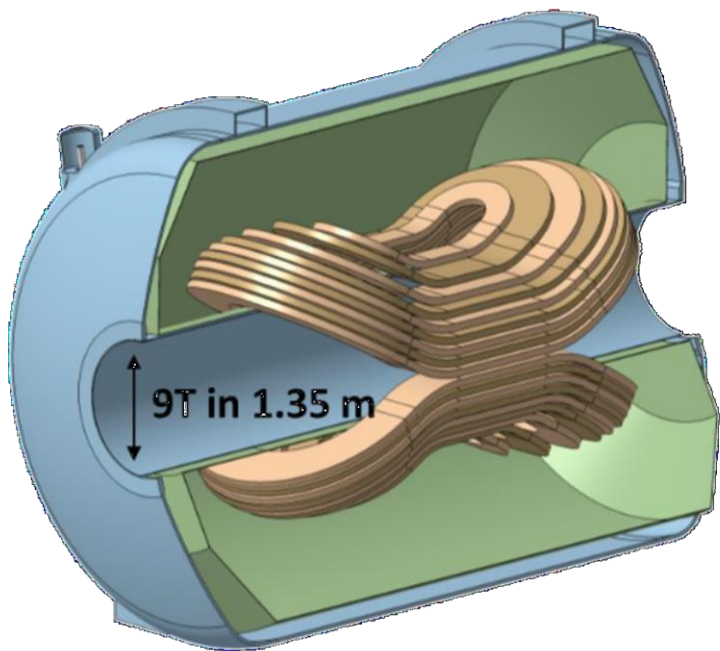
Horn antenna
(+ receiver)





MAgnitized disk and Mirror Axion eXperiment

Magnet: large bore (1.35m) high-field (9.1 T) dipole magnet needed
 → Being developed in cooperation with CEA-Irfu
 → First of its kind!



IEEE TRANSACTIONS ON APPLIED SUPERCONDUCTIVITY

A PUBLICATION OF THE IEEE COUNCIL ON SUPERCONDUCTIVITY



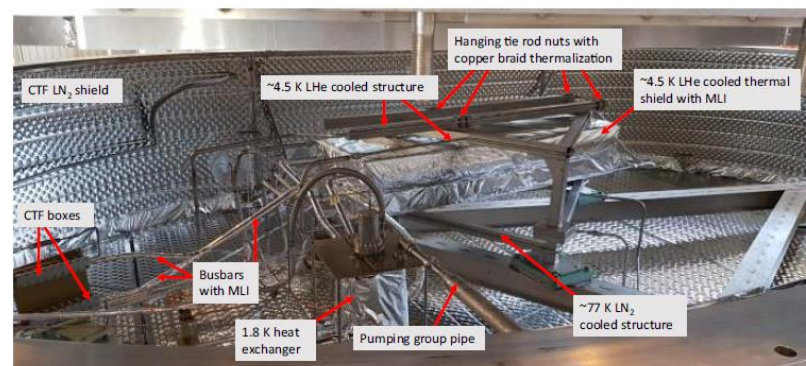
OCTOBER 2023

VOLUME 33

NUMBER 7

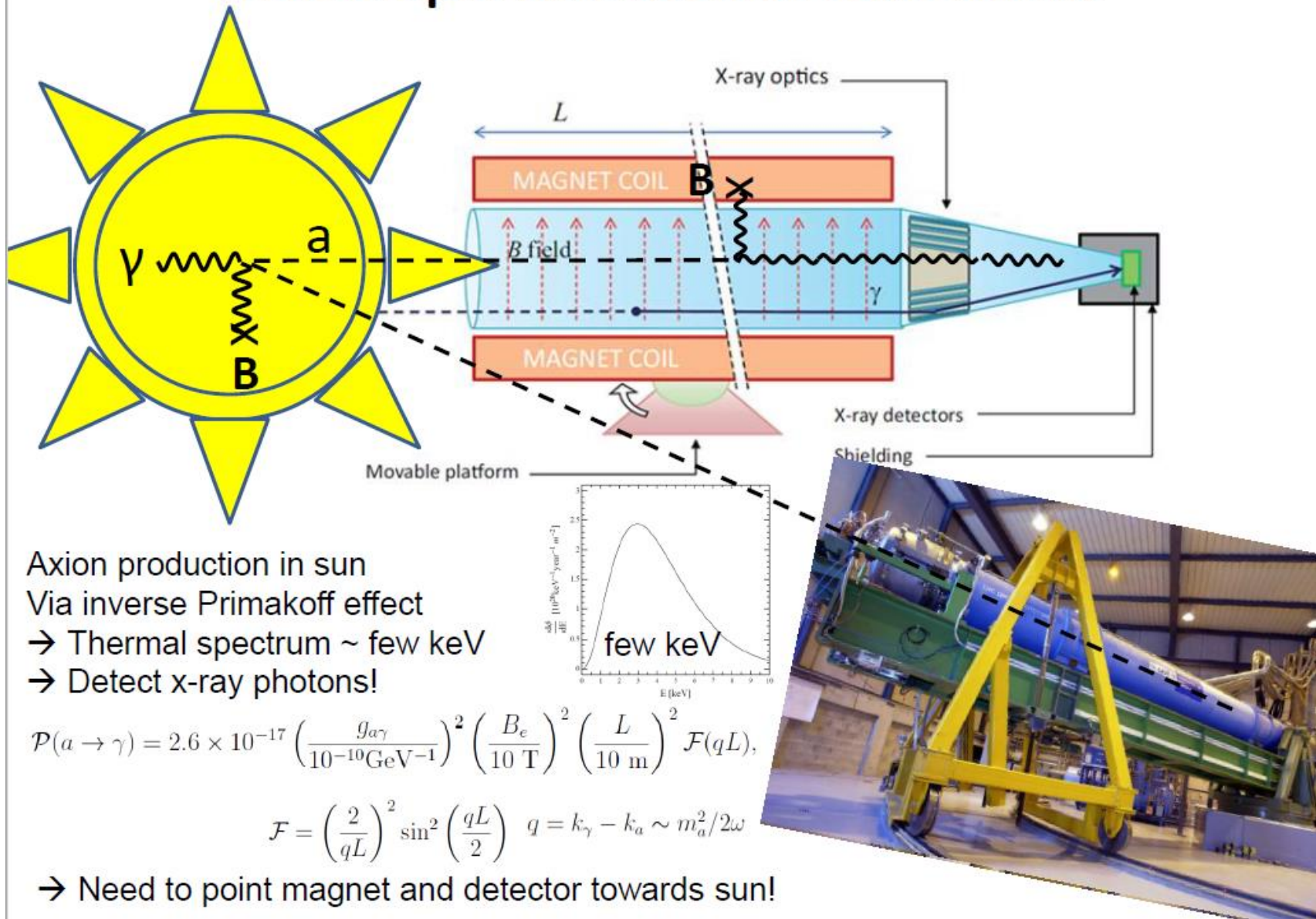
ITASE9

(ISSN 1051-8223)

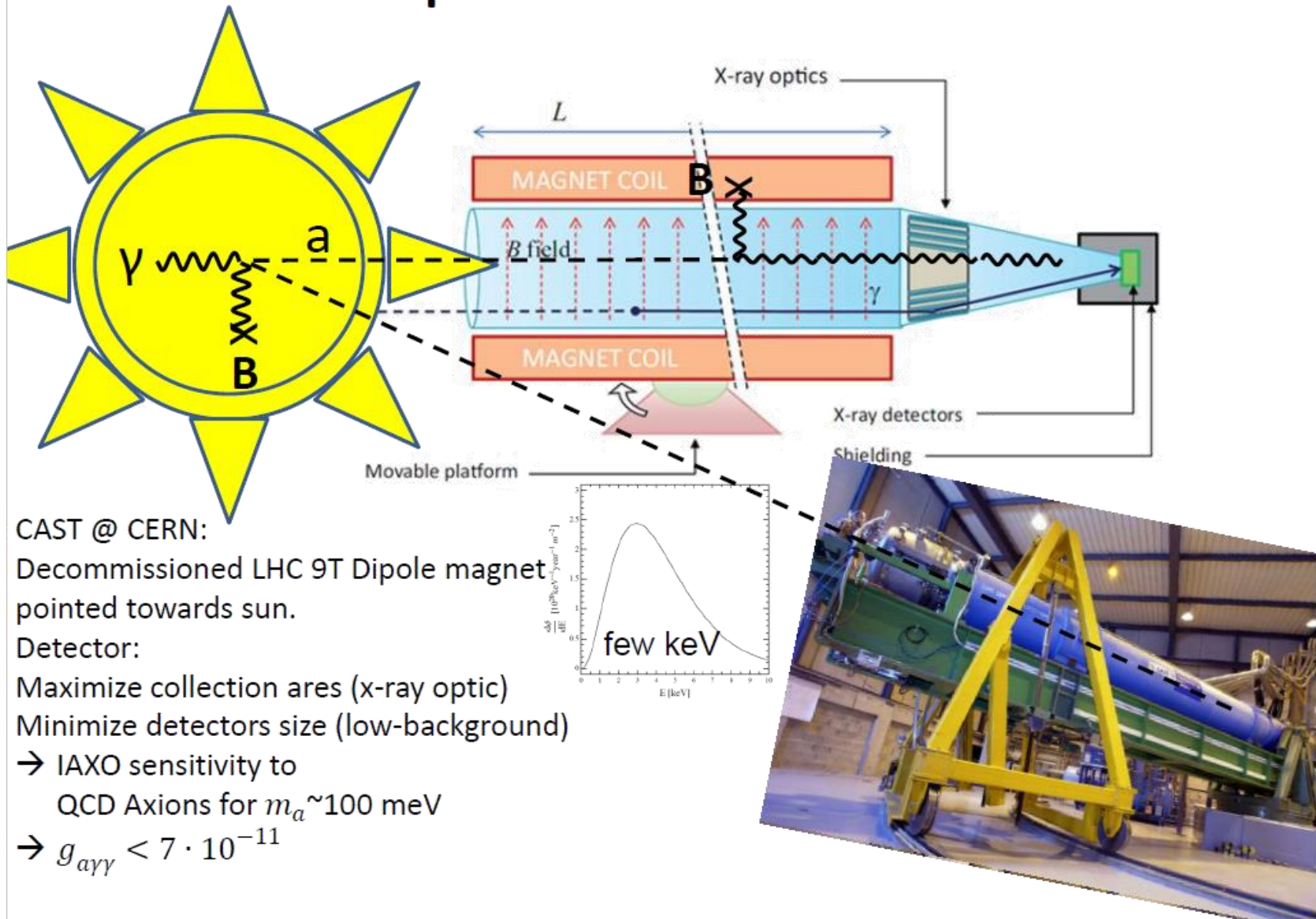


For more, see C. Lorin *et al.*, “Development, Integration, and Test of the MACQU Demo Coil Toward MADMAX Quench Analysis,” Art no. 4500711.

Helioscope: detection of solar axions



Helioscope: detection of solar axions

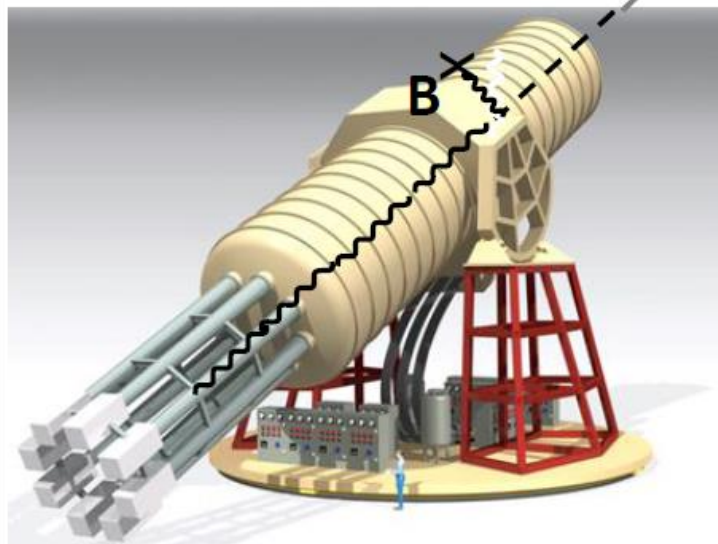


Helioscope: detection of solar axions



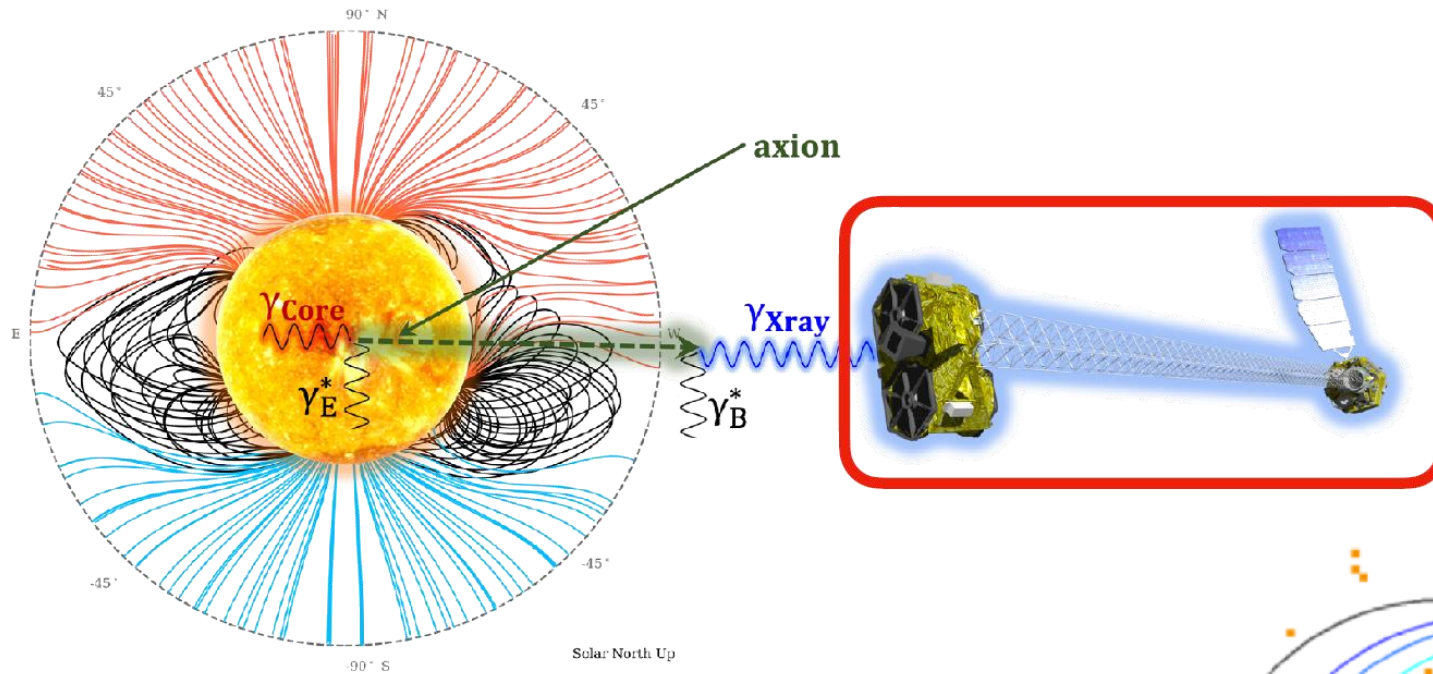
Next generation: IAXO

CAST, Magnets for Colliders,
x-ray optics for satellites,
Low-Background Detectors.



- Toroidal 8-coil magnet $\sim 6\text{T}$
 $L = \sim 20\text{m}$, 600mm bore,
- Locations: probably DESY
- sensitivity to axions
with $m_a \sim 10\text{meV}$
$$g_{a\gamma\gamma} \sim 3 \cdot 10^{-13}$$

NUSTAR as axion telescope



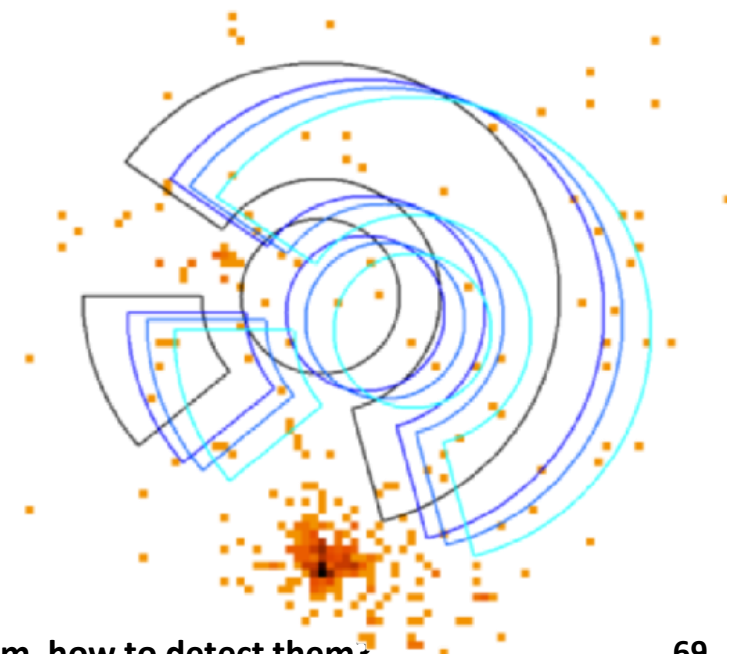
**Observed center of solar disk for 6.4 hours
during 2020 solar minimum in 2020**

Signal region: $r < 0.1 R_\odot$

Bkg. Region: $0.15 R_\odot < r < 0.3 R_\odot$

Remove wedges containing X-ray bright points

E. Todarelli at Partas workshop 2024



NUSTAR as axion telescope

E. Todarelli at Partas workshop 2024

Quiet Sun’s Magnetic Field

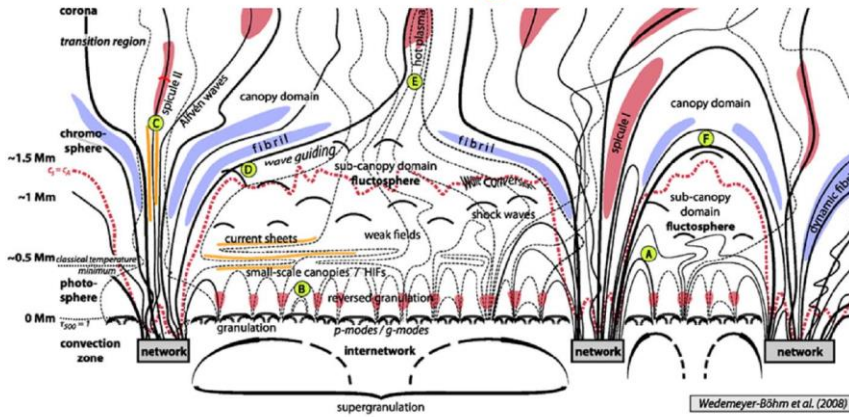
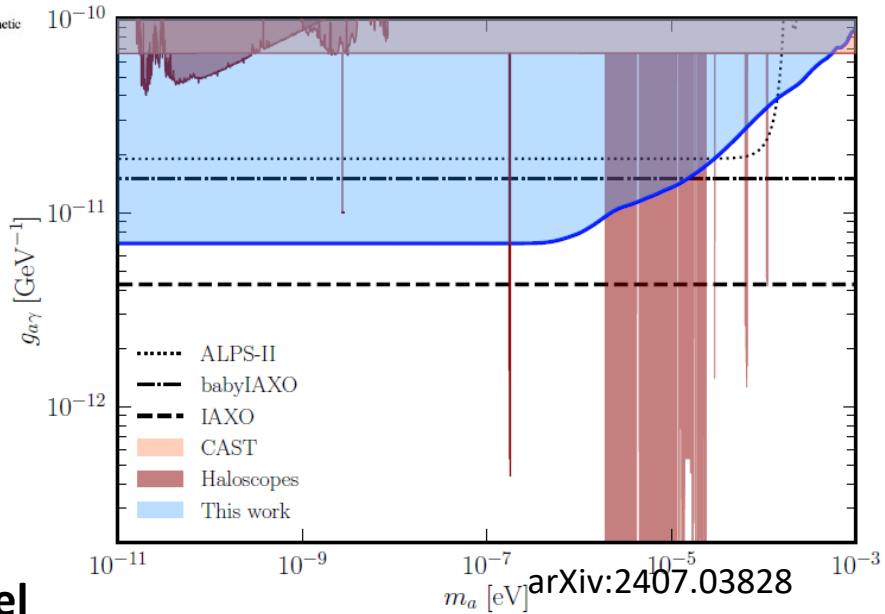


Fig. 16 Schematic, simplified structure of the lower quiet Sun atmosphere (dimensions not to scale): The solid lines represent magnetic field lines that form the magnetic

Axions produced in sun
Convert axions to photons
in solar B-field

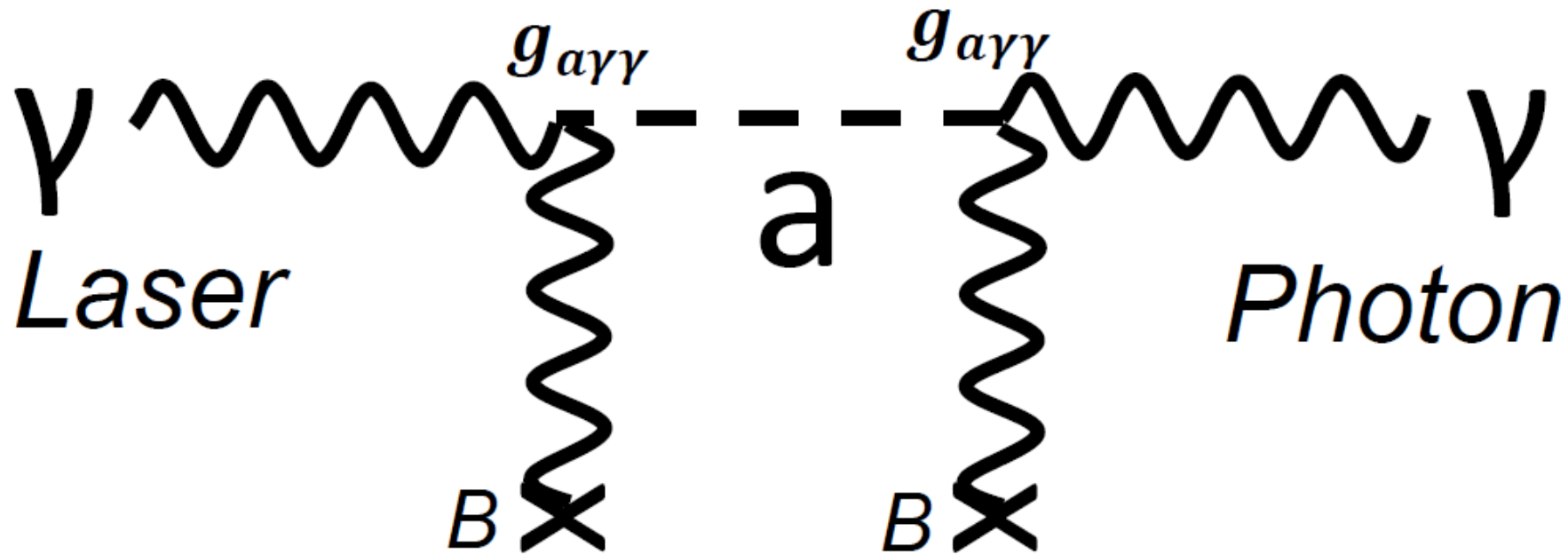


Very competitive limits
Limit depends on solar B-model

Lab experiments:

photon → axion → photon → Detector

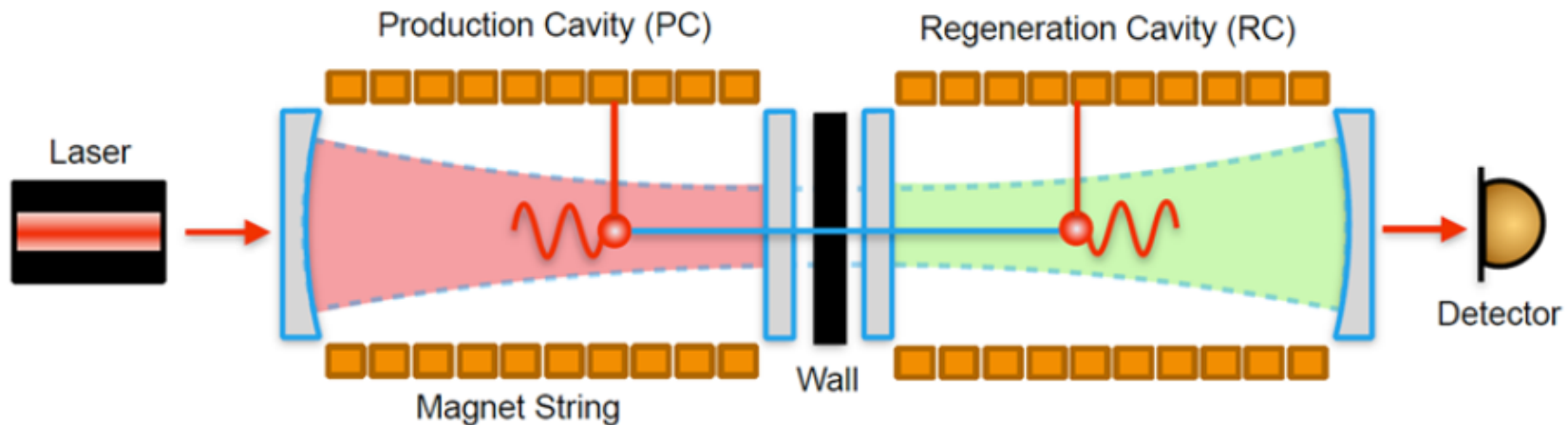
→ No model uncertainty by astrophysics or cosmology!
→ Axions with momentum



$$P_{\gamma \rightarrow ALP \rightarrow \gamma} = 6 \cdot 10^{-38} \left(\mathcal{F}_{PC} \mathcal{F}_{RC} \right) \left(\frac{g_{a\gamma\gamma}}{10^{-10} GeV^{-1}} \right)^4 \left(\frac{B}{1T} \right)^4 \left(\frac{l}{10m} \right)^4$$

Lab experiments:

Light shining through the Wall

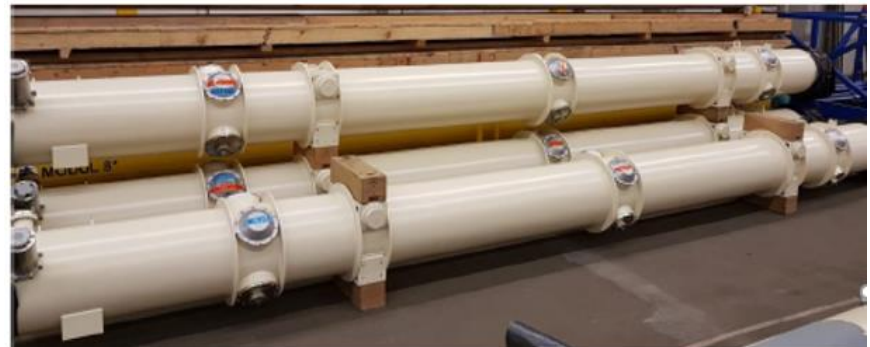


$$P_{\gamma \rightarrow ALP \rightarrow \gamma} = 6 \cdot 10^{-38} \left(\mathcal{F}_{PC} \mathcal{F}_{RC} \right) \left(\frac{g_{a\gamma\gamma}}{10^{-10} GeV^{-1}} \right)^4 \left(\frac{B}{1T} \right)^4 \left(\frac{l}{10m} \right)^4$$

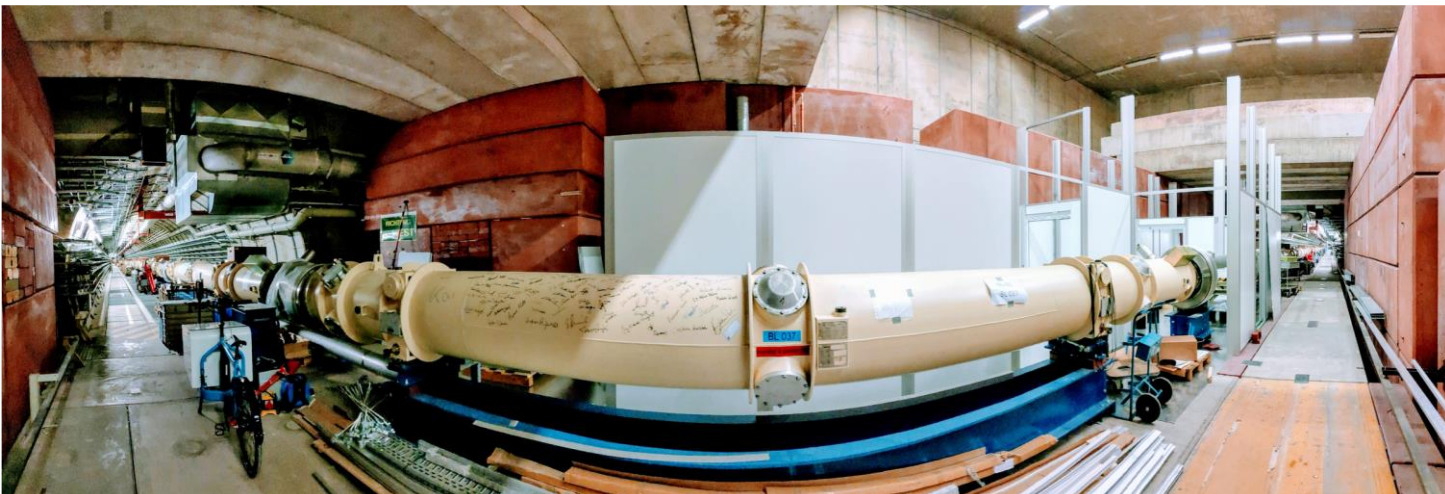
- Maximize magnet length
- Optical generation and regeneration cavities with high Finesse: „recycle light“
- Optical cavity technology from gravitational wave detectors!

ALPS II at DESY

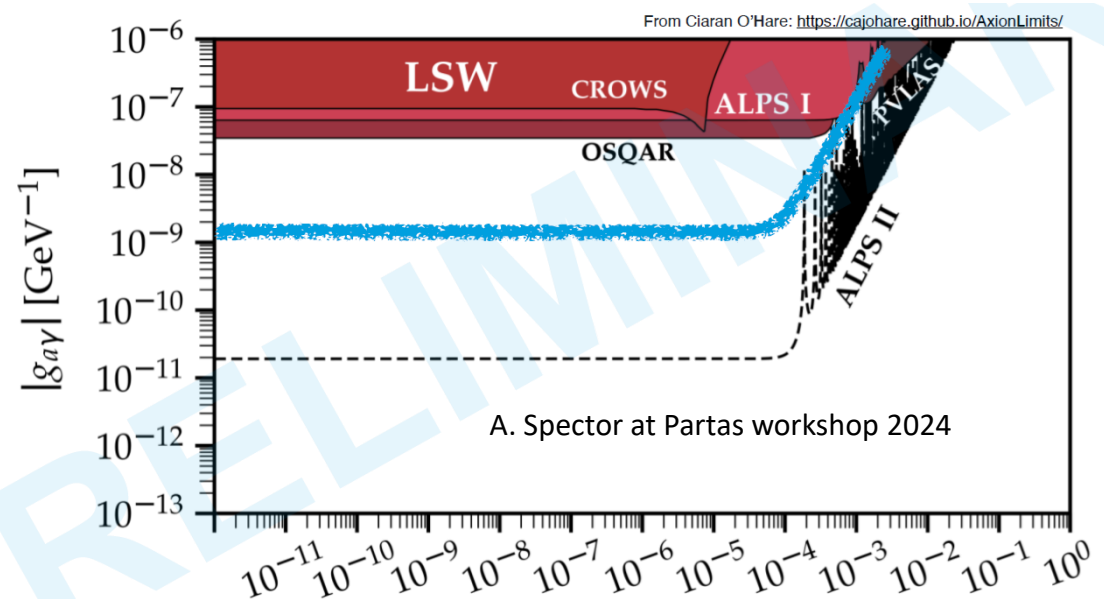
- **2x strings of 12 HERA dipole magnets:
5.3 T, 106 m**
- **Cryogenic infrastructure**
- **High power laser (HPL) system (30 W)**
- **World record storage time: 7.17 +- 0.01 ms**
- **Heterodyne detection system ($\Delta f \sim 1$ μHz)**
- **3 clean rooms at the different stations of the experiment**



ALPS II at DESY

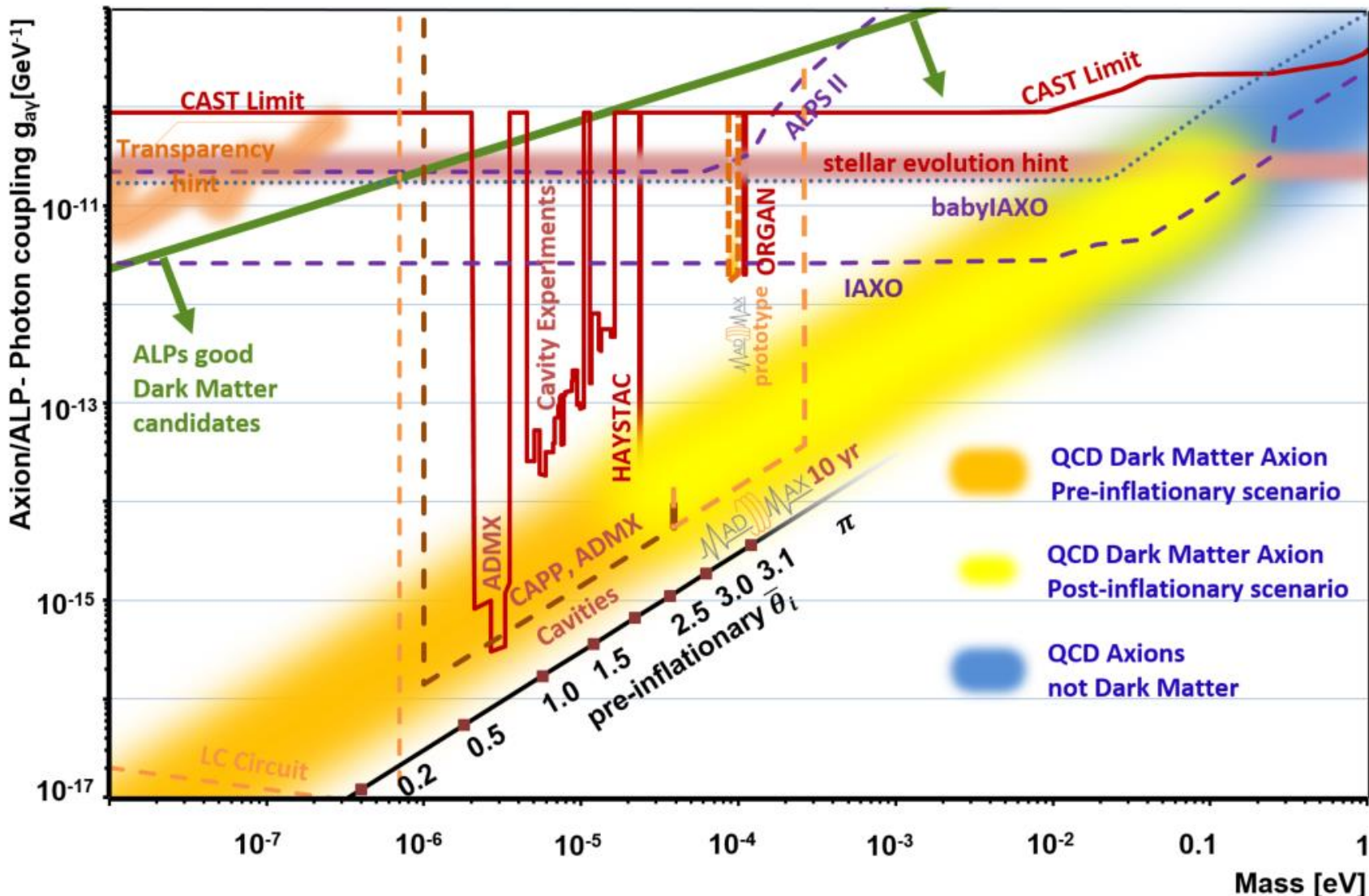


**First data since Feb. 2024
Improve previous limits by
> order of mag.**



Axions and ALPs: where do they come from, how to detect them?

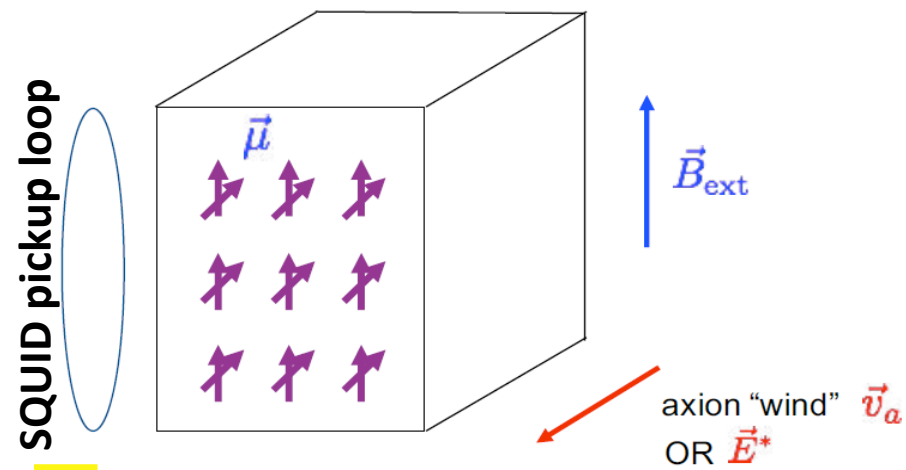
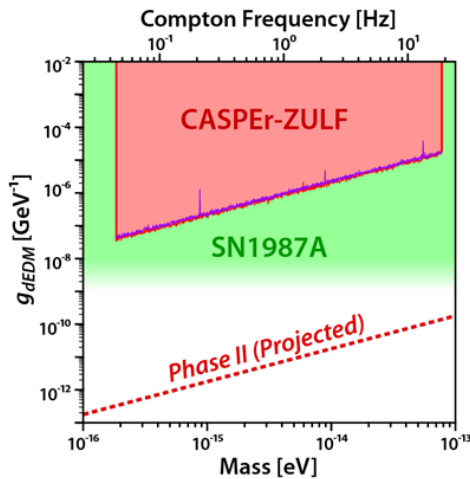
Limits and projections in perspective

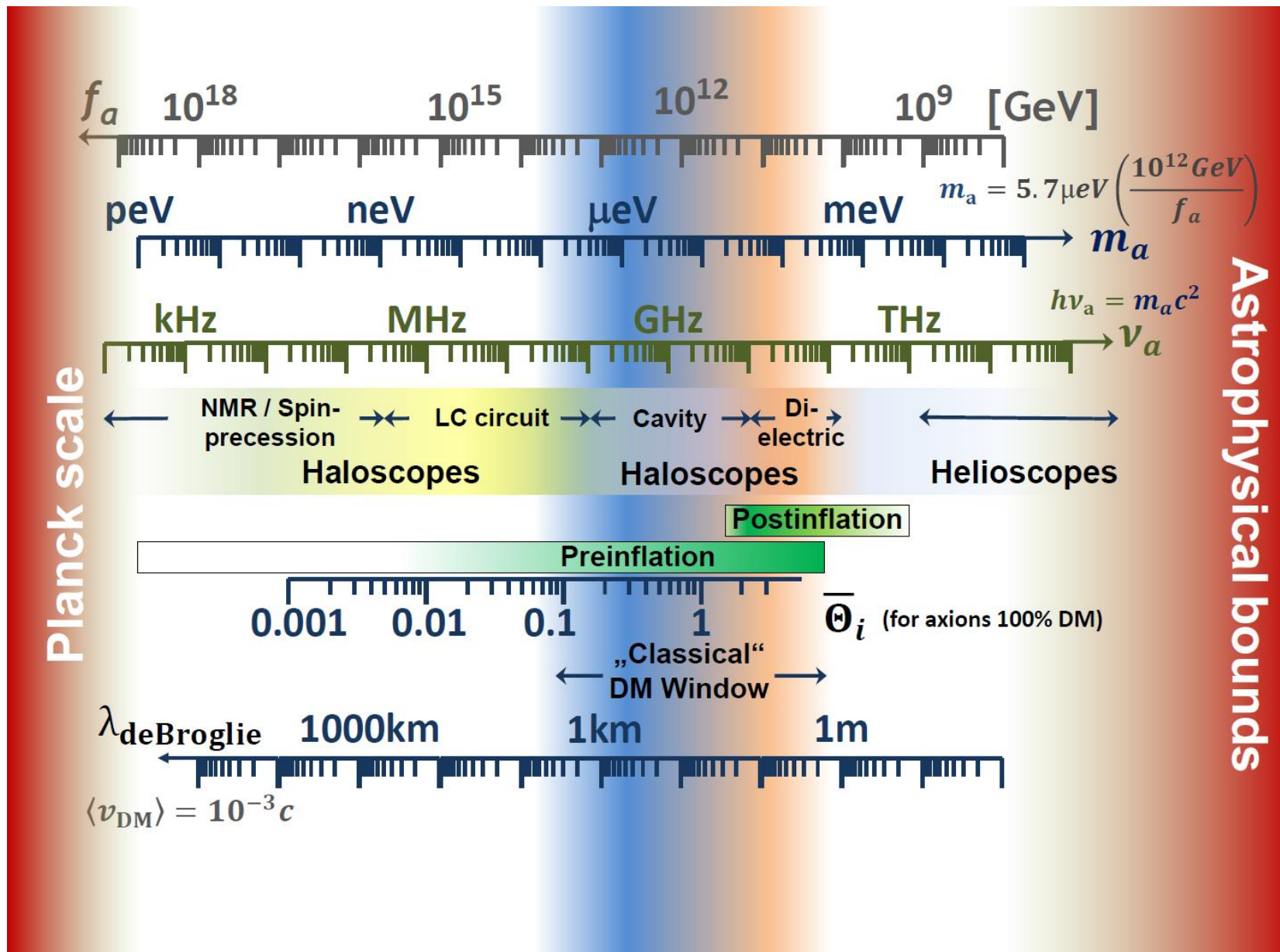


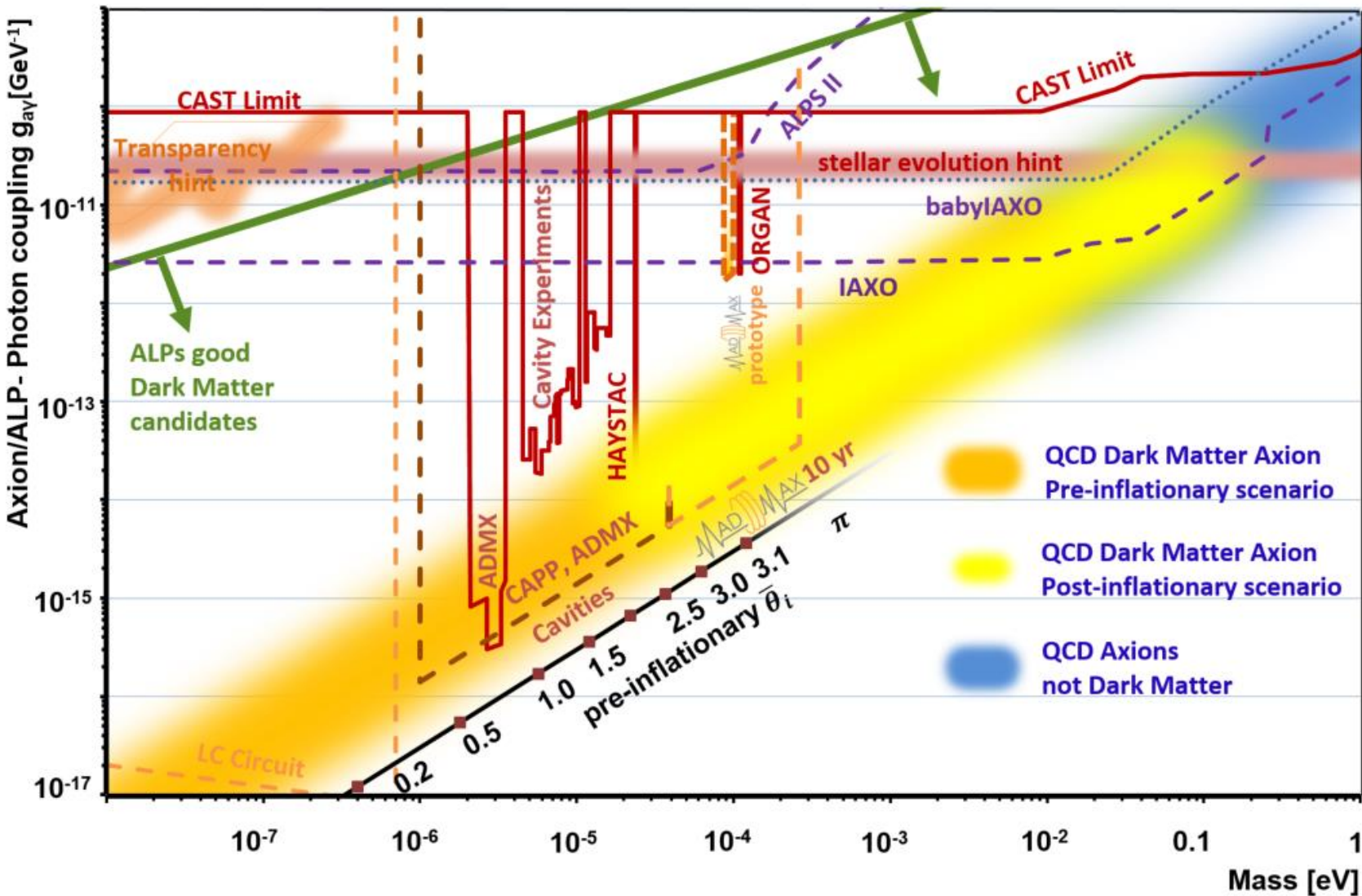
Nuclear Magnetic Resonance:

Axion coupling with nucleus

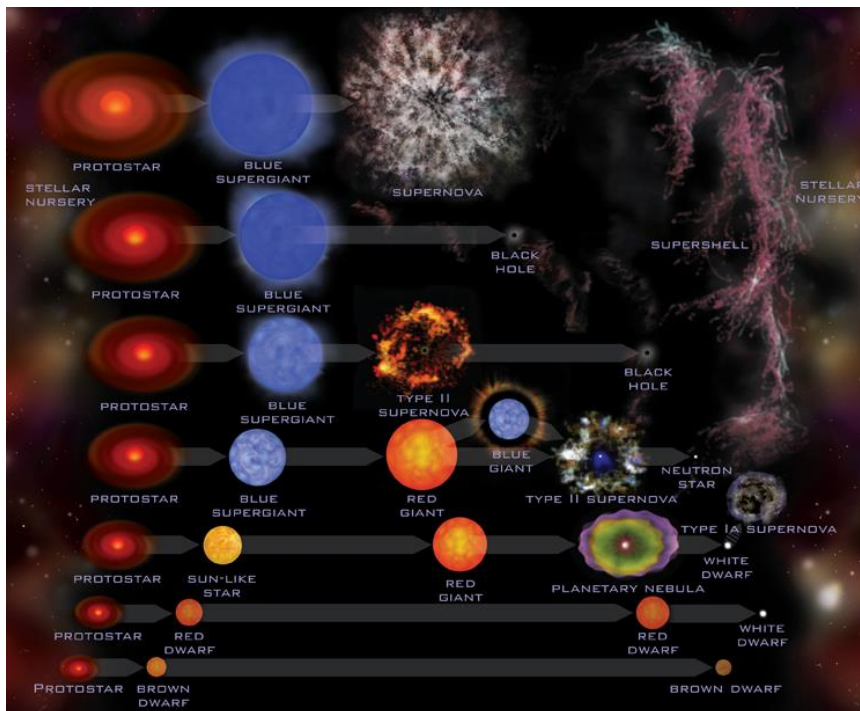
- Oscillating electric dipole moment
- Precession of nuclear spin in material sample in presence of an electric field
- Resonant transverse magnetization
- Measure via precision magnetometry
- Modify B_{ext} to scan different masses (defines sensitivity)







Limits on axion coupling from stellar evolution:



axion couplings with nuclei/electrons/gammas In “hot media/plasmas”:

- emission of axions
 - Additional cooling of stellar cores, supernovae (progenitors), pulsars, ... due to axion emission
 - Stellar evolution influenced depending on coupling strengths
 - Set limits on coupling strength → f_a

Limits from stellar evolution:

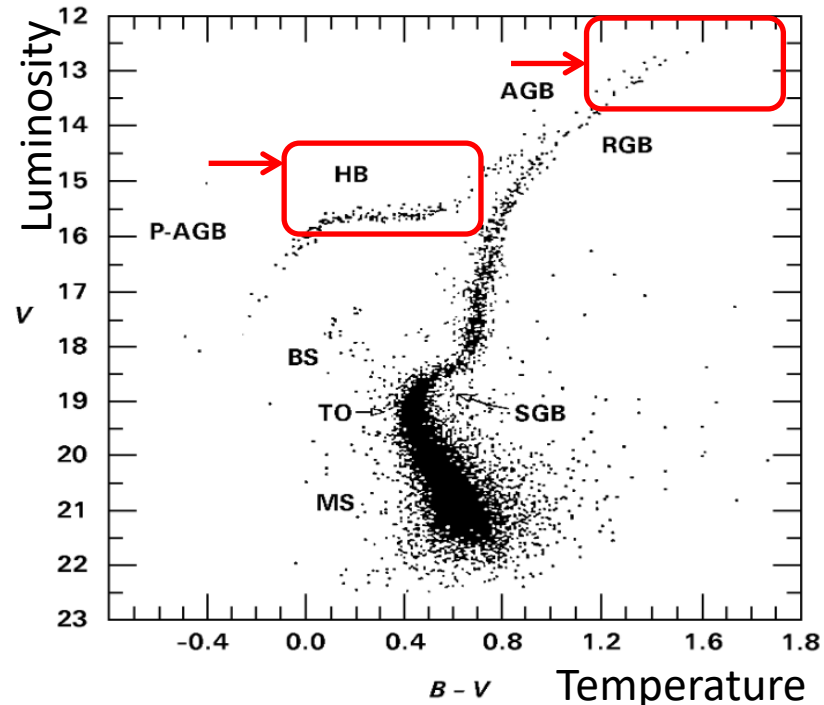
Hertzsprung Russel diagram

Count population

→ Information on duration of given stage of evolution

→ Density depends on cooling rate

→ For example tip of red giant branch



Primakoff energy loss rate proportional to $\frac{T^7}{\rho}$

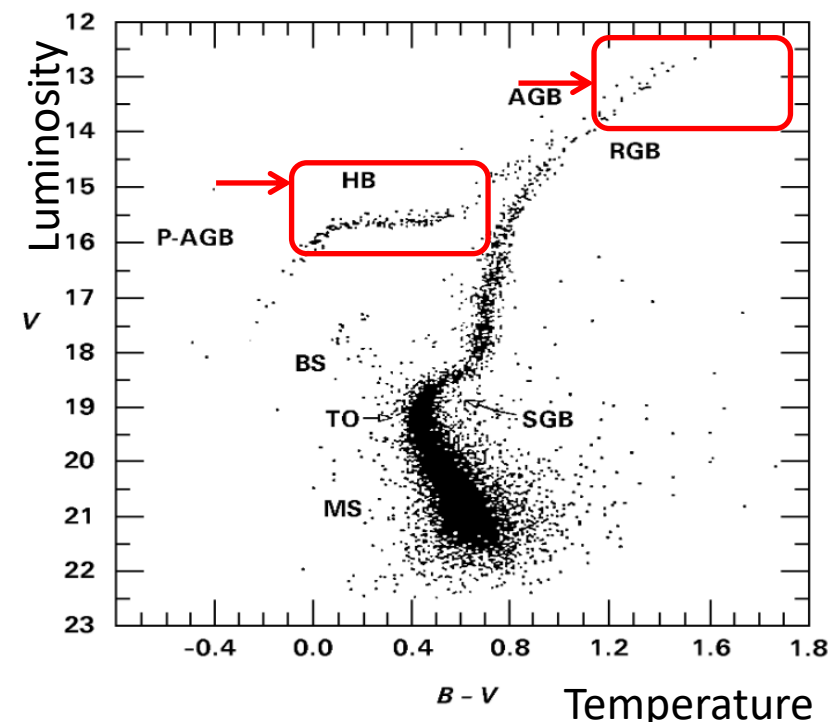
→ axion emission rate depends on sequence in stellar evolution

Globular cluster: Gravitationally bound system of stars that formed at the same time:

Limits from stellar evolution:

Horizontal branch stars (HB): Helium burning stars after **Red Giant Branch (RGB)** stage: **very hot**
→ Axion couplings could significantly shorten lifetime

Count number of stars in HB and compare to RGB expectations based on standard cooling.



Limits from stellar evolution:

Most sensitive analysis (Raffelt, MPP): **Length of neutrino signal from SN87a:**

Core collapse SN: creation of a proto-neutron start with short life time.

During life time of neutron star with $T \sim 10\text{ MeV}$:

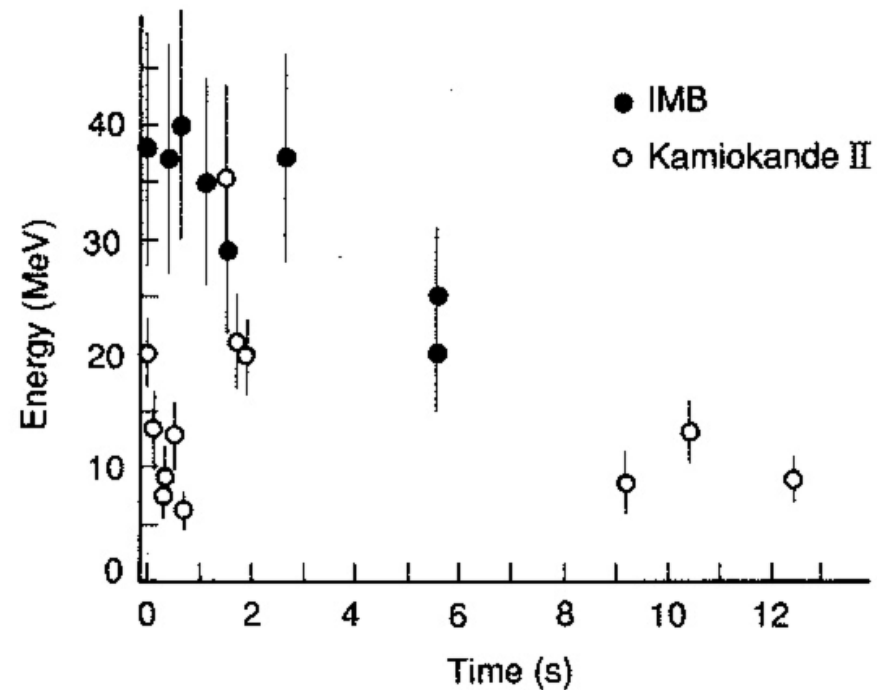
Neutrino emission (almost 20 neutrinos observed during several seconds)

Life time of neutron star would be shortened by emission of axions due to “**axion nuclear Bremsstrahlung**”:

→ Length of neutrino burst:

limit on axion Bremsstrahlung

→ $f_a > 10^8 \text{ GeV} \rightarrow m_a < 1 \text{ eV}$



Hints from stellar evolution:

Some systems show cooling anomalies, i.e. more energy loss than expected:

Pulsating white dwarf G117-B15A with P=215s:

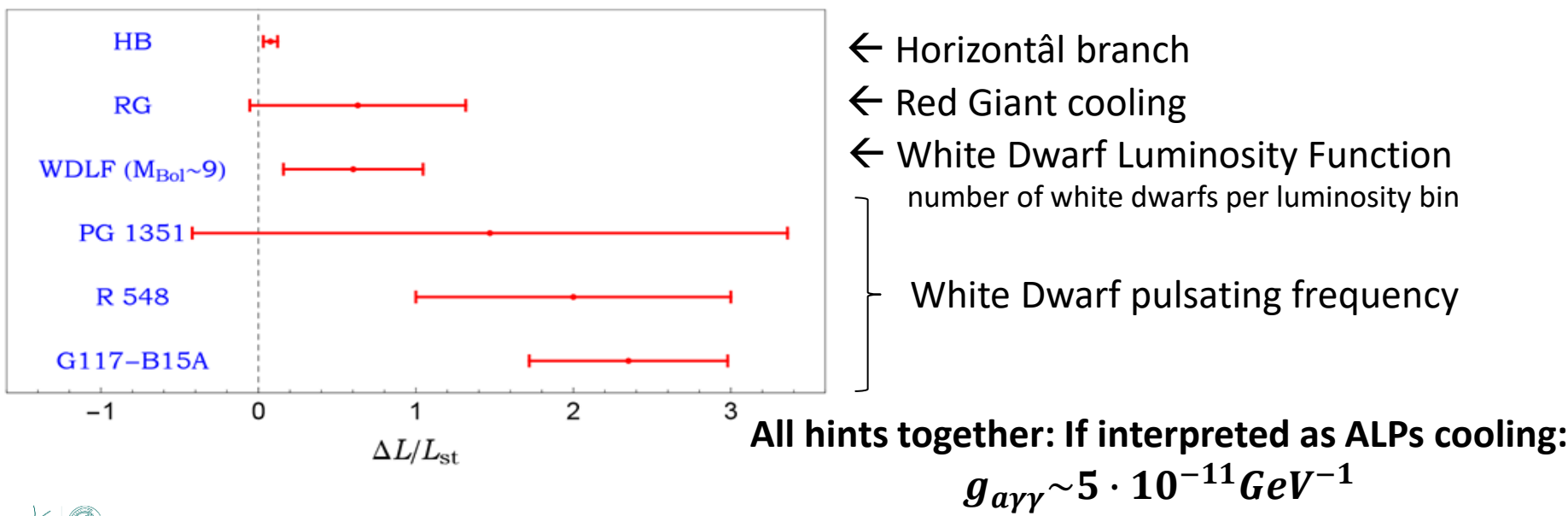
Frequency is decreasing due to cooling:

Expected: $\dot{P}_{th} = (2 - 6) \cdot 10^{-15} \text{ ss}^{-1}$

Measured: $\dot{P}_{obs} = (12.0 \pm 3.5) \cdot 10^{-15} \text{ ss}^{-1}$

(two more variable white dwarfs with slightly too efficient cooling found:
R548, PG1351)

Possible loss mechanism in white dwarfs: “axion electron Bremsstrahlung”



Hints from transparency of the universe:



Some astrophysical sources can emit very high energy gamma rays $\gg 1 \text{ TeV}$. Especially for blazars (AGN with jet pointing towards earth): can be detected on earth using Cherenkov telescopes → MAGIC, HESS, CTA

Photons can interact with infrared band of Extra Galactic Background Light (EBL) resulting from stars, interstellar dust emission, etc.

- High energy gamma rays are absorbed (pair creation)
- Optical depth τ not zero
- Flux is attenuated

$$\Phi_{obs}(E_\gamma) = \Phi_s(E_\gamma) \cdot e^{-\tau(E_\gamma, z_s)}$$

Φ_s and Φ_{obs} : fluxes emitted by source and observed at earth, z_s is the red shift of the source .

Hints from transparency of the universe:

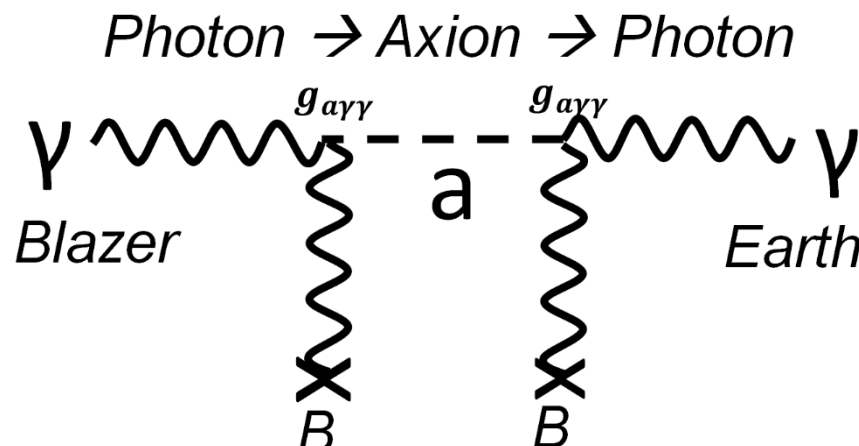
Transparency is given by:

$$\tau(E_\gamma, z_s) = \int_0^{z_s} \int_{E_{th}}^{\infty} \sigma_{\gamma\gamma}(E_\gamma, E) \cdot n_{EBL}(z, E) \, dE \, dl(z)$$

with $l(z)$ the path of the photons, taking into consideration cosmological evolution (expansion), $n_{EBL}(z, E)$ the EBL density at redshift z and energy E and $\sigma_{\gamma\gamma}(E_\gamma, E)$ the angle averaged pair creation cross section.

Photons can evade EBL scattering by: $\gamma \rightarrow ALP \rightarrow \gamma$

Photon to ALPs conversion in magnetic field of source or intergalactic medium



Hints from transparency of the universe:



Source: **blazers**: few mG on 10pc scale,
intergalactic medium: μG on hundred kpc scale,
back conversion in (inter)galactic magnetic field: μG over more than 10kpc,

Depending on line of sight:

Calculate oscillation probabilities as function of direction.

→ Investigation of energy dependent flux from blazars, compare to expectations taking into account $\tau(E_\gamma, z_s)$

→ For ALP scenario: expected flux as function of energy will be different, depending on line of sight (different back-oscillation probabilities).

Analysis of high energy spectra from 12 high z_s sources consistent with ALPs with $g_{a\gamma\gamma} \sim 2 \cdot 10^{-11} \text{ GeV}^{-1}$ for few hundred neV ALP mass.

